APPLYING OPTICALLY STIMULATED LUMINESCENCE (OSL) TO AN ARCHAEOLOGICAL SITE UNDER WATER

A Thesis

by

SHERI LOUISE KAPAHNKE

Submitted to the Office of Graduate and Professional Studies of
Texas A&M University
in partial fulfillment of the requirements for the degree of

MASTER OF SCIENCE

Chair of Committee,	Deborah Carlson
Committee Members,	Christopher Dostal
	Timothy Dellapenna
Head of Department,	Darryl de Ruiter

August 2020

Major Subject: Maritime Archaeology and Conservation

ABSTRACT

The study of archaeology does not exist without understanding stratigraphy. Terrestrial archaeologists frequently utilize studies in sedimentation to understand a site's stratigraphic history, but many tools have not been translated to underwater sites. Current studies in optically stimulated luminescence (OSL) are proving incorrect many assumptions of a stratigraphy's characteristics by identifying disturbances invisible to the human eye. OSL methodologies allow measurements of the last time quartz was exposed to the sun. The preliminary screening and calibrated screening methods, provide a relative chronology of underwater stratigraphy with the added possibility for absolute dates in the future. The stratigraphy of a shipwreck is often thought of as a time capsule, but even though the artifacts from a shipwreck are of the same time and "context" there is often a horizontal stratigraphy that can aid archaeologists in reconstructing artifact disturbances. OSL was applied to marine sediment samples and cores from Maroni *Tsaroukkas,* Cyprus to understand patterns of sediment movement, environmental changes, and to test the application of the portable OSL reader on shallow sites (less than 6.0 m depth). Preliminary screening by means of the portable OSL reader provided the expected results. Samples could be distinguished by high, moderate and low OSL signals, which in turn determined which to bring forward to more intensive processing for calibrated results. Comparisons between data from the screenings made it possible to identify which artifacts had moved recently, and areas of sand accumulation. Finally, initial stratigraphic conclusions determined that the sand on site is being thoroughly

bleached, and the accumulation and erosion of silt changes drastically between the northwest and southeast sectors of the site.

DEDICATION

To My Grandparents, Robert Matthews, Donna Matthews, and Peter Kapahnke

ACKNOWLEDGEMENTS

This thesis was made possible by the hard work of my committee Dr. Dostal and Dr. Dellapenna, as well as committee chair, Dr. Carlson, whose editing and formatting suggestions were exceptionally helpful. In equal measure, I must thank Dr. Timothy Kinnaird of St. Andrews University who I first nagged about this thesis idea on an island in Greece in 2017. He has since patiently guided me through the process of measuring and interpreting optically stimulated luminescence (OSL). I am eternally grateful to him and the Luminescence Dating Laboratory in the School of Earth and Environmental Sciences, University of St. Andrews, Scotland for the use of their facilities to conduct OSL measurements.

Thanks must also be given to Dr. Carrie Atkins, director of the Maroni *Tsaroukkas* Anchorage Survey Project (part of the Kalavasos and Maroni Built Environments (KAMBE) project), for housing me in Cyprus and allowing me to collect sediment samples. In the field, it was Dr. Chris Monroe who deserves all my gratitude for his help lugging supplies around under water and aiding me with sample collection as I hobbled across the sea floor with a sprained ankle.

Finally, I will take the opportunity to thank my family, my friends and my partner for their endless care and support.

CONTRIBUTORS AND FUNDING SOURCES

This thesis was supervised by a committee consisting of Dr. Deborah Carlson (advisor) and Dr. Christopher Dostal of the Nautical Archaeology Program in the Department of Anthropology at Texas A&M University, and Dr. Timothy Dellapenna of the Department of Marine and Coastal Environmental Science at Texas A&M University – Galveston.

The OSL data interpretations of Chapter II and Chapter III are a result of collaboration between Dr. Timothy Kinnaird of St. Andrews University, and the author.

All sediment samples were collected by the author, and all OSL measurements were completed by the author under the guidance of Dr. Timothy Kinnaird

Funding Sources

Research for this thesis was supported by scholarships provided by the Department of Anthropology at Texas A&M University, and the generous support of SSHRC, the Honor Frost Foundation, National Geographic and the University of Toronto Mississauga who fund the Maroni *Tsaroukkas* Anchorage Project.

NOMENCLATURE

Aliquot	A very small sub-sample of grains dispensed onto a 10.0 mm stainless steel/aluminum disc.
Bleaching event	The exposure of a sample either to daylight or artificial light. During a bleaching event, stored electrons are released from traps within sediment grains and photons are emitted.
Dose Rate	Total level of radioactivity which a sediment sample has been exposed to. A measurement needed to calculate a luminescence age.
Equivalent Dose	The amount of radiation needed to produce the same OSL signal naturally produced by a sediment sample. The SAR protocol is used to find this value which is needed to calculate a luminescence age.

Gray (Gy)	Measurement of a dose of radiation. 1 Gy is equal to 1 joule of energy deposited in 1 kilogramme of sediment.
Inductively Coupled Plasma Mass Spectronomy (ICP-MS)	A method of determining what elements are present in sediment by atomic weight. This is needed to calculate the dose rate.
Infrared Stimulated Luminescence (IRSL)	Luminescence stimulation using Infrared light, this wavelength of light stimulates feldspars, but not quartz, and is often used when there is feldspar present in the sediment, but very little quartz.
Kiloan (ka)	One thousand years.
Luminescence Dating	The umbrella term for dating methods that involve stimulating sediment with light (OSL) or heat (TL).
Natural OSL signal	The OSL signal (photons/energy) emitted during stimulation of a sediment sample after a period of burial.

Optically Stimulated Luminescence (OSL)	Luminescence dating using blue light, these short wavelengths stimulate both quartz and feldspar.
Readout	The stimulation of a sediment sample and measurement of the signal during calibrated screening.
Sensitivity	The increase of the efficiency of electrons to become displaced by radiation and released during stimulation. Measured as number of photons per Gy.
Single Aliquot Regenerative-Dose protocol (SAR)	A cycle of tests that a quartz sample is put through to determine the equivalent dose. Cycles produce three measurements: (a) Stored dose, the natural signal produced by the release of electrons stored during burial, (b) Regenerative Dose, the signal produced by known doses of radiation administered in the laboratory, and (c) the

	Test Dose, which is the resulting signal from a standard dose of radiation given to the sample after every readout used to track sensitivity changes in the grains.
Thermoluminescence (TL)	Luminescence dating using heat to stimulate electrons.
Luminescence Trap	A site within a crystal where electrons accumulate and remain stored. Formed by structural defects.

TABLE OF CONTENTS

Page

LIST OF FIGURES

Page

LIST OF TABLES

Page

CHAPTER I

OPTICALLY STIMULATED LUMINESCENE (OSL) AND ARCHAEOLOGY: AN INTRODUCTION

Archaeologists are aware of the effects currents and wave action have on the movement of artifacts, and understand the importance of studying sedimentation on underwater sites, but publications on the subject often focus only on the preservation issues that sediment movement can cause.[1] Ford et al. discuss geomorphic properties of underwater sites and the various tidal, wave, and current actions that can expose, bury, and move artifacts.[2] They also mention the likelihood that "denser" material will "settle in place" despite sedimentation processes.[3] As a site-monitoring strategy with Tesla-BOEM, Keith and Evans used remote sensing and sediment coring to build site-specific models to animate the broad effects of wave, current, and storm action on shipwrecks.[4] Within these publications about sedimentation, there is little focus on how artifact movement affects the interpretation of artifact finds. A method to quantify disturbance at an archaeological site under water is needed. In this chapter, optically stimulated luminescence (OSL) is considered as a methodology that may offer insight into

[1] Ford et al. 2016, 19; Keith and Evans 2016, 44.
[2] Ford et al. 2016, 20-22.
[3] Ford et al. 2016, 20.
[4] Keith and Evans 2016, 54-64.

stratigraphic sequences, specific artifact movement and wider environmental changes on underwater sites.

Methodologies for terrestrial excavation and site formation principles are addressed before explaining the properties of OSL, and how it has helped terrestrial archaeologists interpret sites. Terrestrial and underwater approaches to excavation will be outlined before suggesting how OSL can amplify underwater excavation methods. The underwater environment creates challenges for OSL sampling, and these concerns will be discussed at the end of this chapter.

The introduction of OSL to underwater archaeological excavation can provide more certainty about artifact distribution and post-depositional processes. This chapter will outline the different applications of OSL sampling programs: dating, profiling, and sensitivity measurements.

I.1. Terrestrial Archaeological Principles and Theory

The single-context recording methodology for terrestrial archaeological sites, known as the Harris Matrix, was popularized by Edward Harris in 1979 and forms the foundation for interpreting archaeological sites. The methodology is based on disassembling an archaeological site by sediment layer in the opposite order of deposition: that which is latest is taken up first.[5] The separation of these layers can be quite subjective during excavation. The layers removed can be used to inform

[5] Harris 1989, 113.

lithostratigraphic strata, but these strata are broad and defined by uniform sediment. During excavation, uniform sediment often can be split into smaller layers based on other factors such as artifact distribution.[6] Therefore, the term 'context' will be used here to describe the layers taken up during excavation. Archaeological projects have also used terms such as 'excavation units' and 'baskets' to describe contexts.[7] Each recorded context represents a period of sedimentation caused by human activity or environmental processes during occupation and after abandonment. The contexts are differentiated by changes in appearance of sediment (color, consistency, etc.) or artifact density. However, excavators may choose to arbitrarily split a large uniform context to make artifact associations more intelligible. The formation of contexts can be defined by deposition or extraction: collapse, burial pits dug through strata, or a few millimeters of floor surface can all be separated while excavating. It is understood that sediment contexts and strata are older as they are deeper, but they can be horizontal, vertical, additive or subtractive. Identification and separation of complex stratigraphy is necessary in order to clarify the sequence of events. Once contexts and features are discerned, a date must also be determined, whether through relative artifact sequences (lithics, ceramics, coins) or absolute dating such as radiocarbon dating. The identification of context change is crucial for accumulating accurate insights to the lives of people in the past, especially if an area has been occupied for millennia.

---

[6] See Farrand and Jacobsen (2000, 40) for the post-excavation lithrostratigraphic analysis of the excavations of Franchthi Cave in Greece.
[7] Farrand and Jacobsen 2000, 25.

The separation of contexts is not an easy task. During the excavation of Franchthi Cave, a prehistoric site in Greece, contexts were identified by sediment type or color changes, human made features such as hearths or floors, and post-depositional disturbances. When no clear stratigraphy could be discerned due to lack of sediment change, caused by bioturbation or other disturbances, thin layers of a few centimeters were removed as arbitrary contexts.[8] This was done to avoid collecting multiple unidentifiable contexts as one large context. In general, sediments in Franchthi Cave accumulated at a slow rate of 1.0-2.0 cm every 100 years, making identification of changes a matter of millimeters.[9]

The complications involved of separating strata in the field through visual interpretation has been discussed for decades. Peter Clark addressed the issue in 1992 and explains that single-context recording aims to pinpoint a context by defining environmental processes through visual description, but in reality, environmental disturbances sometimes do not change visual properties.[10] OSL data have been used to understand the environmental processes of bioturbation, post-deposition, and environmental disturbances that Clark described.

[8] Farrand and Jacobsen 2000, 27.
[9] Farrand and Jacobsen 2000, 27.
[10] Clark 1992, 17-18.

I.2. OSL Processes and Methodology

Current studies in OSL are testing many assumptions about stratigraphic characteristics by identifying disturbances, such as bioturbation, that can distribute artifacts without notable changes in context.[11]Araujo provides an example from a site in Central Brazil where older lithic artifacts traveled upwards and were found in strata above the layer of their assemblage. The possibility for OSL to identify the upward movement of sand grains is mentioned and bioturbation through insect activity is blamed.[12] OSL methodology allows for differentiation between (a) contexts created during human occupation, where artifacts could be perceived as in a sediment pocket directly associated with their time of use (primary context), and (b) contexts disturbed and mixed by natural processes.

Identification of different burial dates among different sediments is possible because luminescence studies measure a building signal within quartz and feldspar, which accumulates from the last time the minerals in the sediment were exposed to light or heat.[13] Luminescence dating was first applied to archaeological sites in the 1960s with the thermoluminescence (TL) dating of ceramics, determining the last time ceramics had been exposed to high temperatures (i.e. fired in a kiln).[14] OSL, which measures the last time sediment was exposed to light, was developed in the 1980s.[15]

---

[11] Clark 1992, 17-18
[12] Araujo 2013, 2124.
[13] Huntley et al. 1985, 105; Aitken 1998, 2. The build-up of luminescence does reach a point of oversaturation. A date for sediment beyond 200,000 years old is rarely found (Roberts et al. 2015, 53).
[14] Kennedy and Knopf 1960, 13; Aitken et al. 1968, 442.
[15] Huntley et al. 1985, 105.

Luminescence is caused by exposure of minerals (i.e. quartz and feldspar) to incoming cosmic radiation and naturally occurring ionising radiation present in all sediments (^{235}U, ^{238}U, ^{238}Th and ^{40}K). Radiation travels as alpha, beta and gamma particles that cause energy, or electrons, to accumulate in defects in a mineral's crystal lattice, gradually building up over time (Fig. 1).[16] Exposure to light or heat during

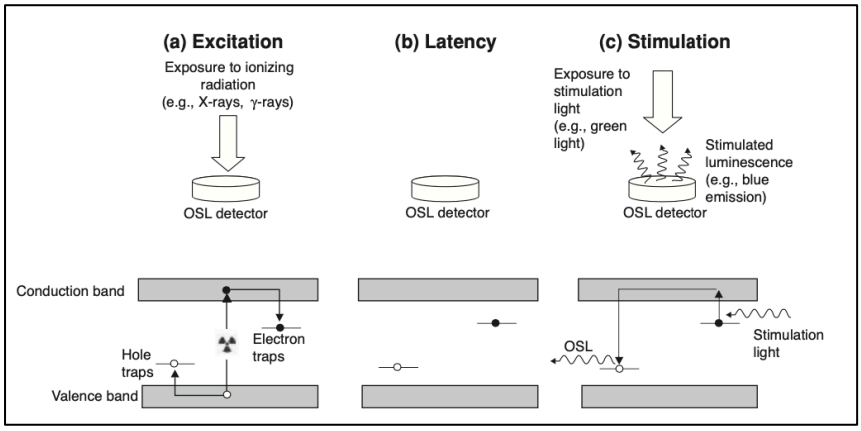

Figure 1. Electron Deposition into Traps and Stimulation Resulting in OSL
This image displays a) radioactivity which dislodge electrons from the conduction band into electron traps, b) the trapped electrons during latency, and c) stimulation expelling electrons to luminescence traps (hole traps) and the release of photons (displayed as OSL). (After Yukihara and McKeever 2011, with permission).

sediment transportation will reset this accumulation to zero. Upon reburial, the energy or trapped charge starts to accumulate in the crystal lattice again (Fig. 2).

The release of this energy can be stimulated in the laboratory using light (OSL) or heat (TL). Luminescence readers use a photomultiplier to count the number of

[16] Aitken 1998, 13, 37-38.

photons released when the electrons are stimulated.[17] Infra-red light is used to stimulate feldspars in a process known as Infrared Stimulated Luminescence (IRSL), while the smaller wavelengths of blue light can stimulate both feldspar and quartz (OSL).[18]

Luminescence readers, which are equipped with radiation sources, heating units and light sources, are used to find the 'stored dose' (the energy accumulated in the sediment during burial), and the 'equivalent dose' (the amount of radiation needed to recreate the stored dose), the latter of which is one of two values needed to calculate age.

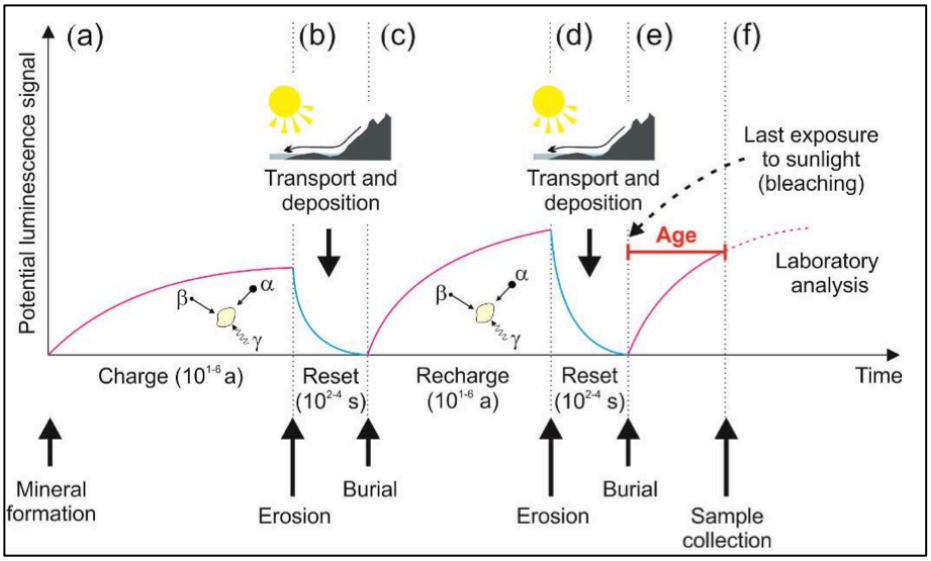

Figure 2. The Accumulation of Luminescence Signal Over Time Displaying the cycle of accumulation of luminescence signal (charge), and bleaching events (After Mellett 2013, this material is available under public license: CC BY 4.0, https://www.geomorphology.org.uk/sites/default/files/geom_tech_chapters /4.2.6 _LuminescenceDating.pdf).

[17] Aitken 1998, 9.
[18] Aitken 1998, 69.

The heating unit is needed to introduce a pre-heat before light stimulation, in order to remove any electrons from unstable traps such as the 110° C TL trap.[19] After irradiation, this trap will become filled, but will lose its electron charge over a number of hours without stimulation.[20] The electrons stored in this trap are therefore not present in the natural signal and must be removed before measuring the equivalent dose.[21] The second value needed for age calculation is the 'dose rate'. This is the radioactivity of the sediment itself, along with any possible cosmic radiation that could have affected the sediment.[22] This measurement can be determined (a) using Inductively Coupled Plasma Mass Spectrometry (ICP-MS), which quantifies the concentrations of radionuclides in the sediment that can produce this radiation, (b) by means of in-situ gamma spectrometry, or (c) with a dosimeter used on site for an extended period of time. A luminescence age is a quotient of equivalent dose over dose rate.[23]

OSL is often used to determine age, but signal intensities and sensitivity measurements can also be very useful on their own. When a project employs OSL it is often to understand the exact date of a structure or pinpoint a time of natural change in the landscape by dating a stratum of sediment. However, age calculations require a series of tests and processing. Recording the differences in the luminescence signal as a relative chronology, without determining an exact date can also be useful for

---

[19] Franklin et al. (1995, 317) describes the peaks of TL, which Chen and Pagonis (2011, 271) and Roberts et al. (2018, 172) outline its effects on OSL measurements.
[20] Roberts et al. 2018, 172.
[21] Chen and Pagonis (2011, 271), outlines a pre-heat regimen during the SAR protocol, beginning at a maximum of 260° to empty both the 110° and 230° TL traps.
[22] Kinnaird et al. 2007, 52.
[23] Aitken 1998, 7.

understanding complex stratigraphy. When sampling a sequence of strata, one can expect to find either a logical signal depth-progression (strata at depth have been buried longer, therefore more luminescence has grown in situ) or areas of reworking, collapse, and/or other construction or damage (which has exposed the sediment to light). Utilizing the luminescence signals to create a relative chronology is referred to as OSL profiling, and often will accompany dating.[24] An OSL profile result from a preliminary screening where sediment samples are left in bulk and unprocessed, or through a calibrated screening. The standard process to prepare samples for calibrated OSL determinations includes sieving and chemical etching. Samples are sieved because different grain sizes move differently on the surface of the earth, affecting the rate at which they are bleached.[25] Large and small grains are also affected differently by the penetration of radiation and have different luminescence responses. When sieving the sediment samples into different grain sizes, these issues can be taken into consideration.[26] Additionally, organic matter and feldspar can obscure the reading of OSL from quartz.[27] Therefore, the sediment is chemically etched with hydrochloric acid and hydrofluoric acid to remove carbonates, organics, and feldspars. The outer-surface of the quartz grains is also removed in this process, in order to eliminate the influence of the alpha-irradiated surface. This is because alpha particles behave unpredictably and it is difficult

---

[24] Sanderson et al. (2001, 893, 896) discuss creating OSL profiles from stored dose determinations performed in the laboratory; Sanderson and Murphy (2010, 299) discuss OSL profiling using a portable OSL reader.
[25] Aitken 1998, 164.
[26] Aitken 1998, 41.
[27] As outlined by Aitken (1998, 68) feldspar and quartz build luminescence at different levels and must be separated.

to reconstruct their influence on the sediment.[28] By eliminating sieving and chemical etching, profiling can be done quickly and in the field with portable OSL readers. The preliminary OSL results acquired through a portable reader can save time in the laboratory by characterizing complex stratigraphy, and identifying the most promising targets for dating or anomalies that need clarification.[29]

Finally, the sensitivity of quartz can provide important information about a stratum. Quartz sensitivity is determined during calibrated screening by comparing the luminescence signal after a standard dose of radiation administered in the laboratory. If the luminescence signal produced is higher in one layer than another, then there is a difference in how efficiently the luminescence is building in those grains. Sensitivity differences may occur due to different origins of the grains, exposure to heat or excessive irradiation and bleaching cycles.[30] These changes in sensitivity within a given stratigraphy can indicate a large-scale change in sedimentation dynamics, such as chaotic erosion events, fire, or change in grain provenance.

I.3. OSL and Stratigraphy on Terrestrial Sites

OSL sampling and profiling performed at the Neolithic site of Kissonerga *Mylouthkia* on Cyprus provides one example of applications of OSL dating on a terrestrial site. Samples were taken to determine the age of two pit-like features, in order

---

[28] Aitken 1998, 41.
[29] The use of portable OSL readers for these purposes was first introduced by Sanderson and Murphy (2010, 299).
[30] Sharma et al. 2017, 646.

to understand whether they are related to other Neolithic features in the area, which broadly date between the early 8th and mid-9th millennium BCE.[31] Stainless steel tubes approximately 15.0 cm in length were inserted into the profile of the pit fill. These tubes were then placed in a light-proof bag and transported to the Luminescence Research Laboratory at the Scottish University Environmental Research Center (SUERC). The two samples went through standard processing for calibrated screening, including sieving and chemical etching. Small aliquots of the remaining grains were dispensed onto discs and set into the Risø TL/OSL automated machine to determine the luminescence signal.[32] This process will be elaborated further in Chapter II (section II.5).

After a series of tests and the SAR protocol to determine equivalent dose (mentioned on pp. 6-7), ages were calculated at 8.37 ± 0.61 ka and 9.12 ± 0.49 ka which fits well with dates from other Neolithic features on site.[33] In the event that excavation is not possible, the OSL results allow responsible government agencies to decree this site important in the face of local construction. With further work, conclusions can be drawn about some of the earliest human habitation on Cyprus and the first instances of animal and plant domestication on the island.[34]

One of the most common uses for OSL on archaeological sites is to find a date for features that lack organic material or artifact associations, but occasionally archaeologists would also like to know the range of ages or luminescence signals within

---

[31] Kinnaird et al. 2007, 53.
[32] Kinnaird et al. 2007, 53.
[33] Kinnaird et al. 2007, 55.
[34] Kinnaird et al. 2007, 56.

an archaeological trench, a naturally occurring cliff face/scarp, or define sediment chronologies from a core. OSL results from a stratigraphic record can provide information about areas where deposition mechanisms have caused sediment to not bleach thoroughly or have a mix of bleached and unbleached grains. The strength of the signal related to location and associated artifacts can indicate disturbances in the stratigraphy from bioturbation and erosion to broad environmental changes. On a single archaeological site, or across whole cultural landscapes, these processes can be related to human activity through time. For example, luminescence profiling was used in Catalonia, Spain not only to date the initial construction of ancient terraces, but also to evaluate the history of damage and reconstruction they have undergone.[35] Preliminary screening using the SUERC portable OSL reader outlined three phases to the terraces: (a) a ploughed surface characterized by an inverted stratigraphy at the top, (b) an upper retaining wall, and (c) the initial construction of a lower terrace wall built much earlier in time.[36]

Samples for luminescence profiling can either be collected and brought to the laboratory to be read, or preliminary observations can be determined in the field using a portable OSL reader. The portable reader was initially developed by the Scottish University Environmental Research Center in 2005.[37] Using a portable OSL reader in the field allows for a larger sampling program, and a more comprehensive understanding of

[35] Kinnaird et al. 2017, 67-68.
[36] Kinnaird et al. 2017, 73.
[37] Sanderson and Murphy 2010, 299.

an area's depositional history to take place. An initial test of the portable reader was performed on canal sediments in Cambodia. Verified in the laboratory by the SAR protocol, the portable OSL reader was able to identify between archaeological sections, older substrates, and mixed and re-deposited sediments.[38] Preliminary screening using the portable reader allows researchers to: (a) gather real time data about what is in a primary context or what has been disturbed, (b) calculate depletion indices indicating whether the sediment was well bleached before deposition, and (c) monitor influences from feldspar in the quartz signal using infra-red light (IRSL) followed by blue light (OSL). OSL measurements with the portable unit are performed on unprocessed sediment samples. This means factors that can alter the signal are removed or controlled in the laboratory for calibrated results (grain size, alpha irradiation and sensitivity). Nevertheless, preliminary screening determinations can allow sediment without a signal, or a mixed signal to be distinguished, which can save valuable time in the laboratory.[39] The process is expanded upon in section II.4.

The sensitivity of quartz and feldspar grains to irradiation and bleaching must be normalized to provide accurate readings, but recording the sensitivity changes can also provide valuable information about the characteristics of the sediment or activity in the area. It is not well known how electron accumulation and stimulation within the grains become more efficient, but there are many factors that cause a sensitivity change: frequent cycles of bleaching and irradiation, exposure to high temperatures, and the

[38] Sanderson and Murphy 2010, 299.
[39] Sanderson and Murphy 2010, 299-300.

nature of the source-rock from which the sediment grains are derived.[40] Usually a large amount of radiation means a large number of electrons become trapped in luminescence centers. However, with an increased sensitivity, a small amount of radiation will cause a large number of electrons to become trapped. It is very important, therefore, to track sensitivity changes during calibrated screening when the sample goes through multiple cycles of irradiation and bleaching. In an experiment performed on sediment from the Otindag desert in China, scientists heated, irradiated and bleached samples 20 times in the laboratory. Afterwards, the sensitivity was found to be 6 times higher, and therefore collecting a much higher luminescence signal with the same amount of radiation.[41] Sensitivity changes are tracked during multiple cycles of irradiation and bleaching in order to correct the luminescence signal.[42] A heightened sensitivity can also be indicative of exposure to high temperatures, such as from a fire.[43] OSL samples collected at the Vasilikos and Dhiarizos valleys on Cyprus see a change in sensitivity in different strata; this is interpreted as a result of seasonal burnings associated with agricultural practices.[44] Sensitivity of TL and OSL can also depend on the number of traps in the lattice of the crystal established during the formation of the source-rock from which these grains are derived. Because characteristics are common among grains of the same source-rock, this information can provide researchers with the geographical provenance

[40] Sharma et al. 2017, 646.
[41] Zheng et al. 2009, 536.
[42] Murray and Wintle 2000, 58.
[43] Aitken (1998, 195) records temperature to induce sensitivity change at 200-550° C.
[44] Kinnaird et al. 2013, 57.

of sediment, and pinpoint time periods when two different sediment features with different provenances were brought together.[45] This aspect is especially relevant for archaeologists attempting to identify severe erosion on a site.

I.4 Underwater Archaeology Principles and Theory

Shipwrecks that have come to their current position through a single event, are seen as a time capsules, capturing one moment in history in a horizontal stratigraphy.[46] This is different from terrestrial sites with many layers of occupation which rarely represent a single period of time in any great detail. However, it is incorrect to think that pristine underwater sites such as the so called 'tumulus wrecks', that still have the structure of the ship and their cargoes preserved, are the only sites we can hope to learn from. Even the most disarticulated underwater sites can provide information not replicated on land, but predictably these sites often have a much more complicated depositional history.[47] Many wrecks in more dynamic environments have been tackled, such as the Marzamemi "Church Wreck" first excavated by Gerhard Kapitän in the 1960s-1970s and revisited by Justin Leidwanger from 2013 to 2019.[48] The site has not only suffered disturbance from previous excavation, but it is located in shallow water (7-9 m) and susceptible to storm activity.[49] Intrusive material has been found in even the lowest layers of the site, and artifacts are found under and amongst reef fragments, with

---

[45] Zheng et al. 2009, 535.
[46] Bowens 2009, 16.
[47] Parker 1981, 316.
[48] Kapitän 1969, 122; Leidwanger 2018, 330.
[49] Leidwanger 2018, 341.

large boulders spread across an area greater than 30.0 x 30.0 m.[50] The Nautical Archaeology Society (NAS)'s *Guide to Principles and Practice in Underwater Archaeology* suggests excavating these sites with "careful investigation" and provides a daunting list of all the complications to a shipwreck's stratigraphic record that might be identified visually while excavating: scouring, silting, collapse, trawling, burrowing organisms, and looting.[51] Understanding that the processes of sediment movement are continuous, especially on shallow sites, how are archaeologists expected to see disturbances such as these when trawling lines, holes, or scouring can be filled in and flattened?[52] Although careful excavation and record keeping to track the associations and positions of artifacts might help us visualize a site, using a methodology based only on artifact location in a frequently changing site is like trying to understand all the behaviors of fish by looking at a snapshot of them in the water column. Dynamic underwater sites deserve attention to formation processes similar to terrestrial sites. Sometimes it is not possible to see evidence of scouring, trawling or looting, and know exactly which artifacts have been affected and how. When a ship's hull has deteriorated and artifacts are strewn across the sea floor in no discernable pattern why should archaeologists draw conclusions only based on visual recording? There is potential for OSL to help underwater archaeologists understand formation processes on such a site, and in turn, extrapolate conclusions with more confidence.

---

[50] Leidwanger 2018, 341-42.
[51] Bowens 2009, 24.
[52] Brennan (2016, 165) discusses the difficulty of identifying trawling effects on site when trawl scares are erased over time.

I.5. Underwater Applications of OSL Dating

On terrestrial sites, the need to turn to OSL as a dating tool comes when there are no organic remains, when the site is too early to date with an artifact sequence (such as relative dating with ceramic sequences), or if a feature has only non-diagnostic artifacts associated with it. Dating using OSL has also been performed on sediments from underwater environments. Sedimentary geologists have performed OSL as a dating tool for deep-sea cores in conjunction with other analyses to reconstruct ancient environments and climate cycles.[53] However, this use for OSL measurements is not necessary on many archaeological sites under water. On shipwreck sites, organic remains are frequently preserved and allow the possibility for radiocarbon dating, and the artifacts present on site are often enough to suggest a range of dates. Another common use of OSL dating is to analyze coastline changes, but it has not been widely utilized in archaeology.[54] For some underwater features such as harbor structures or submerged settlements, OSL dating may be a useful tool to characterize stratigraphic sequences, or determine coastline changes. Due to the often-shallow vertical stratigraphy, traditional OSL dating methods to characterize long stratigraphic sequences may not be useful. However, OSL measurements do not just date specific features or

---

[53] Jacobs 2008, 525; Olley et al. (2004, 182) collected a core off the coast of northwestern Australia from a depth of 1093.0 m in order to test single-grain OSL dating methods. OSL ages for the core ranged from 1,780 ± 290 years old at the top and 51,100 ± 6,500 years old at the bottom, with approximately 10% certainty.

[54] Jacobs (2008, 511-15) provides an extensive compilation of coastal and marine luminescence dating projects.

strata, the methodology can provide a unique opportunity to understand episodes of burial, relative to artifacts, across a horizontal plane.

I.6. OSL and Stratigraphy on Underwater Sites

Underwater stratigraphic analysis can be useful for shallow archaeological sites such as harbors and submerged landscapes to analyze how environmental has affected the area. The possibility for OSL to illuminate now-submerged terrestrial landscapes is exhibited by the sampling program associated with the DISPERSE project, which aims to understand the movement of hominin and human populations through Arabia.[55] In addition to archaeological survey under water and on land, both OSL profiling and dating were performed on marine and terrestrial cores from the Farasan Islands in Saudi Arabia.[56] From the sea floor at 38.0-80.0 m depth, 18 gravity cores and two box cores were taken from the outer and inner submerged Farasan shelves (identified with bathymetry).[57] The two cores were split in half. One half was used to log the sequence of sedimentation and the other was split into a series of samples for OSL determinations, beginning with preliminary profiling using the SUERC portable reader.[58] Samples with promising dating potential or samples reflecting a clear context change were taken for further characterization and calibrated screening.[59] In this case, IRSL was chosen for

[55] Sanderson and Kinnaird 2019, 685.
[56] Sanderson and Kinnaird 2019, 690.
[57] Sanderson and Kinnaird 2019, 691.
[58] Sanderson and Kinnaird 2019, 691.
[59] Sanderson and Kinnaird 2019, 691.

dating feldspar due to a low quartz content in the sediment.[60] Using the IRSL single aliquot regenerative-additive (SARA, a variant of the SAR protocol mentioned on p.19) dose protocol to determine equivalent dose, core FA6 was found to date solely to the Holocene (1.4 ± 0.2 to 5.9 ± 2.5 ka).[61] However, sub-samples from the bottom of core FA13 at 150.0-200.0 cm depth dated to the Late Pleistocene (15.0 ± 1.5 ka to 21.9 ± 3.2 ka).[62] These dates correspond to a surviving paleo-landscape that has been submerged.[63] This OSL sampling project in the Red Sea demonstrates the potential of OSL profiling with the SUERC portable OSL reader, and calibrated screening to refine questions about underwater stratigraphy and environmental change.

As on terrestrial sites, sensitivity differences in quartz can aid in the characterization of more large-scale sediment movement under water. Sensitivity changes occurring in different parts of a core, or in different areas of a site, can raise questions about the sedimentary changes that have occurred in those times and areas. The ability of quartz grains to store luminescence often depends on the nature of the source of the grains. For example, Fitzsimmons found that in Australia, quartz from sandstone sources is more sensitive than quartz from metamorphosed schist.[64] As on land, these changes in underwater stratigraphic sequences can aid in identifying times of erosion, or severe storm action and their effects on coastal sites.

---

[60] Sanderson and Kinnaird 2019, 694.
[61] Sanderson and Kinnaird 2019, 694.
[62] Sanderson and Kinnaird 2019, 694.
[63] Sanderson and Kinnaird 2019, 696.
[64] Fitzsimmons 2011, 199.

I.7. OSL and Artifact Movement Under Water

Although the DISPERSE project focused on questions regarding environmental change over a long period of time, it is plausible that the same methodology can be applied on a smaller scale to identify intrusive processes and theorize how sediment and artifacts have moved within an archaeological site. OSL has been providing a version of this service to terrestrial archaeologists for years, helping to pinpoint which stratigraphic contexts are disturbed or intact. Simple coring and sediment sampling of an underwater site can provide information a) about the depth of surface sediment that is in frequent movement, b) at what depth and in which areas sediments are not affected by storms and wave action, and c) artifact movement along with the sediments. This information may also be useful when considering in-situ preservation methods. Continuously moving surface sediment, if exposed to adequate daylight, will have a consistently small luminescence signal. Often it is expected that all loose sand is churning on the sea floor. OSL can pinpoint to what extent this is happening, allowing a better understanding of which artifacts are in low or high activity zones. On a terrestrial site, all artifacts are not treated with equal significance. An artifact that is found on the surface, in topsoil, is not considered viable when making conclusions about the site because it cannot be related to a specific context. Artifacts found on or near a shipwreck often will have come from that shipwreck. However, surely artifacts from high activity zones and low activity zones should not be assigned the same archaeological weight when drawing conclusions (such as about cargo distribution on a ship), and this information must be explained clearly in

publications. On most shipwreck sites, it may seem simple to distinguish between disturbed and undisturbed artifacts by assuming those exposed at the surface are those which have been displaced. However, processes that disturb artifacts such as looting, previous excavation, fishing via net, trawl or dynamite, and collapse of the hull can produce upheavals that affect buried artifact along with those on the surface. Underwater sites apart from shipwrecks can also benefit from an understanding of artifact and sediment movement, especially if a site has an uneven artifact distribution. If a site under water has assemblages of material that do not seem to fit together, OSL measurements of the surrounding sediments could identify different depositional events that may provide an explanation. This very situation is seen at Maroni *Tsaroukkas*, which the author sampled in 2019 and will be discussed in Chapter II.

In order to answer questions about artifact movement, the natural deposition patterns need to be determined from cores taken either on site, or near to site as long as there is not a drastic change in landscape. Luminescence signals from the cores may then be compared to isolated samples taken beneath large artifacts in an attempt to identify a depositional change. If the stratigraphic sequences below an artifact registers archaeologically meaningful luminescence doses, the artifact is likely to be close to an original position. If an artifact were to be redeposited, the sediment beneath it now is likely to have been exposed to the sun more recently. Therefore, if the OSL signal of the sediment beneath an artifact is higher than from the equivalent substrate of a core, this could mean that the artifact has prohibited light from reaching the sediment underneath it. Cores taken on site are useful for interpreting the signals seen in those sediments not

affected by the presence of artifacts. From these cores, OSL results can also pinpoint areas of a site with low or high activity, unrelated to specific artifact movement. If coring on site is a concern, small layered sediment samples on site can also be collected.

There is great promise for OSL to aid our understanding of the deposition and movement of artifacts, but potential is limited by the type of site. The possibility for sediment to wash underneath artifacts creates concerns about drawing conclusions from the OSL signal. A site where artifacts rest on a dense sediment such as a mud, clay or silt would eliminate some of this concern. Less sediment may also have been washed beneath large, heavy artifacts such as stone blocks, ingots or amphoras. When working with heavier artifacts, the next consideration is whether they have sunk deeper into the sediment than other artifacts, creating the illusion that they were deposited earlier. This issue is another reason cores are taken on or near to site, to create a point of comparison for the sediment beneath the artifact. If an artifact's lower surface is only found by removing 10.0 cm of dense clay, then this sediment can also be collected in a series of samples or a small core to determine whether the sediment is similar to the chronological range collected from the comparative core. An impact with enough force to lodge an artifact into dense sediment may have produced a disturbance in the stratigraphic record. The OSL methodology is in its infancy, but the implementation of this tool and the results may change the way we think about the relationship between sediment and artifacts at underwater sites.

I.8. Challenges and Limitations of OSL Under Water

There are a couple of important constraints to OSL sampling under water. In general, the methodology can only be done in an environment that has quartz and/or feldspar. This can be determined by studying the bedrock geology, and should be done before OSL sampling is attempted. Areas with volcanic (basalt) or limestone bedrocks generally do not have enough quartz for OSL measurements to be successful.[65] In fact, the Mediterranean is viable for OSL for the most part because fine quartz grains from the Sahara are frequently carried on wind currents.[66]

The second limitation is that the site must be in shallow water (less than 10.0 m), where the sediment will receive enough sunlight for adequate bleaching as it is redeposited on the surface. The same issue will arise if the site is located in turbid water, where particles in the water column affect how much light reaches the sediment. However, not enough research has been done to say how water clarity and depth influence results. Bleaching experiments were performed with optical spectronomy and spectral radiometry at Angkor Borei in the Mekong Delta in Southern Cambodia.[67] At the height of day, wavelengths of light reaching 1.5 m into the disturbed water were only 5% of what they were at the surface.[68] However, conditions will always differ from place to place. Cores from a low-energy tidal mudflat in the north of the Wadden Sea in Denmark were taken for OSL profiling and the results provided accurate ages in the

[65] Thiel et al. 2015, 27.
[66] Stuut et al. 2009, 237.
[67] Sanderson et al. 2007, 324.
[68] Sanderson et al. 2007, 324.

core, beginning at 9 ± 3 years old and up to 305 ± 16 years old in these murky conditions.[69] The small errors indicate that the surface is well bleached even through the water column.[70]

The accuracy of OSL measurement depends strongly on the sediment bleaching when it gets churned to the surface and exposed to the sun. Wavelengths of light toward the ultraviolet end of the spectrum create a faster emission of electrons from luminescence traps within the crystals. However, the ultraviolet component of sunlight is absorbed in water, creating an environment where it is less likely that the sediment is completely bleached at all times.[71] This uncertainty undermines the resolve to spend time coring, taking samples, and performing extensive laboratory work, but the methodology developed by SUERC can rectify some of the challenges of uncertain bleaching. Preliminary screening through the portable OSL reader does not produce dates, rather it can create a relative series of signal intensities. Developed for terrestrial sites, this device allows patterns in a stratigraphic record to be understood. The portable reader collects the average signal from a larger sample rather than from a few grains.[72] It is a much friendlier and faster methodology for complicated depositional environments, allowing disturbed contexts to be identified quickly.[73] This is important for an archaeologist's understanding of a site, but also useful for finding the most suitable

---

[69] Madsen et al. 2005, 259.
[70] Madsen et al. 2005, 259.
[71] Aitken 1998, 16-17.
[72] Samples for the portable reader are usually read in a 50.0 mm diameter petri dish (maximum volume of about 0.039 cm^3).
[73] Sanderson and Murphy 2010, 299.

material for further study (i.e. material well bleached prior to deposition with a high signal for dating). Different bleaching rates in a sample will yield uncalibrated results, but combined with sedimentological and stratigraphic observations, these samples can provide detailed narratives about site formation processes.[74] Preliminary screening allows more samples to be taken, providing simple identification of outliers in the dataset.[75] The portability of SUERC's OSL reader allows samples to be measured on site and areas of problematic mixing to be understood and taken into consideration during excavation and sampling.[76]

The luminescence signal in quartz and feldspar grows in relation to radiation in the environment, however radiation behaves differently under water and this must be taken into consideration as well. In all environments, nuclei from various elements (U, Th, K) decay and emit radiation in the form of alpha, beta, and gamma rays. This radiation as well as cosmic radiation will penetrate the sediment to different lengths and causes electrons to become detached and recombine at defects in the crystal lattice, beginning the accumulation that will create the luminescence signal.[77] However, radioactivity attenuates in water, causing radiation levels to be three orders of magnitude lower in a waterlogged environment.[78]

Lower radiation under water does not mean it is impossible to perform OSL measurements, but determining the dose rate can require extra work. The change in

---

[74] Sanderson and Murphy 2010, 301.
[75] Stang et al. 2012, 315.
[76] Sanderson and Murphy 2010, 300.
[77] Aitken 1998, 37-38.
[78] Aitken 1998, 38.

exposure to radiation because of water content plays a large role in determining dose rates (how much radiation the sediment has received) on site, a value needed to calculate dates using OSL. Issues arise with sediment that has had varying water content since burial.[79] Dose rate measurements assume that radiation conditions are stable, but if the sampled sediment has been waterlogged, the dose rate changes with time. Knowledge of the sediment's life span in and out of submergence is necessary to determine the proper dose rate.[80] In the case of the OSL sampling project at the Oga Peninsula in Japan, the sampled sediment had been exposed to changes in water content due to fluctuations in sea-level over time. To reconcile this, the average of present-day water content and saturated water content was calculated.[81] The result was then used to estimate the lifetime of water content in the sediment and calculate an estimation for the amount of radiation the sediment would have been exposed to.[82]

Today, the most common use of OSL is to date specific features or sites. However, there are different applications of OSL that could benefit underwater archaeologists. Relative chronologies of luminescence signals on a site can help clarify artifact deposition and sedimentation patterns without determining an absolute date for the sediment. There are a number of steps beyond measuring the natural luminescence

---

[79] Aitken 1998, 43-44, see also: Madsen et al. 2005, 261-62.
[80] Aitken 1998, 43.
[81] The present-day water content can be determined by weighing the sample as it is, with its natural moisture content and subtracting this weight by the weight of the sample after it has dried in the furnace. The saturated water content can be determined by weighing the sample after enough water has been introduced only to fill the spaces between the grains with water molecules and subtracting this weight by the sample's dry weight. See Thiel et al. (2015, 22) for details.
[82] Thiel et al. 2015, 22.

signal in order to arrive at a date for the samples. Though determining a date from some samples can be useful, it can be an unnecessary effort for an entire sequence. However, using only a luminescence signal to draw conclusions does have its drawbacks. OSL data may determine if the sediment beneath an artifact has a higher luminescence signal than the surface sediment. In that case, that artifact may be not be in frequent movement, but we also cannot say definitively that the artifact is in a context belonging to the time period to which it has already been dated. It would be most beneficial not to separate OSL dating from OSL profiling, but rather use relative dating and absolute dating in tandem to learn the most about underwater environments.

I.9. Conclusion

Terrestrial archaeologists are often able to distinguish the visual characteristics of complicated stratigraphic changes, altered by bioturbation, human interference and environmental disturbances. However, these issues are more difficult to identify visually on archaeological sites under water. The tumultuous conditions courtesy of storm activity, currents and waves are joined by trawling, animal activity, and looting, and can create unintelligible stratigraphic sequences, vertically and horizontally. Additionally, sediment underwater is often very uniform and separate contexts cannot be identified. Excavations will often group artifacts by grid squares that divide up the site.[83] This however, does not address disturbances in a reliable way. OSL has the potential to

[83] Bowens 2009, 126; Leidwanger 2018, 343.

clarify processes of sedimentary deposition and the distribution of artifacts along with it. This can be done through a collection of cores on or near a site, and the collection of isolated sediment samples associated with artifact finds. OSL signal intensities can be joined by sensitivity measurements to understand changes to the underwater landscape via changes in quartz characteristics that represent the introduction of new sediment. There are two OSL methods that can be exploited: (a) preliminary screening methods using portable OSL equipment and (b) calibrated screening measurements are discussed in Chapter II. In Chapter III, overall conclusions will be drawn about the significance of OSL sampling and new strategies will be discussed that may eliminate some of the concerns regarding this methodology.

CHAPTER II

OSL SAMPLING AT MARONI *TSAROUKKAS,* CYPRUS

II.1. The Late Bronze Age Anchorage at Maroni *Tsaroukkas,* Cyprus

A series of Late Bronze Age (1650-1100 BCE) stone anchors and ceramics have been documented on the sea floor off the coast of Maroni *Tsaroukkas* in southeast Cyprus. During the initial underwater survey project conducted from 1993 to 1996, 35 Late Bronze Age stone anchors were recorded, along with a condensed area of ceramics (Late Cypriot I A, mid-17th century BCE) in the northwest corner of the survey area.[84] The current (since 2017) survey project is directed by Dr. Carrie Atkins of the University of Toronto, and aims to record newly exposed finds, check artifact distribution from the previous survey, and create photogrammetric models of the site (Fig. 3).[85]. This project is in conjunction with the Kalavasos and Maroni Built Environments (KAMBE) project, a widespread survey and excavation project in the area under the auspices of Cornell University, the University of British Columbia, and the University of Chicago. Within the current survey area of 225.0 x 200.0 m the seabed slopes from 2.0 m to 8.0 m in depth, and patches of natural cobbles and boulders cover the silty sea floor, with larger

[84] Manning et al. 2002, 114, 152; Atkins 2020, 14.
[85] Fulton et al. 2016, 17-8.

areas of sand. [86] Not far inland are scattered Late Bronze Age structures, a concentration of buildings at Maroni-*Vournes,* and tombs along the shore, which were explored as early as the late 1800s (Fig. 4).[87]

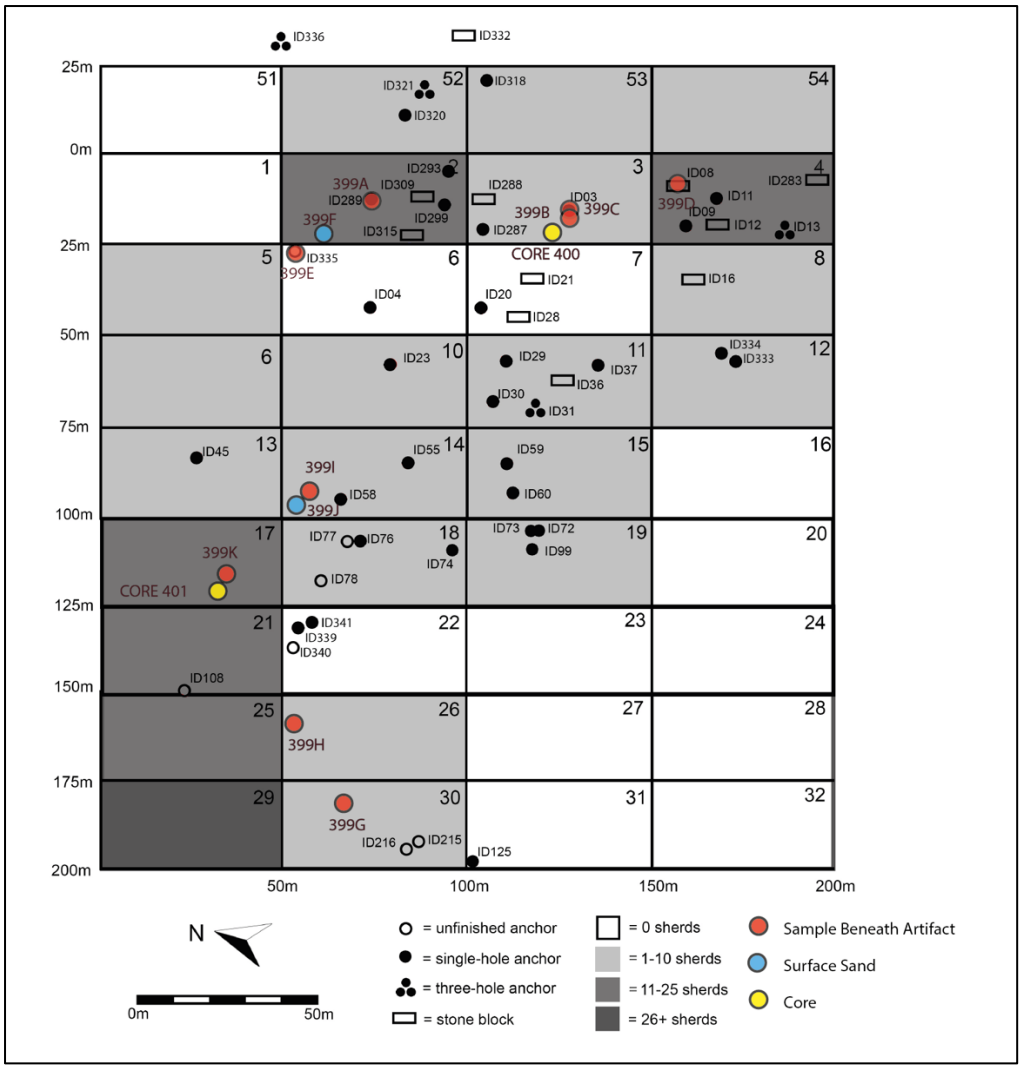

Figure 3. Site Plan of Anchorage at Maroni *Tsaroukkas* (Adapted from Carrie Atkins, unpublished)

[86] Manning et al. 2002, 113. Sediment is classified using the Udden-Wentworth scale outlined by Folk (1980, 23).
[87] Cadogan 1992, 123; Manning et al. 1998, 297.

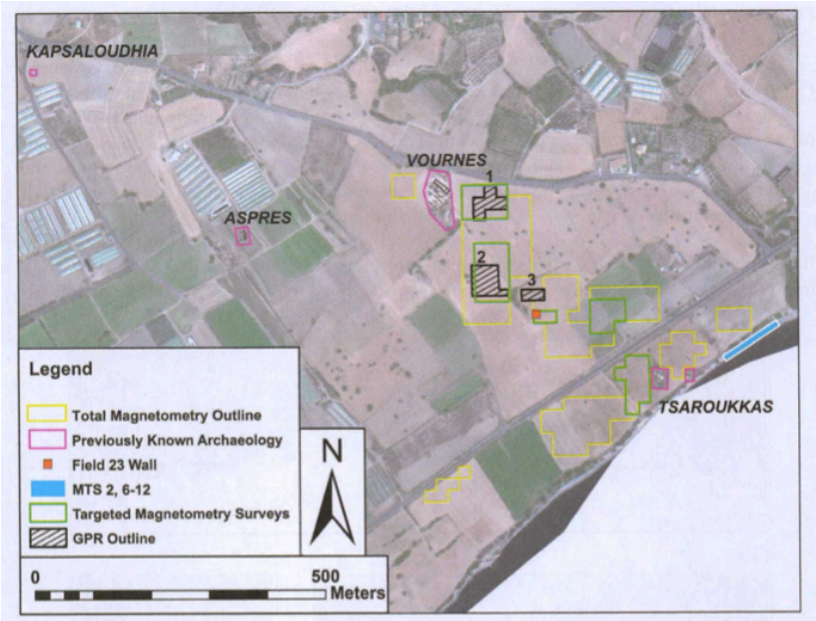

Figure 4. Map of Archaeological Sites near Maroni *Tsaroukkas*, Cyprus (After Manning et al. 2014, with permission).

In June 2019, the experimental OSL sampling project was conducted alongside the current underwater survey. This anchorage was chosen for optically stimulated luminescence (OSL) testing under water because of its shallow environment, the presence of large artifacts, and the hope OSL could answer questions about the anchorage. These include: (a) how these anchors relate to the ceramic assemblage and the architectural blocks found on site, (b) whether the artifacts ended up in the sea from erosion and sea-level change, or as debris from maritime activity, and (c) what the sedimentation patterns of the site look like. It has been suggested that this area may have

once been a sheltered inlet.[88] Erosion and sea-level changes have certainly altered the local shoreline, but it is uncertain if and how the site has been affected.[89]

The varied environment of the anchorage is ideal to test the application of OSL on underwater sites, and assess whether a full-scale sampling program has the capacity to answer some or any of the questions listed above. In this chapter, I examine whether the OSL sampling program can (a) clarify sedimentation/ deposition processes, (b) identify artifact movement, and (c) determine whether preliminary screening measurements could be effective for future on-site evaluations at Maroni *Tsaroukkas.*

Through methodologies of relative luminescence profiling, I hope to establish a new tool for understanding stratigraphic records and quantifying the effects of post-depositional disturbances on underwater sites. In this chapter, I will discuss the methodologies behind processing sediment samples and quantifying the luminescence intensities, and conclude with a description of the results.

II.2. The OSL Sampling Program

II.2.1 Underwater sampling

Sampling at the anchorage of Maroni *Tsaroukkas* resulted in two cores and 11 isolated samples. Nine of the 11 samples were collected from beneath artifacts, while the remaining two contain surface sand to determine if the sediment is being bleached

[88] Manning et al. 2002, 113.
[89] Andreou (2018, 1) introduces an ArcGIS model to monitor current erosion levels on the south-central coast of Cyprus.

thoroughly at the surface. Sampling was performed in three dives over two days. Before heading to the site, a map was drawn on a slate indicating the position of anchors from beneath which sediment could be collected. Once an anchor was located, divers hand-fanned around the edge of the artifact. If it was sitting on cobbles, the artifact was not sampled since it was almost certain that sediment has washed through the spaces between these cobbles. When a suitable anchor sitting flat on the sediment was found, the bottom edge was located, and a horizontal tunnel was created to collect samples from beneath the artifact. A light-proof tarp with arm-holes, created from a film-changing bag, was used to block the sampling area from light exposure. To ensure consistency, I alone collected samples by pushing my arms through the arm holes of the tarp with spoon and sample cup in hand. The labelled sample cup had been previously covered in black duct tape to minimize light exposure. On site, once my arms were in place, I used the spoon to remove one more layer in the tunnel, cleaned the spoon of any silt that adhered, and then scooped sediment into the sampling cup. Contamination from sand suspended in the water-column was possible when sampling, but care was taken to ensure that it was negligible. The majority of sediment seemed to settle quickly, and the sample cup was kept in position under the anchor until the lid was closed. After the sample was collected, it was placed into an aluminum-lined bag, as an extra precaution against light exposure. In some cases, when tunneling beneath an artifact, it was discovered that the bottom edge of the anchor was sitting on silt, and that sand had washed in around the curved edges. In one case, sand and silt were collected in separate samples (**399B** and **399C**) to assess the differences in the OSL signals between these sediments. Six isolated

samples (**399A-399F**) and the first core (**400**) were taken on the southeastern side of the site (Table 1). The isolated samples from this part of the site were from large stone artifacts (**399A-399E**) along with one sample of surface sand (**399F**). The five samples

Southeastern Isolated Marine Samples				
Sample Number	Artifact Type	Sediment type	Tunnel length under artifact (cm)	Depth below sea-level (m)
399A	Stone Anchor ID 289	Silt	20.0	3.0
399B	Stone Anchor ID 03	Sand	30.0	4.5
399C	Stone Anchor ID 03	Silt	20.0	4.5
399D	Architectural block ID 08	Sand, pebbles	15.0	6.0
399E	Unfinished Anchor ID 335	Sand	20	3
399F	Surface Sand	Sand	--	4

Table 1. Isolated Marine Samples collected in Southeastern Sector of Site

from underneath artifacts on the northwestern part of the site were collected to test the application of OSL measurements on sediment beneath smaller artifacts (Table 2). The northwestern sector of site is comprised of cobbles among large ceramic sherds, mainly from Late Bronze Age storage jars. Ceramics were selected if they were large (more than 10.0 cm length) and resting on sediment in more "secure" positions, such as wedged underneath a cobble. When in a more precarious position, the ceramic sherd was loosened once surrounding sand was fanned away, and had to be removed. The sediment underneath was then collected, and the sherd was replaced. Most of the ceramics were

Northwestern Isolated Marine Samples			
Sample Number	Artifact Type	Sediment Type	Depth below sea-level (m)
399G	Ceramic sherd	Sand, pebbles	2.0
399H	Ceramic sherd	Coarse sand	2.0
399I	Ceramic sherd	Coarse sand	2.0
399J	Surface sand	Sand	2.0
399K	Ceramic base	Silt	2.0

Table 2. Isolated Marine Samples collected in Northwestern Sector of Site

sitting on sand, and only one large base (**399K**) was sitting flat on silt. The base fragment was large enough that it remained in place and a tunnel could be made to the center of the base. Taking samples from beneath ceramics was a more difficult task. The sand was coarser in this area, with small pebbles. Sample collection was performed to the best of my ability, but while working under the tarp, often more pebbles were collected than sand.

Two cores were collected, one for the southeast sector and another for the northwest sector. Both cores were approximately 125.0 m away from the furthest sample. To collect the cores, tubes of PVC, 2.0 cm in diameter were covered in duct tape. Once in position on site, the tubes were driven into the sediment with a hammer. Because of the dense silt, the area around each tube had to be dug out with a spoon requiring a large amount of manpower and time. After the tubes were removed, the top was plugged with duct tape and a cap was affixed to the bottom. On shore, they were placed in the shade and the ends were further secured with duct tape. The first core (**400**) from the southeastern sector of site captured 30.0 cm of sediment, while the second (**401**) from the northwest only collected 16.2 cm. In core **400**, the top 9.9 cm was sand,

and the remaining 20.2 cm was silt. In the second core (**401**), the top 6.3 cm was sand, and the remaining 9.9 cm was silt.[90] The aim was to collect a core with close to 1.0 m of sediment, and the small collection achievable with our methods created a concern that little information would be learned about the site.

II.2.2. Terrestrial Sampling

Samples were collected from the anchorage under water (marine samples), as well as on shore adjacent to the survey site (terrestrial samples; Fig. 5). On the shore

Figure 5. Terrestrial Scarp next to Anchorage which was the source of the environmental and archaeological samples.

[90] There are no photos of the lithostratigraphy of these cores since the sediment could not be exposed to light.

there are a series of previously excavated Bronze Age tombs. Samples were collected from an archaeological section and a nearby environmental section without archaeological material (Fig. 6).[91] Terrestrial samples were collected for comparison between terrestrial and underwater bleaching rates and luminescence behaviors, as well as to see if more could be learned about the area around the site. Although it is small, the

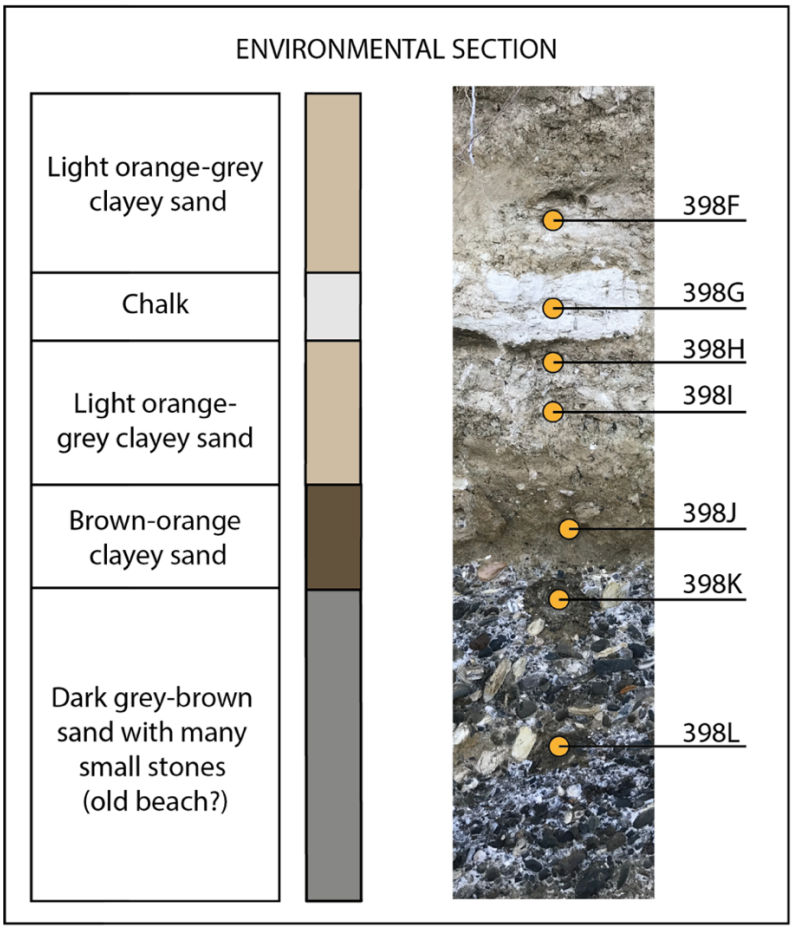

Figure 6. Terrestrial Samples: Environmental Section

[91] Coordinates for the environmental section: N34° 44.623' E33° 23.209'. Coordinates for the terrestrial section: N34° 44.640' E33° 23.236.

archaeological section (Fig. 7) was chosen because it had a clear stratigraphic sequence. Much of the archaeological material in the scarp is collapsed and mixed, but the plaster layer in this section below the layer of stones/cobbles was considered a feature that may preserve intact stratigraphy.

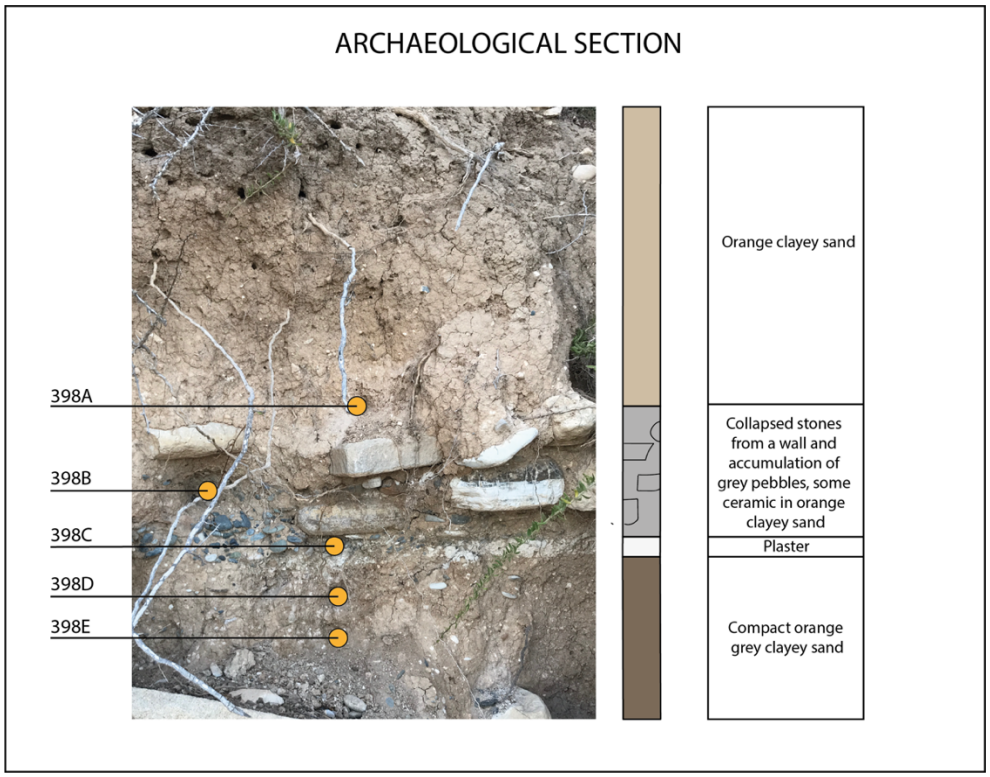

Figure 7. Terrestrial Samples: Archaeological Section

Samples were collected at night in order to protect them from sun exposure, allowing enough light to see the outline of the strata, but not enough to stimulate the electrons stored in the sediment. Metal markers were placed in each visible stratum

during the day in order to ensure samples collected at night were taken from the correct areas. The first 2.0-3.0 cm of sediment was removed in order to prevent contamination from bleached grains. Sediment was then collected in numbered 50.0 ml plastic containers with lids. To prevent exposure to the sun, the containers were covered in duct tape before sampling and once the sediment was collected, the containers were placed into an aluminum bag. Depending on the density of the sediment, the containers were often not filled completely, especially from the chalky stratum (**398G**), and the old beach strata (**398K** and **398L**). The weight of the sampled sediment ranged from 21.5 g-42.4 g. In retrospect, it is regrettable that more sediment was not removed before sampling was performed; Murray and Funder advise that approximately 10.0 cm should be removed to ensure no light-contaminated material was collected.[92] Sediment in this area becomes covered in a layer of calcium carbonate forming a hard crust on the surface.[93] We attempted to remove this, but it is unlikely that we managed to cut all the way through it. Time constraints, lack of proper equipment to remove large amounts of compacted sediment, and concern for the integrity of the scarp created hesitancy when sampling. These factors are taken into consideration when interpreting the results.

[92] Murray and Funder 2003, 1179.
[93] This is known as kafkalla (Cypriot term) or caliche and is caused by precipitation of moisture in the sediment leaving behind a hard crust residue, see Schirmir (1998, 116) for details.

II.3. Data Interpretation

The OSL signals determined through preliminary and calibrated screening are displayed as a curved graph known as a decay curve (Fig. 8).[94] The graph represents the depletion of electrons from the traps in the sediment crystals as they are stimulated by light. Preliminary screening with the portable OSL reader displays this signal intensity as a photon count, while the calibrated screening with the Risø OSL reader displays the normalized results as a stored dose in units of grays (Gy).[95] The vertical axis of the decay curve is the luminescence measured in photon counts or stored dose (Gy). The

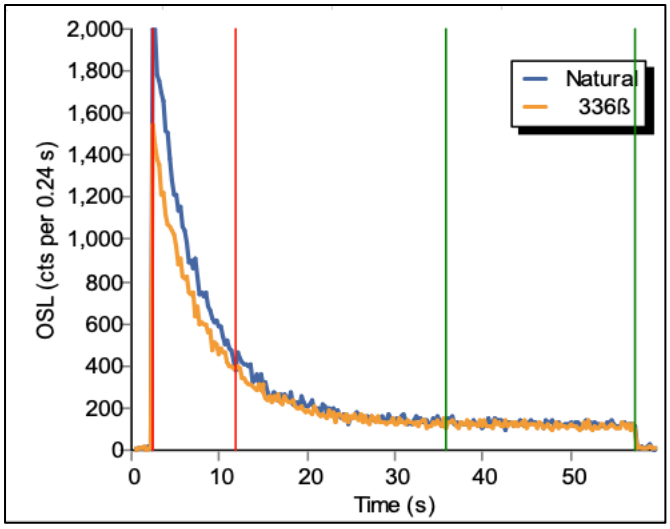

Figure 8. Example of an OSL Decay Curve This decay curve is from an aliquot of sample **399A** during the SAR protocol during a cycle after an administered radiation dose of c. 30.0 Gy. The red lines are the boundaries of the first integral (fast component) and the green are the boundaries of the second integral (background).

[94] Aitken 1998, 25.
[95] The stored dose is normalized to the test dose, which is the term for the result produced from the stable amount of irradiation given after the natural signal is determined.

horizontal axis represents time in seconds. The decay curve is derived from a composite of decay curves occurring as different traps within the crystals are depleted. The most light-sensitive traps are called the 'fast' component. Since they bleach quickly and reliably these are what OSL measurements are based on.[96] The signals after this fast component can accumulate as the aliquot goes through subsequent cycles of irradiation and bleaching and this can be erroneously included in the calculation of the fast component. These subsequent cycles occur in all sequences of the calibrated screening (described in section II.5). Therefore, the fast component must be isolated. This is done by selecting windows of focus (integrals) along the decay curve after the samples have been read. The first integral (shown in red) selects the signal from the fast component at the beginning of the curve. The second integral (shown in green) is used to calculate the background of the signal at the tail end of the curve by taking the average of the selection and multiplying it by the numbers of channels in the first integral. The first integral is then subtracted from the background to retrieve the net signal of the sample.[97] Integral lengths change from study to study. For the SAR protocol, integrals were chosen between (a) 2.6 and 7.2 seconds, and (b) 36 and 57.6 seconds. The first integral begins at 2.6 seconds because there are a few seconds of background count before the light is turned on.[98] For the SAR protocol, the first integral was changed to 1.6 to 12 seconds (as seen in the figure), this was done in order to have a little more room to extract a signal

[96] Roberts et al. 2015, 44.
[97] Duller 2016, 32.
[98] Carter et al. 2018, 267.

from the insensitive material. The difference between the stored doses resulting from these changes was negligible.

Once the signal intensities (counts, as obtained from preliminary screening) or stored dose (Gy, from subsequent calibrated screening) have been determined for isolated samples, they are plotted to look for different patterns. For the stratigraphic sequences examined (cores **400** and **401** and the terrestrial sections), the stored dose and sensitivity distributions provide the first indication of the chronological range. If the sediment stratigraphy is intact, then signal intensities and stored dose values may be expected to increase with depth (normal signal depth-progression), and can be seen in the graphs. The stored dose values are displayed in these graphs on a logarithmic scale in order to facilitate comparison. The data from the 11 isolated marine samples and displayed in tables rather than graphs, as they do not form a stratigraphic sequence.

A few factors that affect the results are the chronological limitations of luminescence dating, error values, and sensitivity values. Luminescence dating is most commonly used to measure ages younger than 200,000 years. However, some exceptions allow older ages to be retrieved due to lower than average environmental radiation.[99] The luminescence saturation limit varies in different quartz grains. Generally, grains will have a saturation point of approximately 150.0-255.0 Gy.[100] However, some can be saturated with doses as low as 20.0 Gy, or as high as 400.0 Gy, as seen in grains from

[99] Roberts et al. 2015, 53.
[100] Heydari and Guérin 2018, 97.

the Australian dunes.[101] This information will be important in section II.5 to contextualize the calibrated screening results, some of which will be quantified in terms over 700.0 Gy. Aliquots with error values (which are caused by low sensitivity) greater than 20% of the natural signal, or sensitivities calculated to below 100 counts were removed from the results.

II.4. Preliminary Screening

11.4.1. Background and Methodology

After the sediment samples and cores were collected, they were packaged and shipped to the Luminescence Dating Laboratory in the School of Earth and Environmental Sciences, University of St. Andrews in Scotland. There I processed and put the sediment through OSL determinations under the supervision of Dr. Timothy Kinnaird. The cores were first opened under subdued lighting, and small isolated samples were collected at intervals of c. 1.5 cm spacing down the core, minding the boundary between sand and silt. After drying in the furnace at 50° C, the samples were presented for measurement in the SUERC portable OSL reader in 50.0 mm diameter plastic petri-trays. This was done to determine whether (a) preliminary screening with the portable unit can produce useful distinctions and could be useful in the future to make on-site determinations, and (b) the sediment is viable for more intensive calibrated screening. Although the portable device is designed for use in the field, it was

[101] Roberts et al. 2015, 53; for high saturation points in Australian sand see Yoshida 2000, 32.

economical to perform these first tests in the laboratory, to understand accuracy and ability before bringing the device to site. In order to determine whether the preliminary screening results are useful to this specific site, the results will be compared to the calibrated results in Chapter III.

The portable reader measures both infrared-stimulated luminescence (IRSL) and optically stimulated luminescence (OSL), by (a) shining a red light to stimulate feldspars but not quartz, (b) shining a blue light to stimulate the quartz, and (c) counting the photons that result from each stimulation (readout of the signal). By monitoring the change in the ratio between IRSL and OSL signals, changes in the representation of quartz and feldspar can be quantified. Since these signals are recorded from bulk, unprocessed sediment samples, the signal intensity is not accurate enough for dating determinations. Factors that can confuse the signal – such as grain size, uncertainties from alpha irradiation and mixed sensitivities – are usually controlled with chemical etching, sieving into grain fractions, and laboratory testing such as that performed for the calibrated screening seen in section II.5. However, the profile of signals can provide useful initial conclusions.

Depletion indices are also recorded. This is the ratio of photon counts during the first half of the stimulation time to those in the second half of stimulation time.[102] This index displays how quickly the signal is depleted. The faster the signal is depleted the better it was bleached prior to burial. If the value of the first half of the signal divided by

[102] Sanderson and Murphy 2010, 300.

the second half is above 2.0 then the sample is well bleached. A sample can also be read as poorly bleached if there is a mixture between well-bleached and unbleached grains. If a sample is not bleached thoroughly before deposition, the results will be inflated because they carry a residual signal collected during the previous period of deposition. This is a large concern for the marine sediments being examined from Maroni *Tsaroukkas.*

II.4.2. Preliminary Screening Results

II.4.2.1. Core **400**

Core **400**, taken from the southeastern sector of the anchorage from 406.6 to 436.6 cm below sea level, was split into 20 sub-samples **400A-400U**. The preliminary screening (Fig. 9) shows that all seven sand sub-samples collected between 406.6 and 416.5 cm depth in the core, were characterized by consistently small OSL signal intensities from 1,152-1,933 photon counts. The last two sub-samples of sand (**400F and 400G**) from a depth of 415.1 to 416.5 cm were characterized by higher signal intensities of 2,111-2,702 photon counts. **400G** and **400F** seem to represent a thin layer of 'older' sand, suggesting that there is a subtle chronology present in the sand. However, there is some possibility that **400G and 400F** contain contamination of grains from the underlying silt that are contributing to the composite signal. IRSL is not detectable in the core at a depth of 406.6-415.1 cm. **400G** is the first sample to return an IRSL signal of 111 counts. The signal intensity remains comparatively small throughout the core, ranging from 111-12029 counts, and IRSL:OSL ratio values are low, with an average of

0.09. The first sub-sample of silt, **400H**, returns signal intensities 24 times greater (66,679 counts) than the sand sample immediately overlying it. The remaining silt sub-samples can be separated into two groups categorized by their ranges of signal intensity. In group one, the five sample between 419.7 to 426.5 cm have OSL signal intensities ranging from 71,012 to 95,429 counts (average of 83,506). In group two, the last eight samples between 427.9 to 436.6 cm have smaller signal intensities that range from 40,336 to 58,596 counts (average of 46,811).

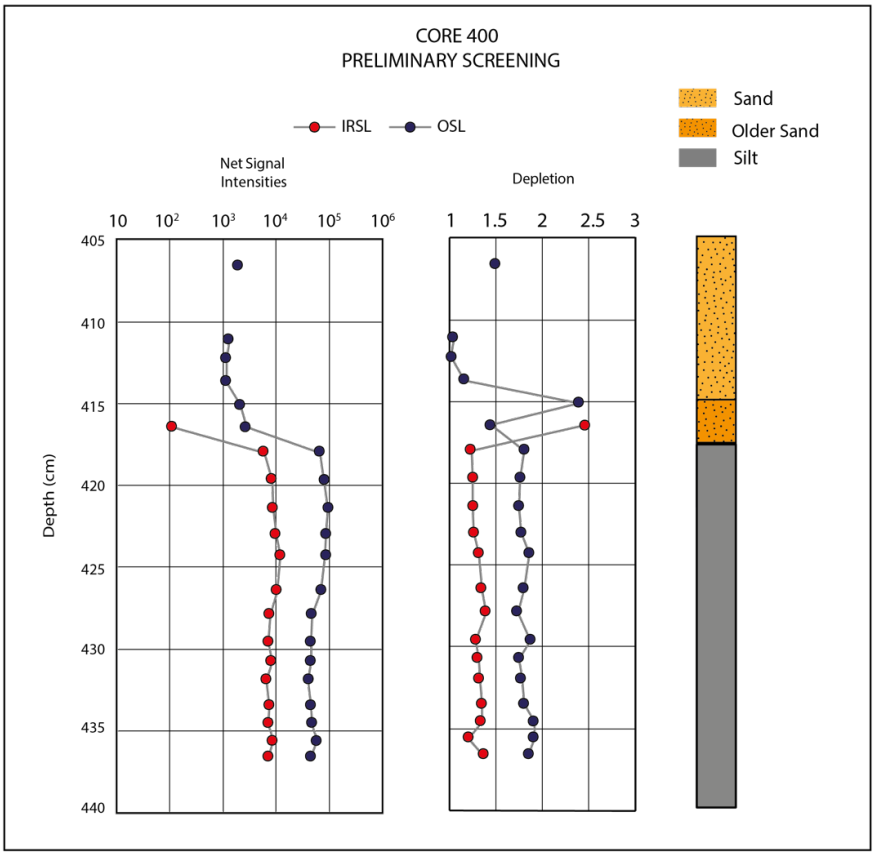

Figure 9. Preliminary Screening for Core 400 The graph to the left records net signal intensity measured in photon counts while the graph to the left portrays depletion indices. To the far left is an image depicting the lithostratigraphy of the core.

The depletion indices for the majority of the sand and silt are low, varying between 1 and 1.86; this might indicate that the OSL signals are drawn from mixed age sediments, with residual luminescence remaining from prior burial periods. At a depth of 415.1 cm, sand sub-sample **400F** is an exception with a depletion ratio of 2.4, suggesting the luminescence may have grown entirely in situ. This also indicates the sand from this sample is more sensitive, and may be from a different provenance.

In summary, the majority of the sands in core **400** appear to be mobile, with luminescence signals that were recently reset. There is some evidence that an older sand unit is preserved above the silt. The silt shows a complex depositional history, spanning a considerable length of time. The five upper silt samples from 418 to 426.5 cm hold higher signal intensities than those below them. This suggests that either the sediment has been reworked, with older sediments redeposited on top of a younger sediments, or that this section holds residual luminescence.

II.4.2.2. Core **401**

Core **401,** collected from the northwestern sector of site at a depth of 201.1-217.3 cm below sea level, is shorter than core **400** and is split into 18 sub-samples. The top seven sub-samples consist of sand, at a depth of 201.1 to 207.5 cm within the core (Fig. 10). The bottom 11 sub-samples are of silt at a depth of 208.6 to 217.3 cm within the core. The sand samples once again have very small OSL signal intensities and only a detectable IRSL signal from only two samples: **401A** (201.0 cm depth) and **401G** (207.5

cm depth). As in core **400**, the base of the sand (**401G**) has a higher OSL signal. Its photon count is 10,462, which is approximately 22 times higher than in the previous sand sub-samples. One explanation for this could be contamination through human error while splitting the sub-samples. It is also possible that this higher signal intensity is indicating that there is a pocket of 1.0 cm or so of sand that is not in frequent movement.

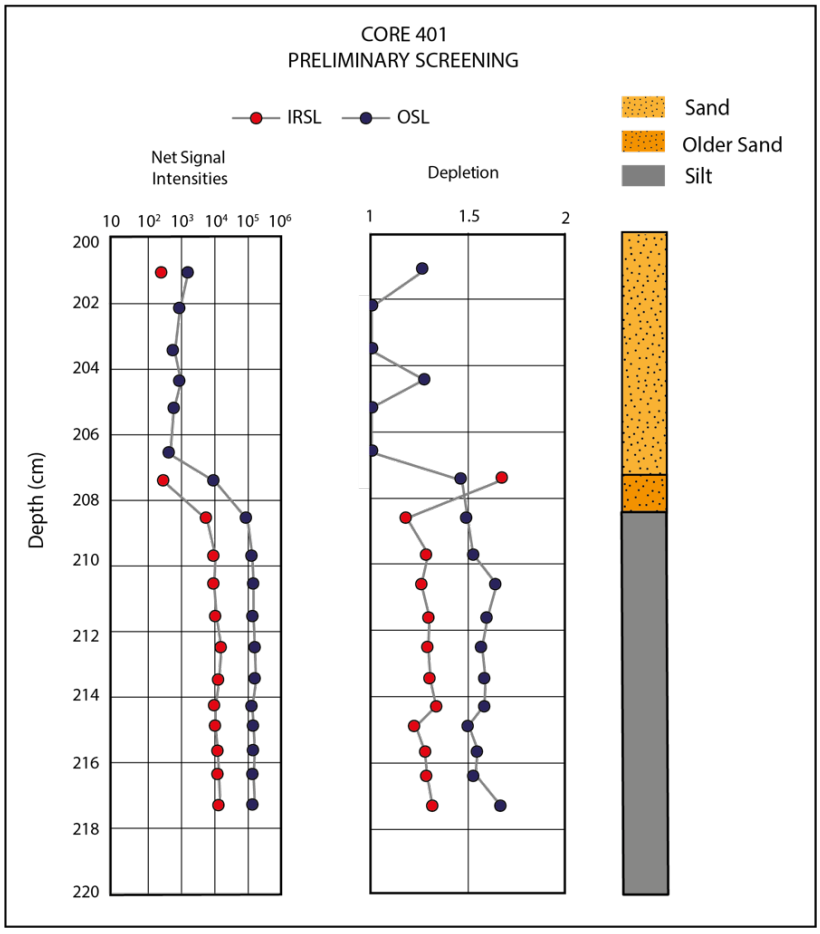

Figure 10. Preliminary Screening for Core 401 The graph to the left records net signal intensity measured in photon counts while the graph to the left portrays depletion indices. To the far left is an image depicting the lithostratigraphy of the core.

Excluding this sub-sample, the signals in the sand are more varied than in core **400**, ranging from 462 photon counts to 1,578 counts. The first silt sample (**401H**) registers a signal intensity 9 times higher than the sand sub-sample above it. The next two sub-samples, at a depth of 209.7 to 210.6 cm, gradually increase in OSL signal. The last eight sub-samples, from a depth of 211.6 to 217.3 cm have approximately the same signal, suggesting a rapid accumulation of sediment within this 5.7 cm section.

The IRSL signal is not registered at the top of the core **401** from 201.1 to 206.6 cm depth, but gradually increases with depth after the last sand sub-sample (207.5 to 217.3 cm depth). In core **401**, IRSL:OSL ratios average 0.02, which is lower than in core **400**. However, in both cores IRSL contribution is minimal.

The depletion indices of **401** are as low as those observed in core **400**. There is not a single sub-sample in core **401** with a depletion index over 2.0 which indicates that the sub-sample was bleached before deposition. However, it is clear from the signal intensities that the sediment is being bleached to zero when deposited on the sediment surface.

In summary, Core **401** shows a signal-depth progression that is consistent with normal age-depth progression. The sand is being bleached sufficiently as it travels across the sea floor, with the exception of the last sub-sample **401G**. Signal intensities from the silt increases with depth in the first three sub-samples, while the remaining eight register a similar signal intensity.

II.4.2.3. Isolated Marine Samples

There are two approaches to identifying artifact movement through OSL measurements from Maroni *Tsaroukkas*. The first approach requires silt beneath artifacts to have a higher signal than the first silt sub-sample in the core. This would infer that the artifact has been obscuring that silt from the sun. However, variation in OSL signal across the silt surface has not been categorized. Therefore, comparisons are only made to understand whether the signals from this environment are sufficient for further study. The second approach may help understand the accumulation of sand at different parts of the site through the sand samples that have signals higher than all the sand in the cores. The results discussed below are from the preliminary screening; in section II.5 these results will be compared to the calibrated results from the calibrated screening.

Of the five samples that were taken from underneath stone anchors or architectural blocks in the southeast sector of the site (Table 3), two were of silt (samples **399A** and **399C**). Both of these samples have OSL signals higher than the signal from the equivalent sediment layer in the core (the top sub-sample of silt in core **400)**. However, sample **399C** seems too high and sample **399A** may be too low to conclude that these samples indicate the anchors have not moved recently. Sample **399C** has photon count of 159,531 which is higher than all the silt in core **400**. This is one of the only samples to have a depletion index above 2.0, which may indicate it was well-bleached before deposition and not carrying any residuals from a previous bleaching event. This

Preliminary Screening						
Sample Number	IRSL Photon Counts	IRSL Depletion	OSL Photon Counts	OSL Depletion	IRSL/OSL	Significance / Comments
399A	12,430 ± 117	1.5	82,899 ± 290	2.1	0.15	Higher than core equivalent
399B	194 ± 37	1.5	3,032 ± 65	1.9	0.06	Higher than surface sand
399C	19,628 ± 145	1.5	159,431 ± 402	2.3	0.12	Higher than core equivalent
399D	98 ± 37	2.6	4,078 ± 73	1.7	0.02	Higher than surface sand
399E	-42 ± 39	0.1	1,396 ± 53	1.4	-0.03	Higher than surface sand
399F	-48 ± 36	5.0	566 ± 43	1.0	-0.08	Surface sand, much lower than sand samples from under artifacts
400H	5922 ± 84	1.2	66,679 ± 260	1.8	0.09	Silt surface in core

Table 3. Preliminary Screening Results for Southeastern Isolated Marine Samples The top sub-sample of silt from core **400** is also provided at the bottom for comparison.

may not indicate that the artifact has remained in place, but rather that the silt layer here has been eroded to expose older sediment before the anchor was deposited. Sample **399A** taken from the silt beneath a stone anchor, is 1.24 times higher than the first silt sample in core **400**. This suggests that the sediment below the anchor has not been exposed to light for 1.24x longer than the top of the silt in the core. Results from the calibrated screening (section II.5) and SAR protocol (II.6) will clarify these preliminary results. Additionally, samples **399B** (sand) and **399C** (silt) were taken from beneath the same anchor, and were collected to understand if the sand settling around the ridges of

the anchor is travelling with the same frequency as the surface sand. **399B** registers a small signal intensity of 3,032, which is much higher than the intensities from the surface sand samples (**399F** with 566 photon counts and **399J** with 319 photon counts).

From the southeastern sector of the site at a depth of 6 m, two of the three samples of sand taken from beneath artifacts meet the requirements of the second approach: their signal is higher than all the sand in the core. **399B** has a signal 5.5 times higher than the surface sand, but only a couple hundred counts higher than the sand of core **400**, which is not a significant difference. However, **399D**, from a depth of 6.0 m below sea level, is approximately 1.5 times higher than the sub-sample of sand in core **400** with the highest signal. It is difficult to use this to assume anything about the movement of the architectural block superposing the sediment. This is a complicated environment with many cobbles and boulders that allow sand to move beneath a stationary artifact. However, this signal does show the possibility for the preliminary screening to differentiate between signals of sands that are not bleached to the same degree. The higher signal intensity could indicate that sediments are collecting here and moving less frequently than in other parts of the site. The depletion index from the preliminary screening provides a value of 2.27 indicating that this sample was reset before deposition and has yielded a signal without residual luminescence.

From the northwest sector of site, at a depth of 2 m, most of the isolated samples of sand from beneath ceramics have OSL signals within the range of signals from core **401** (Table 4). **399K** is the only isolated sample of silt from this region, taken from underneath a ceramic storage jar base that was wedged next to a cobble. The silt it was

lying on top of has an extremely high signal intensity, 2.6 times higher than the highest signal in core **401**. It is exceptionally strange because the core was taken no more than 30.0 cm away from this sample. At the same sediment level (the top of the silt) within core **401** (the top of the silt), the sample from underneath the ceramic base is 43 times higher. This seems to be an anomaly, resulting from different mineralogical characteristics.

Northwestern Isolated Marine Samples						
Sample Number	IRSL Photon Counts	IRSL Depletion	OSL photon counts	OSL Depletion	IRSL: OSL	Significance/Comments
399G	--	--	--	--	--	No signal
399H	29 ± 34	3.1 ± 0.7	946 ± 46	1.1	0.03	Higher than surface sand
399I	--	--	1489 ± 55	1.1	-0.03	Higher than surface sand
399J	--	--	319 ± 42	1.1	-0.18	Surface Sand
399K	29201 ± 175	1.3 ± 0.02	457408 ± 679	1.8	0.06	Sample is much higher than compared core sample
401H	6008 ± 86	1.2 ± 0.03	100438 ± 319	1.5	0.06	Silt surface in Core

Table 4. Preliminary Screening Results for Northwestern Isolated Marine Samples. The top sub-samples of silt from core **401** is also provided in the bottom row for comparison. No IRSL signal intensities were detected for samples **399I** and **399J**, and no IRSL or OSL signal intensities were detected for **399G**.

The two samples of surface sand can provide some indication of what the photon count and OSL depletion indices look like for samples with more exposure to the sun. The samples came from a depth of 4.0 m (**399F**) and 2.0 m (**399J**) below the sea surface.

Sample **399F** has a photon count of 566, and **399J** has a photon count of 319. The lower photon count of **399J** corresponds to its shallow depth and better access to the sunlight. The photon counts correspond well to the sand in core **401**, but the photon counts of core **400** are in the 1000s. This could be an indication that residuals are carried at the increased depth of 4.0 m (core **400**).

In summary, preliminary screening using the portable OSL reader was able to distinguish (a) between modern sands which have recently moved (small signal intensities, moderate depletion indices), (b) the sediments that register geological doses (high signal intensities, low depletion indices), as well as (c) the artifacts that rest on sediment that may register archaeological doses (moderate signal intensities).

II.4.3.4. Terrestrial Samples.

The preliminary results of the archaeological section indicate that the first and third sample at 70.0 cm and 88.0 cm depth, respectively, remain close to 3,500 photon counts, with a spike in intensity in the second sample, reaching 63,000 photon counts (Fig. 11). This suggests that the first 14.0 cm, associated with what may be a collapsed wall, caused the sediment to become mixed. Samples **398C** and **398E**, from above and below a plaster surface at 88.0-95.0 cm depth, also remain close to 3,500 photon counts. These samples were of particular interest to identify a possible intact stratigraphic record from below the plaster surface. The signals of these two samples were quite similar, suggesting a short chronology, which is consistent with a destruction event. IRSL signal

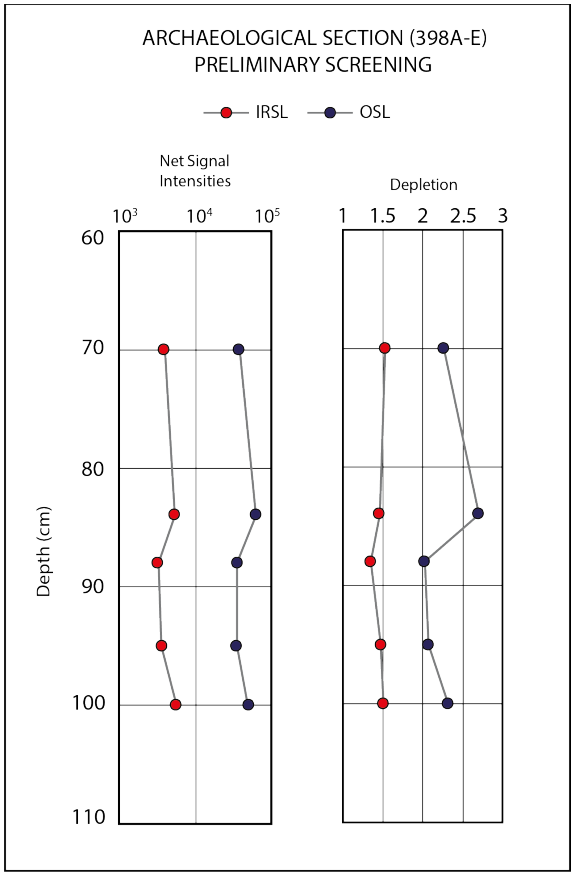

Figure 11. Preliminary Screening for Terrestrial Archaeological Section (398A-F**)**

intensity remained low, ranging from 3,246-3,894, with IRSL:OSL ratios averaging at 0.10.

The preliminary results of the environmental section show a spike in signal intensity from sample **398F** to **398G** (100.0 cm-117.0 cm depth), which reaches to 85,804 photon counts. The next two samples (**398H**-3**98I**), from 129.0 to 135.0 cm depth, remain in this range (71,880-92,678 photon counts). The last three samples (**398J**, **K**, **L**), from 135.0-179.0 cm depth, have a much smaller signal intensity from 45,031 to 36,094 (Fig. 12). The much higher signal intensities at the top of the stratigraphy

compared to the bottom suggest the possibility that grains exposed to the sun remain in the bottom samples.

Depletion indices are much higher than in the marine samples, with 42% registering a depletion index above 2.0, suggesting less residual luminescence. IRSL signal intensity also seems different from the marine samples, with a wider range signals (1,848-12,855), and with IRSL:OSL ratios averaging 0.12. This may be due to the

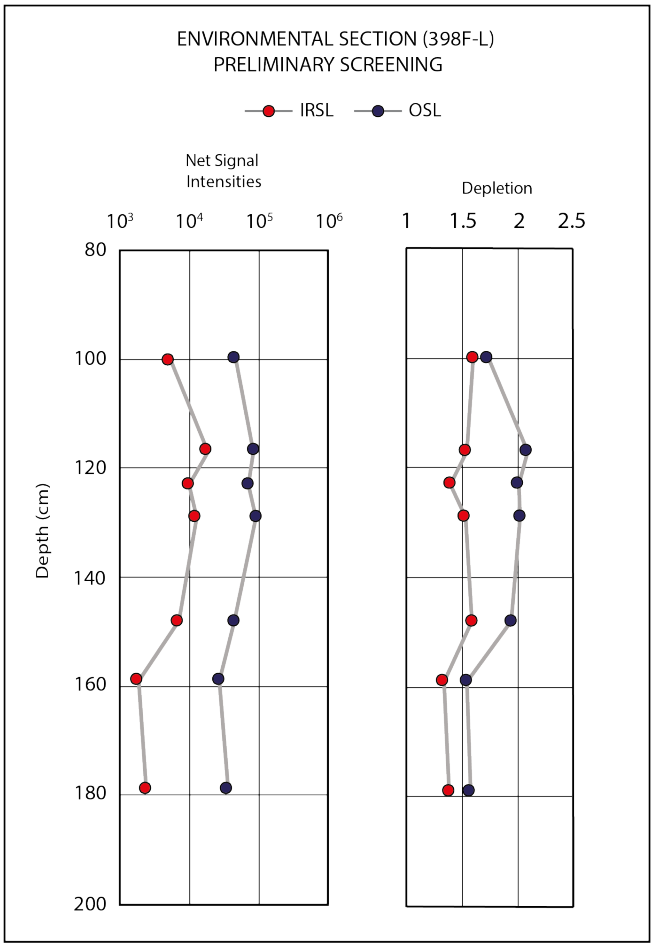

Figure 12. Preliminary Screening for Environmental Section (398G-L**)**

different sediment types on land and under water, and not better conditions. Both batches of terrestrial and marine samples seem to register useful signal intensities.

In sum, preliminary screening results of the terrestrial sections show that the archaeological section has relatively similar signal intensities, c. 35,000 photon counts, with spikes of 63,190 (at 84.0 cm depth) and 49,211 (at 100.0 cm depth). In the environmental section, signal intensities show signal-depth progression from 46,034-92,678 photon counts (100.0-135.0 cm). Below this, from 150.0-179.0 cm, signals begin to decrease from 45,031 to 36,094 photon counts. These lower samples were taken from a rockier environment, less of the outer surface could be removed, and less sediment was collected from between the cobbles, resulting in a lower signal intensity. These results will be calibrated in the next section with aliquots all of similar amounts of quartz (section II.5.2.5).

II.5. Calibrated Screening

II.5.1. Background and Methodology

Following preliminary screening, samples were subjected to mineral purification and analysis using the Risø TL/OSL DA-20 automated dating system.[103] In order to prepare the samples, sand-sized polymineral (90-250 μm) was extracted from the

[103] Equipped with a $^{90}Sr/^{90}Y$ β-source for irradiation (dose rate at time of measurement, 1.10 Gy/s), blue LEDs emitting around 470 nm and infrared diodes emitting around 830 nm for optical stimulation. OSL was detected through 7.5 mm of Huoya U-340 filter and detected with a 9635QA photomultiplier tube.

sediment by wet sieving.[104] Only half of each sample was sieved in order to leave some material for future testing. The polymineral fractions were then treated with 1 M hydrochloric acid (HCl) for 10 minutes to remove any organics, and chemically etched with 40% hydrofluoric acid (HF) for 40 minutes to remove the outer layer of the grains affected by alpha radiation. This was followed by a second treatment of 1 M HCl for another 10 minutes to remove any fluorides precipitated during the HF treatment which could luminesce. Thus, concentrates of quartz were prepared for all 62 samples. Two aliquots of HF-etched quartz were then dispensed onto the center of 10.0 mm stainless steel discs sprayed with a thin layer of silicone oil to aid adhesion. The Risø TL/OSL system is comprised of a radiation source (Co^{60}), stimulation collar, a heating unit, photomultiplier, and a carousel capable of reading 48 aliquots (Fig. 13). The cycle

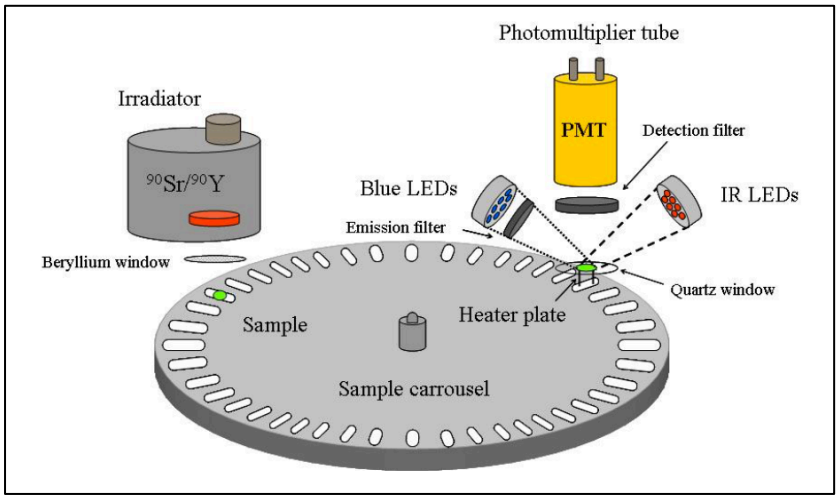

Figure 13. Organization of the Risø TL/OSL Reader (Image courtesy of DTU Nutech, Denmark, 2015).

[104] All samples are stored at the Luminescence Laboratory of St. Andrews University.

begins with a pre-heat at 220° Celsius for 10 seconds, the carousel then moves the sample under the light source and photomultiplier while temperature is maintained at 125° C as a blue LED light stimulates the sample for 60 seconds (readout). After the 'natural' cycle, the sample is given a test dose of approximately 1.0 Gy, followed by a pre-heat and readout. The test dose of radiation is used to monitor for sensitivity changes in the sediment.

The two aliquots of quartz, once measured, allow for an indication of the homogeneity of the sediment, and whether it was well or poorly bleached. The lowest signals will be used to draw conclusions about age, since it is more likely that an aliquot with a higher signal is carrying a residual signal from insufficient bleaching prior to burial.

II.5.2. Calibrated Screening Results

II.5.2.1. Thermal Stability and Bleaching Tests

Initial characterization tests were performed on a selection of samples to understand the thermal stability and bleaching characteristics of the quartz at Maroni *Tsaroukkas*. Thermal stability tests, or pulsed annealing tests, are used to select the ideal pre-heat temperature treatments for this sediment. This is needed because the aim of the SAR protocol is to recreate the natural OSL signal with a known dose of radiation. In order to do this, an ideal pre-heat temperature must be used that both (a) removes electrons that were not present in the natural signal, and (b) does not disturb those

electrons in the heat-sensitive traps that could not be bleached before re-deposition of the sediment.

Thermal stability tests involve cycles of pre-heat, irradiation and readout. The OSL signals were recorded at a range of temperatures between 100°C and 400°C, using a short stimulation (1 second at 10% power). The experiment was repeated after a nominal dose of 500.0 Gy to test repeatability.

Two aliquots of sample **398A** (terrestrial, compact, fine clayey sand from the archaeological section) were subjected to thermal stability tests. The quartz from **398A** is characterized by moderate to low sensitivities, and the burial dose is low; such that, the pulsed annealing curve is poorly constrained and not displayed in the graph. However, the natural OSL signal shows some stability through 100°C to 200°C, with a suggestion of some thermal transfer between 150°C and 200°C. From 200°C the signal is depleted as the temperature is increased. The regenerated signal steadily declines with increased temperature, decreasing more rapidly after 200°C, and is depleted entirely after 300°C (Fig. 14). A pre-heat between these two temperatures for the SAR protocol would suffice.

The second characterization was undertaken to assess the response of the Maroni *Tsaroukkas* quartz to stimulation with light. These bleaching experiments were performed in the Risø TL/OSL reader, using a small aliquot procedure: irradiation, 'stimulation' using the blue LEDs, preheat, and OSL readout. For each cycle, the length of time the sediment was bleached was increased by intervals of 1, 10, 100, 1,000, and

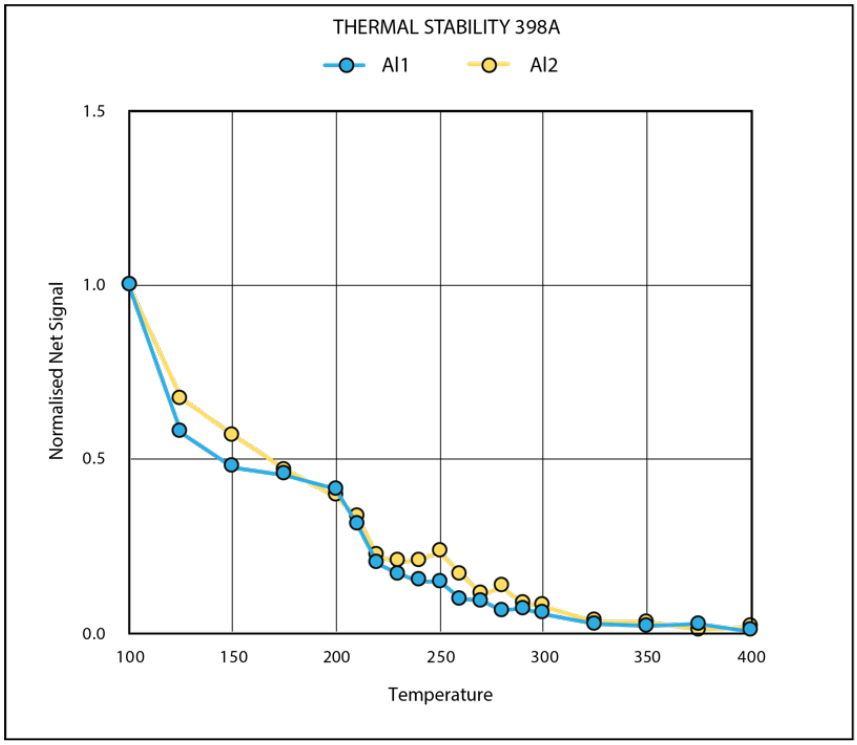

Figure 14. Regenerative Thermal Stability in 398A Natural signals have been left off the chart as they obscure comparison.

10,000 seconds. Sensitivity changes were monitored using a test dose of approximately 1.0 Gy. The OSL signals from each cycle were normalized to their subsequent test dose. The first bleaching test was performed on samples **398F** and **398L** (Fig. 15). Both of these samples are terrestrial samples from the environmental beach scarp. Sample **398F** is from the top of the scarp consisting of a compact light orange- beige clayey sand. **398L** is from the bottom of the scarp consisting of a dark grey-orange sand and many small cobbles. The bleaching test shows that the sediment is bleached quickly after 100 seconds.

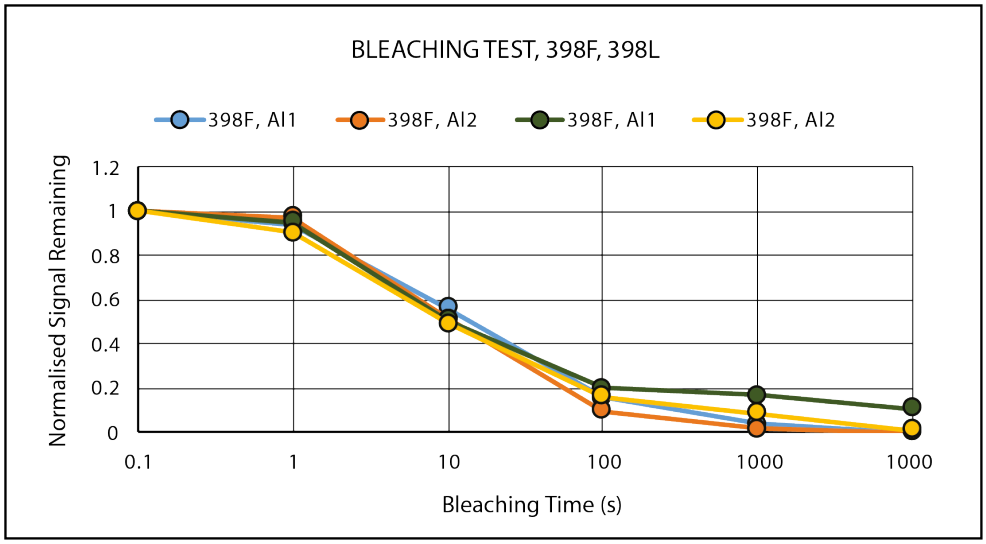

Figure 15. Bleaching Test for Samples 398F **and** 398L

The second bleaching test was performed on marine samples: two aliquots of **399A**, one of **399F,** and **399H** (Fig. 16). Sample **399A** is silt from underneath an anchor, **399F** is surface sand and **399H** is sand from beneath a ceramic sherd. This time, samples **399H** and the second aliquot of **399A** were entirely bleached within 10 seconds. Samples **399F** and the first aliquot of **399A** were bleached in 100 seconds.

These tests show that the 'fast component' of the OSL signal was removed during the first 100 seconds of exposure. However, in regards to the bleaching test, it is important to remember that sediment in the environment is not spread out in a thin layer on a tiny stainless-steel dish and the resulting sample will not exhibit electron depletion in a quick, even manner.

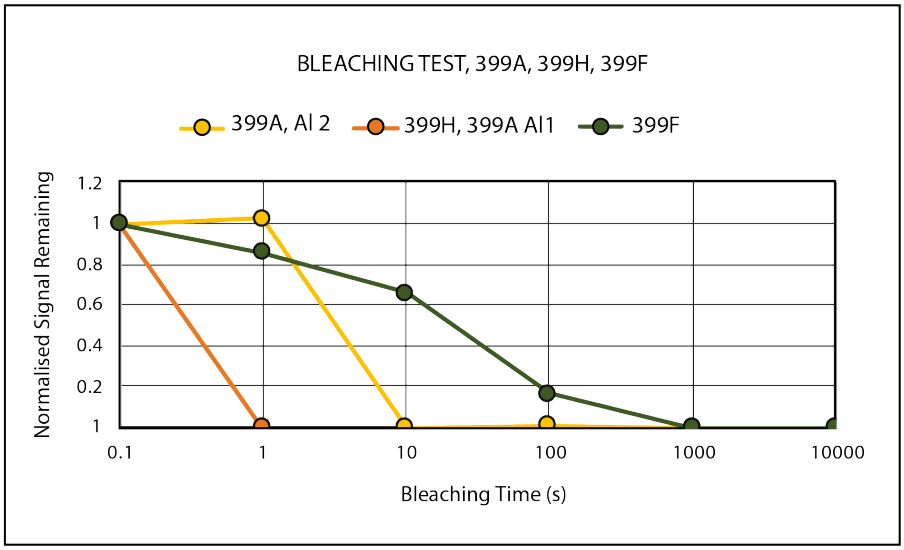

Figure 16. Bleaching Tests for Samples 399A**,** 399F **and** 399H

II.5.2.2. Core **400**

The calibrated screening results for core **400**, taken from the southeastern sector of the site, indicate a very slight signal-depth progression in the silt. The sand in core **400**, from 406.6 to 416.5 cm depth, has stored dose estimates that remain consistently low, fluctuating around zero. This implies that the approximately 10.0 cm of sand was frequently in motion (Fig. 17). From the silt between 418.0 cm and 427.9 cm depth in core **400**, many aliquots have error values more than 20% of the stored dose. This resulted in the removal of five samples from the graph (**400H**, **400J-M**). Additionally, sample **400Q** at 431.9 cm depth was also removed due to high errors. The paired aliquots of the sample from the top layer of silt (**400H**) also have high error values (21% and 71%). However, since aliquot one, with a stored dose of 12.4 Gy, has the smallest error value within the top of silt, it is included for the purpose of comparison with the

isolated marine samples from beneath artifacts. Due to the low number of surviving aliquot pairs, the smallest stored doses are presented in the graph in order to identify the best stratigraphic trend. Within those silt samples with acceptable error values, stored

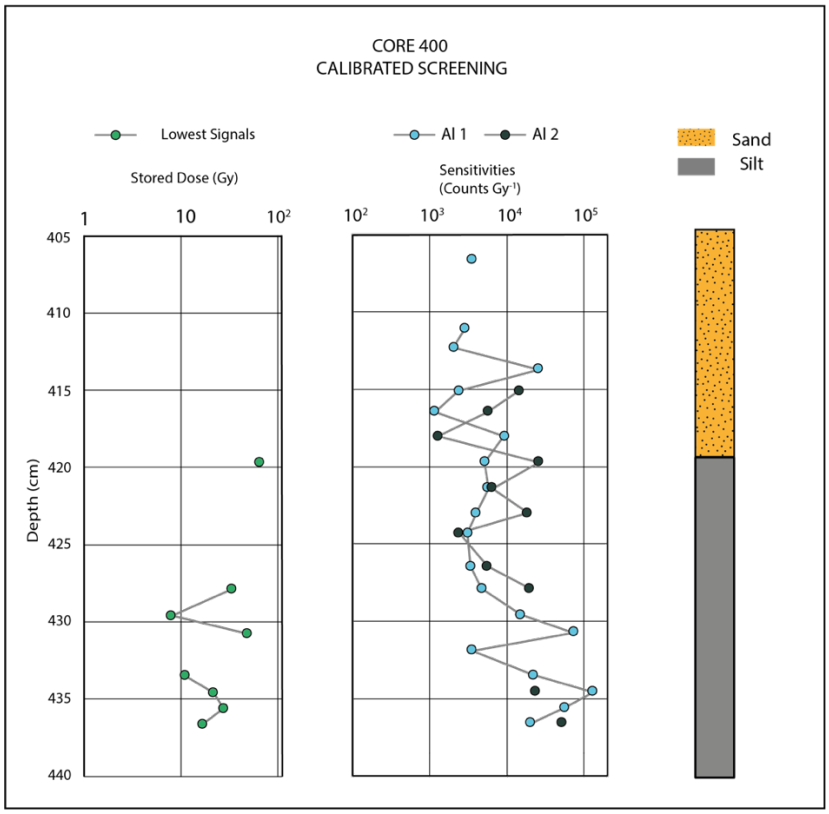

Figure 17. Calibrated Screening for Core 400 The graph to the left records the lowest stored doses from paired aliquots (measured in grays) while the graph to the left portrays sensitivity measured in photon counts per gray. To the far left is an image depicting the lithostratigraphy of the core.

dose values fluctuate between c. 8.1 and 33.8 Gy, with spikes of 49.9, 67.4, and 103.5 Gy. These figures reflect a large scatter implying poor bleaching conditions at deposition. The results for core **400** suggest that the sediment has a heterogeneous

sensitivity distribution, with few grains able to carry a bright signal, and the majority characterized by dim signals.

Sensitivity values are heterogeneous throughout the core, but can be divided into three separate sections. Sensitivity values of the sand, from 406.6 to 416.5 cm depth, range from 116 to 1,432 Gy^{-1}, with one large outlier at 2,597 Gy^{-1} (average of 723 Gy^{-1}). The top section of silt underneath the sand from 418.0 cm to 429.6 cm depth with sensitivities ranging from 127 to 1,970 Gy^{-1} (average of 870 Gy^{-1}). From 430.8 cm to 436.6 cm within the core has sensitivity values ranging from 355 to 13,291 (averaging 12,779 Gy^{-1}). It seems that the sediment at the bottom of the core likely has a different provenance.

In sum, core **400** presents challenges to OSL dating in the form of samples with a mix of bleached and unbleached grains, and grains with sensitivities too low to register an OSL signal. Despite this, sensitivity values effectively separate core **400** into three distinct sections: (a) the sand with low sensitivity, (b) the top 11.6 cm of silt with moderate sensitivity, and (c) the bottom 5.9 cm with high sensitivity values.

II.5.2.3. Core **401**

Core **401**, which was taken from the northwestern sector of the site, produced stored doses that cannot be considered in the final results. The first silt sub-sample (**401H**) must be discounted due to high error values and sensitivity below 100 Gy^{-1}. Therefore, the top of the silt was assigned about 1.0 cm lower at sub-sample **401I**. This sub-sample has a mean signal of 41.5 ± 6.2 Gy, and sensitivity well above 100 Gy^{-1},

implying a more accurate reading. For the same issues of high error above 20% of the signal, sub-samples **401B**, **401D** and **401G** have also been removed.

The sand from 201.10 to 207.5 cm below sea level are characterized by stored dose values that fluctuate around zero, implying that this sand is in frequent motion. The top section of silt from 209.7 to 214.9 remains in a signal range between approximately 40.0 and 50.0 Gy (Fig. 18), while the last 1.7 cm (sub-samples **401P-401R**) have much higher signal intensities, ranging from 761.4 Gy to the last sub-sample with signals of

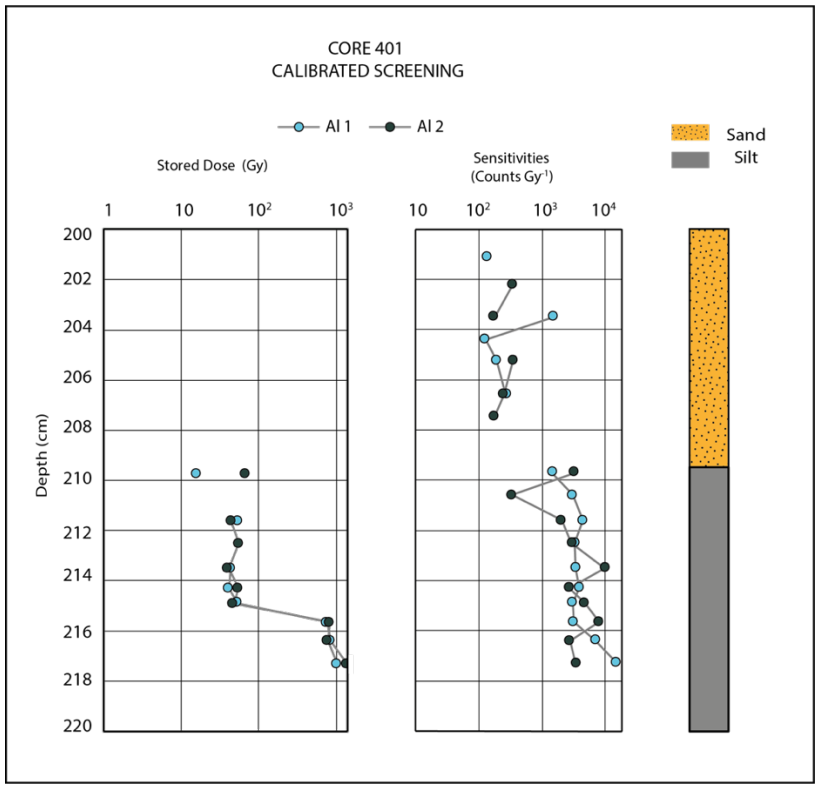

Figure 18. Calibrated Screening for Core 401 The graph to the left records stored doses (measured in Grays) while the graph to the left depicts sensitivity measured in photon counts per Gray. To the far left is an image depicting the lithostratigraphy of the core.

1356.6 Gy and 1031.8 Gy. The silt is therefore characterized by two units: an upper unit between 209.7 and 214.9 cm with stored doses progressing in sync with depth through 15.4-47.6 Gy and a lower unit, from a depth of 215.7-217.3 cm, with stored doses in excess of 828.4 Gy. Because the fast OSL component of the signals in this second unit are saturated, and these dose estimates correspond to ages beyond anthropogenic activity, putting them out of the realm of the present investigations, these were not explored further. There was concern that since this core was only approximately 17.0 cm in total length, there would not be enough material to provide information about the site, but this depth seems to be the maximum range of legible stratigraphy in this area.

There is a clear difference in the sensitivity range of the sand and the silt. The sand (top 6.4 cm) ranges from 128-349 Gy^{-1}, with an outlier of 1,528 Gy^{-1}. The silt (bottom 7.6 cm) ranges from 1,444 to 15,306 Gy^{-1}, with an outlier at 332 Gy^{-1}. As in core **400** there are a lot of mixed sediments, but in general, the sensitivities do represent a difference in luminescence behavior between the two main sediment types.

In summary, cores **400** and **401** indicate a relatively simple sediment stratigraphy: 6.4-9.9 cm of modern, mobile sand and over 18.6 cm of silt. The modern sands share similar luminescence behaviors: fluctuating around zero with a max stored dose of 0.6 Gy. The silts are characterized in both cores by higher stored doses ranging from 12.4 Gy to 103.5 Gy. The magnitude and range in stored dose values observed for the silts in cores **400** and **401**, indicate that the 'chronologies' differ, with silts in core **401** representing a longer preserved stratigraphy.

II.5.2.3. Isolated Marine Samples

Of the 11 isolated samples taken underneath artifacts, only one (**399A)** produced a signal without error values above 20% (Table 5), indicating the majority of samples have low sensitivities. The calibrated results for sample **399A**, taken from silt beneath an anchor, provided a stored dose value of 31.3 Gy. This is 2.5 times higher than the comparative sub-sample in core **400**. Sample **399C**, taken from silt beneath a stone anchor in the

Calibrated Screening					
Artifact and Sediment	Sample Number	Depth Below Sea level (cm)	Mean OSL Stored Dose (Gy)	Mean Sensitivity Counts (Gy^{-1})	Comments/ Significance
Silt from Anchor	**399A**	300.0	31.3 ± 6.2	591 ± 34	Higher than silt surface in core
Sand from Anchor	**399B**	450.0	--	--	
Silt from Anchor	**399C**	450.0	118.8 ± 72.8	92 ± 10	
Sand from Block	**399D**	600.0	--	--	
Sand from Anchor	**399E**	300.0	0.9 ± 2.9	150 ± 17	
CORE	**400H**	418.0	12.4 ± 2.6	518 ± 32	Silt surface in core
Surface Sand	**399F**	300.0	--	--	
Sand from Ceramic	**399G**	200.0	--	--	
Sand from Ceramic	**399H**	200.0	0.02 ± 1.4	118 ± 11	
Sand from Ceramic	**399I**	200.0	--	--	
Surface Sand	**399J**	200.0	0.2 ± 0.2	519 ± 23	
Silt from Ceramic	**399K**	200.0	35.9 ± 15.3	769 ± 39	

Table 5. Calibrated Screening Results for Isolated Marine Samples Taken from the southeastern and northwestern sectors of site. The top sub-sample of silt from core **400** is listed as well. The sub-sample of silt from core **401** is not listed since there are no signals from the northwestern sector to compare to. Stored doses highlighted in pink have errors above 20%.

southeast sector of site, did not produce a viable signal from the calibrated screening of its two aliquots. Error values were above 20% of the stored dose, and sensitivity values were below 100 Gy^{-1}.[105]

The preliminary screening results identified samples **399A**, **399C**, **399B**, **399D** and **399K** as having signals higher than their comparative samples in core **400** and **401**. Samples **399C, 399B**, **399D** and **399K** did not produce signals that agreed with the preliminary results. The two screening methods did agree with sand samples **399E-399J**. In the preliminary screening these samples had very small signal intensities (319-1395 counts), and in the calibrated screening, these samples did not register a signal.

The calibrated screening results are similar to the preliminary screening results only in sample **399A**. The conclusion is, therefore, that **399A** may indicate that the silt from beneath the corresponding anchor has not seen the sun as recently as the silt exposed by the movement of sand.

II.5.2.4. Terrestrial Samples

The calibrated screening results for the first sample in the archaeological section (**398A**) at a depth of 70.0 cm below the top of the scarp, produced a higher stored dose (10.4 Gy) compared to the other samples in that section, suggesting mixed sediment (Fig. 19). The

[105] 24 other aliquots of this sample went through the cycles of the SAR protocol and these aliquots had a higher sensitivity and better results. These will be discussed further in section II.6.2.

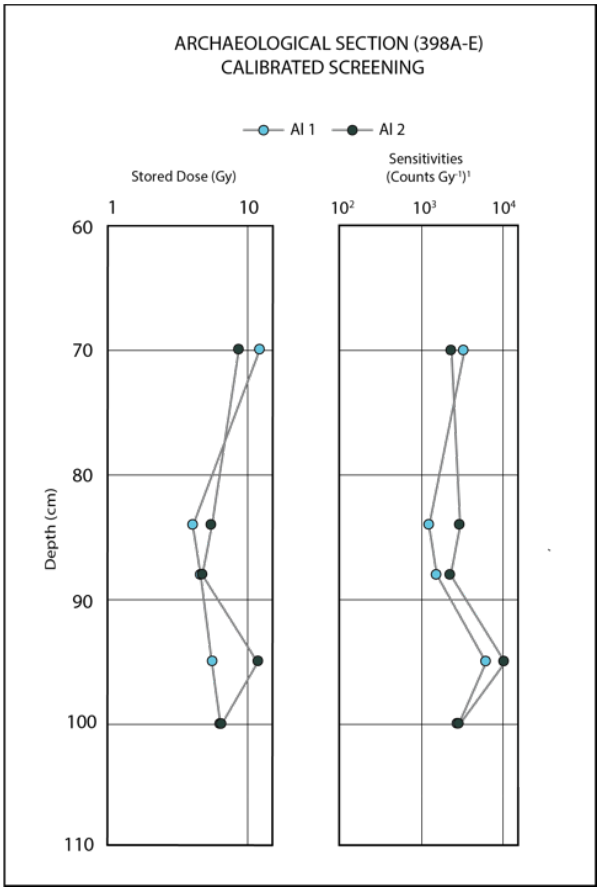

Figure 19. Calibrated Screening for Terrestrial Archaeological Section (398A-E**)**

remainder of the section (**398B-398E**), from 84.0 cm to 100.0 cm have signals progressing slightly with depth, from 4.1 Gy to 6.5 Gy. The average sensitivity measurements between the pairs of aliquots range from 1,922 to 2,881 Gy^{-1}. However, sample **398D** presents an intriguing spike in sensitivity with an average of 8,319 Gy^{-1}. One interpretation of this spike could be a fire in the area, which exposed the quartz to high temperatures and caused an increase in sensitivity.

The calibrated screening for the environmental section was not able to detect a signal from samples **398G** or **398H** at a depth of 117.0 to 129.0 cm below the top of the

scarp. Sample **398G** was collected from the chalk stratum, which yielded a small amount of quartz to be read for OSL (Fig. 20). **398H** on the other hand was taken in the stratum below of orange clayey sand. It is possible this sample contains contamination from the surface that was not properly removed, resulting in bleached grains within the aliquots. The next samples **398F** and **398I**, 135.0 to 150.0 cm below the top of the scarp, also seem to be mixed due to the range in stored doses between the paired aliquots (24.6-76.6 Gy, and 19.5-59.6 Gy). The last three samples **398J**, **398K**, and **398L** have less variance

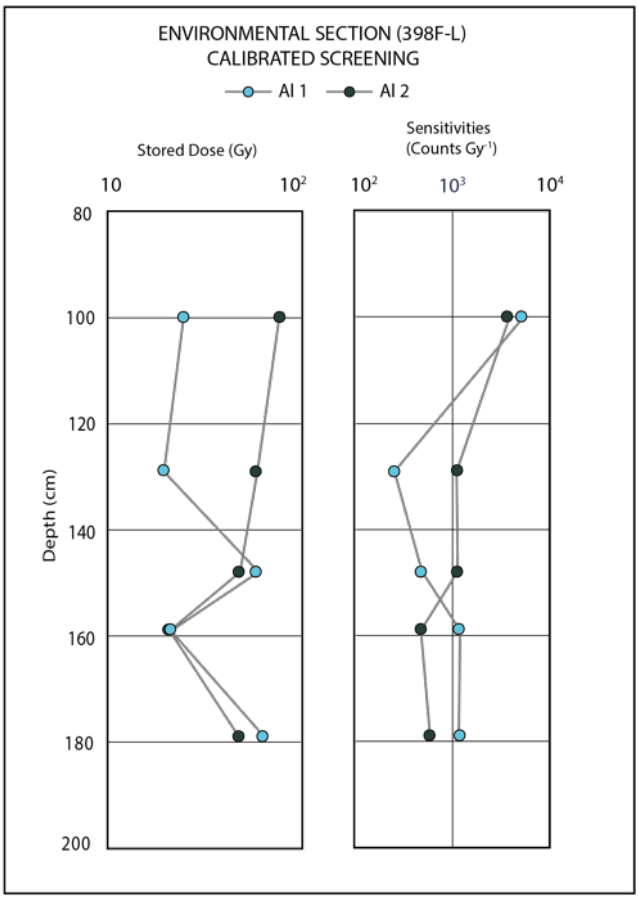

Figure 20. Calibrated Screening for Terrestrial Environmental Section (398G-L)

between paired aliquots and the results from the calibrated screening are similar to the preliminary results. A signal-depth progression can be seen in the lowest signals from the paired aliquots: from 100.0-135.0 cm signals remain close to 20.0 Gy, while from 150.0-179.0 cm the majority of stored doses are approximately 47.0 Gy, with one anomaly at 165.0 cm (**398K**) which registers an average stored dose of 21.0 Gy. Sensitivity values remain in a consistent range between paired aliquots, from the lastfour samples at a depth of 135.0-179.0 cm, each sample has a range from approximately 400-1,200 Gy^{-1}.

In sum, slight signal progression with depth can be observed in both the environmental and archaeological sections. The archaeological section registers archaeological doses, c. 4.0-6.0 Gy, with some collapsed surface reworked at the top (c. 8.0 Gy). In the environmental section with clear geological strata present, a signal-depth progression is seen from c. 20.0 to 47.0 Gy. It is clear that mixed sediment is present in the samples, probably from the outer surface of the scarp that was not fully removed. This is a consistent problem throughout the samples, and yet signal progressions can still be understood. In comparison to the marine samples, terrestrial samples hold more sensitivity and a larger IRSL contribution (seen in the preliminary screening).

II.6. SAR

11.6.1. Background and Methodology

The Single-Aliquot Regenerative-dose (SAR) OSL protocol is used to determine equivalent dose.[106] The equivalent dose is one part of the luminescence age equation. Each aliquot is subjected to cycles of irradiation, pre-heat, and readout. The administered regeneration doses increase with each step in the SAR cycle. The test dose (approximately 1.0 Gy) is administered after each regeneration cycle. The first cycle determines the natural signal, followed by the test dose, the sequence looks like this: pre-heat to 260°C, readout of OSL at 125°C, irradiate to 1.0 Gy (test dose), preheat to 260°C, readout of OSL at 125°C. The latter cycles, to determine regeneration doses, follow the same sequence of preheat and OSL measurement, but follow increasingly higher dose administration: 2.5, 5.0, 10.0, and 30.0 Gy. The test dose after each regenerative dose measurement remains consistent at 1.0 Gy, in order to monitor changes in sensitivity. When sensitivity changes occur during these cycles, the signal is corrected using the results from the standardized test dose. Once corrected, results can be used to estimate the equivalent dose.

There are three additional cycles in the SAR protocol sequence: zero dose, repeat dose and IRSL dose. A zero dose cycle bleaches the aliquots without irradiation to monitor if there is any transfer from heat-sensitive traps to light-sensitive traps. A repeat dose performs the first regeneration cycle (2.5 Gy) for a second time to check the

[106] Murray and Wintle 2000, 57.

consistency of the SAR protocol. Finally, an IRSL dose (2.5 Gy), records any response from IR-sensitive minerals.[107]

Further mineral purification procedures were undertaken to prepare the samples for SAR OSL analysis. First, the grains were separated by density using Lithium Sodium Tungsate (LST) heavy liquids of the densities 2.64 gcm^{-3} and 2.74 gcm^{-3}. This is done in order to separate feldspars from quartz. The 90-250 μm grain fractions that have already been chemically etched (as outlined on pp. 53-54) are first placed into a vial with 2.64 gcm^{-3} heavy liquid. Feldspars float at this density and are collected. The grains that sink are then collected and submerged in 2.74 gcm^{-3} heavy liquid. The grains that float in this liquid are the quartz grains that are collected for sampling. These grains are rinsed with de-ionized water and dried before being sieved into grain fractions of 90-150 μm and 150-250 μm. The processed grains are then dispensed into 24 aliquots, divided between the two grain fractions, adhered to 10.0 mm stainless steel discs with silicone oil spray in the same method used to dispense aliquots for the calibrated screening (outlined on p. 59).

Due to the Covid-19 pandemic that ravaged the globe in 2020, laboratories worldwide have closed and the Inductively Coupled Plasma Mass Spectrometry (ICP-MS) tests needed to identify the elements within the sediment could not be conducted.[108]

---

[107] Roberts et al. 2015, 46; Murray and Wintle 2000, 58.
[108] Worldwide measures to contain the spread of the virus began in March 2020. Prevention included removing all personnel from many laboratories. The St. Andrews Isotope Geochemistry laboratory where the ICP-MS analyses were meant to be conducted, had not reopened in time for the results to be included in this thesis.

This information is needed to calculate the "dose rate", or the level of radioactivity in the sediment. However, since 24 aliquots from each sample have been tested in much the same way as the calibrated screening, the additional stored dose determinations can fill in any blanks, or provide more context to the calibrated results.

II.6.2. SAR Results

The SAR protocol was performed on samples **399A**, **399C**, **399D** and **399F**. These four samples were chosen to represent the range of sediment on site, in an effort to focus on samples taken to recognize artifact movement. **399A** and **399C** are samples of silt from beneath anchors, **399D** is of sand from beneath an architectural block, and **399F** is a sample of surface sand. The 24 aliquots of each sample provide a clearer understanding of the range of signals in the sediment. It has already been stated that the sediment grains are a mix of those that have been bleached (low signal) and those that are carrying residual luminescence (high signal) from prior deposition periods. The aliquot of **399A** with an acceptable error value dispensed for calibrated screening provided a stored dose of 31.3 Gy. The SAR protocol was able to recover a signal from 19 of 24 aliquots for **399A**, however there are only five of these aliquots with error values below 20% (Table 6). From these five aliquots, the sample has an average of 27.7 Gy, with a low of 2.4 Gy and a high of 50.7 Gy. From the calibrated screening results **399A** was highlighted as a sample with a higher signal than the top layer of silt in core **400** (14.9 Gy), which may indicate that the anchor sitting above has been in place obscuring the sediment for a while. The SAR results provide a little more certainty for

399A		
Aliquot Number	Stored Dose	Error %
3	50.7 ± 3.54	7.0
4	26.6 ± 4.72	17.8
6	0.7 ± 0.39	57.5
7	0.3 ± 0.57	192.1
8	6.3 ± 2.67	42.4
9	2.4 ± 0.41	17.0
10	7.0 ± 3.54	50.2
11	21.7 ± 14.37	66.2
12	46.2 ± 7.68	16.6
14	61.2 ± 15.05	24.6
15	37.7 ± 10.20	27.1
17	26.3 ± 9.07	34.5
18	4.9 ± 1.04	21.3
19	12.8 ± 2.21	17.3
20	0.9 ± 0.40	44.0
21	98.9 ± 53.35	53.9
22	26.9 ± 6.49	24.1
23	8.0 ± 5.51	69.2
24	29.5 ± 31.09	105.5

Table 6. SAR Results for Sample 399A This sample was collected from silt beneath an anchor on the northeastern part of site. 19 out of 24 aliquots produced signals. with error values above 20% are highlighted in pink.

this hypothesis. The majority of aliquots (3 of 5) have a signal higher than the equivalent silt sample in the core. Tentatively, we can conclude that the silt beneath this anchor has not seen the sun as recently as the top layer of silt in core **400**.

The calibrated results also produced a higher OSL signal for sample **399C** (118.8 Gy) than the equivalent sample in the core (14.9 Gy), but a very high error of ± 72.8 Gy meant these OSL measurements had to be discarded. The SAR results are once again very mixed (Table 7). Out of 24 aliquots, a signal was detected from 15, but only four of these 15 aliquots have an error below 20%. The four aliquots provide a mean of 16.7 Gy,

with a low of 3.6 Gy and a high of 46.0 Gy. This is a much different result than the calibrated screening. The majority of the aliquots (3 of 4) have a signal below that of the

399C		
Aliquot Number	Stored Dose (Gy)	Error %
2	8.7 ± 2.7	30.9
4	11.7 ± 0.9	7.7
5	0.8 ± 0.6	68.9
6	0.5 ± 0.5	111.1
7	4.6 ± 2.2	46.4
8	1.7 ± 9	523.3
9	8.5 ± 6.9	81.7
13	46.0 ± 5.5	11.9
14	14.9 ± 5	33.2
15	3.6 ± 0.4	12.0
16	7.4 ± 2.1	27.8
17	18.1 ± 10	54.5
20	18.4 ± 8.5	46.0
23	18.4 ± 5.8	31.5
24	5.6 ± 0.8	14.4

Table 7. SAR Results for Sample 399C This sample was collected from the silt beneath an anchor in the northeastern part of site. 15 aliquots out of 24 produced signals. Those with error values above 20% are highlighted in pink.

equivalent sub-sample within core **400**. The silt beneath this anchor seems to have seen the sun more recently than the top of the silt in core **400**.

Sample **399D** was collected from sand beneath an architectural block. Only two of the 24 aliquots produced a signal (Table 8). However, neither of these produced a signal with an error below 20%. This result agrees with the results of the calibrated screening which did not register a signal for **399D**. However, the preliminary screening

399D		
Aliquot Number	Stored Dose	Error %
8	13.6 ± 4.9	36.1
17	1.1 ± 31.7	2772.2

Table 8. SAR Results for Sample 399D This sample is of sand from beneath an architectural block in the northeastern part of site. Only two of 24 aliquots produced signals from this sample and both error values are above 20%.

registered a signal higher than the sand in the core. This is because sensitivity of the quartz is not high enough to produce a signal through calibrated screening and the SAR protocol, as only a few grains are carrying the signal (which are detected by the portable unit). Two interpretations can be drawn for this sample: (a) sand is accumulating in this rocky area and not moving as frequently as the sand in the core, or (b) this sample came from a depth of 6.0 m and may not be exposed to enough sun to bleach the sample as thoroughly as the 4.0 m sand sample. More samples from this depth must be taken in order to understand how the sediment is bleaching.

Sample **399F,** taken from the surface sand under water at a depth of 4.5 m also went through the SAR protocol (Table 9). Out of the 24 aliquots, four aliquots contained

399F		
Aliquot Number	Stored Dose	Error %
5	0.1 ± 0.6	1197.8
6	4.9 ± 3.5	70.6
15	3.8 ± 51.4	1363.2
22	8.9 ± 10.9	122.8

Table 9. SAR Results for Sample 399F Surface sand is collected in this sample. Only four aliquots produced a signal and all have very high error values.

a stored dose, but all had an error above 20%. This makes good sense for a sample of sand that is actively exposed to the light.

The equivalent dose is determined in each aliquot by finding where the natural signal intersects with the curve constructed by the regenerated signals.[109] The results from all the aliquots are displaying in a histogram plot to view the distribution and signal intersects with the curve constructed by the regenerated signals.[110] The results from all the aliquots are displaying in a histogram plot to view the distribution and determine a density probability which instructs the equivalent dose determination for the sample. This was done for samples **399A** and **399C** (Fig. 21). The equivalent dose for

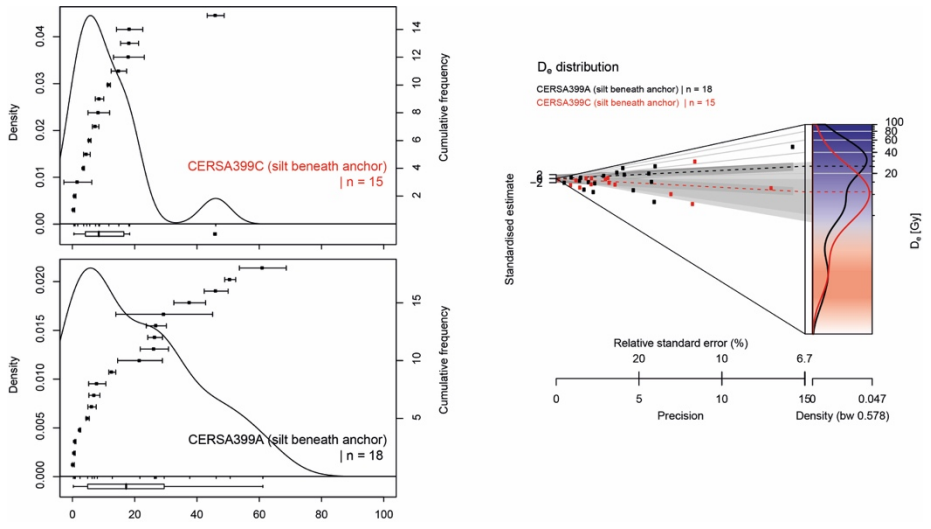

Figure 21. Equivalent Dose Determinations are displayed in a Kernel Density Estimate plot (left) and a combined Abanico plot (right), which combines a radial plot and histogram plot. Towards the left the density of equivalent dose values are extended. If these values were to fall towards the red section at the bottom, they would be more likely to carry archaeological doses. (Image courtesy of Timothy Kinnaird).

[109] Murray and Wintle 2000, 61.
[110] Murray and Wintle 2000, 61.

sample **399A** is 18.0 Gy and for **399C** it is 15.0 Gy. Neither sample is estimate to match archaeological ages but show that the SAR method to derive equivalent dose is applicable to the samples from Maroni *Tsaroukkas.*

II.7. Conclusion

Isolated marine samples, marine cores and terrestrial samples were collected at the ancient anchorage of Maroni *Tsaroukkas* in order to experiment with OSL measurements at an underwater site. The anchorage provided a promising set of OSL results to work towards answering questions about (a) the possibility to gain useful information using preliminary OSL screening, (b) artifact movement, and (c) the categorization of stratigraphy on the seabed. The 62 samples underwent preliminary screening with the SUERC portable OSL reader, calibrated screening with the Risø TL/OSL reader, and the SAR protocol (used to produce a series of regenerative signals to calculate the equivalent dose needed to determine the age of the sediment). Though there were issues of mixed sediment in samples and a lack of bleaching, secure readings and patterns of sediment deposition were still extracted from the data.

The SUERC portable OSL reader is used to characterize signal intensities, and understand if sediment is carrying residual luminescence signals from prior periods of burial. This is often performed in the field to locate suitable sediment for dating. In this case study, preliminary OSL measurements with the portable OSL reader and calibrated results were derived in the laboratory. Details are not expected to be similar from both

methods, but general trends can be seen between both screenings: (a) the signal-depth progression for core **400** is only slight, while for core **401** it is normal, and (b) samples collected from beneath artifacts could generally be categorized by high, moderate and low signals.

Toward the goal of understanding artifact movement on underwater sites, the comparison between the isolated marine samples the sub-samples of the same sediment layer within the cores presented promising results. Nine isolated samples were taken from beneath artifacts, three of silt, and six of sand. Preliminary and calibrated screening results concluded that the sand samples held no signal, and were in frequent movement, as is expected. This left only three isolated silt samples to compare to the core sub-samples, two of which yielded promising signals. **399A** remained consistently higher than the comparative sub-sample in core **400** from the same area. **399C** was not consistent between the preliminary and calibrated screenings, but the 24 aliquots measured during the SAR protocol produced signals lower than the same sediment layer within core **400**. Although the variation of the top layer of silt on site is not well understood, it is fundamentally promising that these results were able to register signals for comparison. Additionally, the preliminary screening was able to discern between sand samples with small and moderate intensities, informing the frequency of sand movement around and under artifacts. The identification of one artifact that has remained in a position longer than another (has been blocking the sun from reaching dense sediment longer than another), and the frequency of sediment movement, is not

commonly made through visual determinations in the field, but may be possible through OSL measurements.

Finally, it was promising to acquire a basic understanding of the submerged stratigraphic record on site using small cores less than 30.0 cm long. This experiment provides insight into how OSL can differentiate between layers of sediment created in an amount of time much shorter than the geological time frames OSL determinations are commonly used for. However, OSL measurements acquired from cores on underwater sites will still often represent a longer time period than that reflected in the archaeological record. The stratigraphic record of site like the anchorage at Maroni-*Tsaroukkas* can be understood via the isolated samples, and the sand and top layer of silt in the core. OSL measurements from these samples have provided two pieces of information: (a) that entire approximately 10.0 cm of sand is in frequent movement and registers not OSL signal, and (b) the silt beneath artifacts and from the top silt layer of the cores registers a variable signal (ranging from 12.4-41.5 Gy) despite frequent movement of the sand above.

CHAPTER III

CONCLUSIONS AND NEXT STEPS

III.1. Summary of the OSL Sampling Program

In June 2019, I joined the underwater survey attached to the Kalavasos and Maroni Built Environments Project to sample two areas of the anchorage at Maroni *Tsaroukkas*, Cyprus, for optically stimulated luminescence (OSL) determinations. These measurements were performed to test the application of OSL on an archaeological site under water. Terrestrial excavations use OSL determinations to understand whether layers of sediment exhibit age progression with depth, or have disturbances. This in turn allows researchers to determine whether artifacts within these disturbed layers are the result of sedimentary processes or anthropogenic activity. The use of OSL provides the unique ability to characterize sediment movement and pinpoint disturbances because it can determine the last time sediment was exposed to the sun (i.e. redeposited). With storm, current, wave, and human activity affecting underwater sites, submerged artifact assemblages can be affected without clear signs of such. OSL analysis of stratigraphic sequences and samples from beneath artifacts permit conclusions about artifact movement and the environmental history at underwater and terrestrial sites alike.

The anchors at Maroni *Tsaroukkas* are spread over 225.0 m x 200.0 m area of accumulated cobbles and sand atop the silty sea floor. However, to the northwest approximately 20.0 m from shore, there are fewer anchors, and a large assemblage of Late Bronze Age ceramic sherds. Anchors and ceramics lie atop layers of sand, cobbles

and silt. In the southeast corner of the anchorage, at a depth of approximately 4.0-6.0 m, five isolated sediment samples (**399 A-F**) from beneath five artifacts, and one core (**400**) were collected. In the northwest corner of site, from a depth of approximately 2.0 m, four isolated samples (**399 G-K**) from beneath four artifacts, and one core (**401**) were collected. Additionally, a surface sand sample was collected from both areas of the site in order to establish whether the sediment is receiving enough sunlight at the surface to reset the luminescence signal. On shore next to the anchorage, samples were collected from environmental (showing no signs of human activity) and archaeological (showing signs of human activity) sections of the scarp, in order to compare mineralogical, and luminescence behaviors between the terrestrial and underwater sediments. The samples were then sent to the University of St. Andrews' Luminescence dating laboratory where preliminary screening, calibrated screening, and the SAR protocol were performed on the sediment.

In Scotland, preliminary measurements were determined first using the SUERC portable OSL reader. This OSL screening method is often performed on site with unprocessed sediment samples to identify those with viable signals for dating purposes. The process was mirrored in the laboratory in order to understand whether this step could be useful for future fieldwork at Maroni *Tsaroukkas.* The preliminary results will be compared to the calibrated screening in section III.2.1. Following preliminary screening, each sediment sample was sieved to a uniform grain fraction, chemically etched, and two aliquots of each were dispensed for calibrated screening with the Risø TL/OSL reader. Select samples were then further refined by density and dispensed into

24 aliquots each for the SAR protocol, a series of regenerative tests to construct the equivalent dose, a measurement needed to calculate age.

Despite the fact that less radiation and less sunlight reaches sediments in an underwater environment, the OSL sampling program at Maroni *Tsaroukkas* produced meaningful results. The two cores taken from opposite ends of the site distinguish two different patterns of sedimentation. Core **400**, collected from the southeast sector at a depth of approximately 4.0 m, emitted relatively uniform signals, with spikes corresponding to more residual luminescence. Core **401**, collected from the northwest sector at a depth of approximately 2.0 m, records a longer 'chronology'. In both cores many samples were unsuccessful due to low sensitivity, which creates high errors. The sand in the cores carries no viable signal, suggesting the sand has been mobile and recently exposed to daylight to remove the luminescence signals. However, in the preliminary screening the sand deeper down in the core emitted a higher signal intensity, suggesting that it has not been reworked as frequently.

In core **400**, the lower dose estimate of the paired aliquots represents the more bleached component, and the one more likely to register depositional ages. These estimates fluctuate around 15.0 Gy through approximately 8.0 cm of silt, indicating these sediments were bleached quickly. Sensitivity measurements from core **400** separate the sediment into clearer sections: (a) the sand from the top 9.85 cm of the core with sensitivity ranging from 116 to 1,432 Gy^{-1} (average of 723 Gy^{-1}), (b) The top 11.6 cm of silt with sensitivities ranging from 127 to 1,970 Gy^{-1} (average of 870 Gy^{-1}), and (c) the bottom 5.85 cm of silt with sensitivity values ranging from 355 to 13,291 Gy^{-1}

(averaging 12,779 Gy^{-1}). Core **401** has higher OSL signals in the silt, starting at 15.4 Gy and ending at 53.7 Gy. The bottommost three samples of core **401** are oversaturated. The signals of core **401** have a more consistent progression without the large spikes seen in core **400**. This is possibly a result of the shallower water depth where **401** was collected, which allows more thorough exposure to the sun. The oversaturated silt only 14.6 cm into core **401** indicates either a very slow deposition of silt, or that the newer silt in this area has been eroded by wave action to reveal older layers. The isolated sand and silt samples collected beneath ancient artifacts (anchors and ceramics) on site solidified the conclusion that the majority of the sand is bleached. The silt from underneath these artifacts did provide promising results that could lead to a comprehensive understanding of artifact movement, with further sampling.

In this chapter I discuss the results in relation to the goals of the sampling program: (a) the possibility for preliminary screening to make determinations during fieldwork in the future, (b) the ways in which OSL can characterize artifact movement through disturbed sediment patterns, and (c) the help OSL can provide to understand environmental changes at an underwater site. In section III.3 I discuss the future steps needed to interpret results and produce more reliable outcomes from OSL sampling programs.

III.2. Significance of OSL Results

III.2.1. Comparison between Preliminary Screening and Calibrated Screening

One of the goals of the experimental OSL sampling program at the anchorage of Maroni *Tsaroukkas* was to determine if preliminary OSL screening could be beneficial for categorizing sediments on-site. The results were compared to those from the calibrated screening, which produced calibrated results from small aliquots of processed sediment. Processing included chemical etching, and sieving into grain fractions in order to retrieve a concentrate of quartz and eliminate contamination from feldspar, carbonates and organics that can confuse the signal. Apart from this, preliminary results can be altered by differences in sediment amounts, and the quartz levels within that sediment. For example, after processing the Maroni *Tsaroukkas* samples in the laboratory, it could be seen that the silt held a much smaller amount of quartz than the sand, which may be why higher signal intensities seen in the calibrated results were not produced by the portable unit. Calibrated screening additionally takes the sensitivity of the sediment grains into consideration, avoiding overestimation of signals. The comparison aims to understand if information can be gathered through the portable unit to draw preliminary conclusions about a site, in order to justify any added cost, time and manpower to fieldwork under water.

The results of the preliminary screening with the SUERC portable OSL reader do show some general consistencies. Core **400** from the southeast corner of the anchorage is characterized by lower signal intensities from both screenings (preliminary and calibrated), while core 401 from the northwest has much higher signal intensities and a

more pronounced signal depth-progression. The portable unit was able to categorize sections of sediment features with minimal effort: the marine cores, marine isolated samples, and terrestrial sections could be categorized by low (bleached), moderate (archaeological), and high (geological, earlier than human occupation) intensities. The preliminary and calibrated screenings provide different proxy data and are not expected to produce similar details. Any variation in the results is due to insensitive grains and complex depositional settings. To have retrieved a chronological signature within the sediment is in itself positive.

III.2.1.1. Core **400**

The preliminary screening of core **400** indicated that the majority of sand moved recently, and that exposure to daylight was adequate to reset the OSL signals. The exceptions are the two lowest sand samples (**400F** and **400G**) from 415.1 to 416.5 cm depth, which have higher signals and are likely older. In the silt, the first three sub-samples (**400 H-J**) have higher signals than the rest and subsequent samples **400K** to **400M** regress in signal with depth. Among the lower silt sub-samples **400N-400U** signal intensities remain small. The higher signals in the silt at the top of the core suggest there is interference from different mineralogical variations removed during processing. The calibrated screening similarly showed that there is no signal in the sand, and very little signal-depth progression in the silt (Fig. 22). The top section of silt did not produce higher signals than the lower section, and sand samples **400F** and **400G** does not have higher signals than the other sand samples. The majority of the sand grains are too

insensitive to produce a signal through the calibrated screening, but the signal intensity produced by the few sensitive grains that store a signal was determined by the preliminary screening and is sufficiently valid to conclude the sand holds a small signal-depth progression.

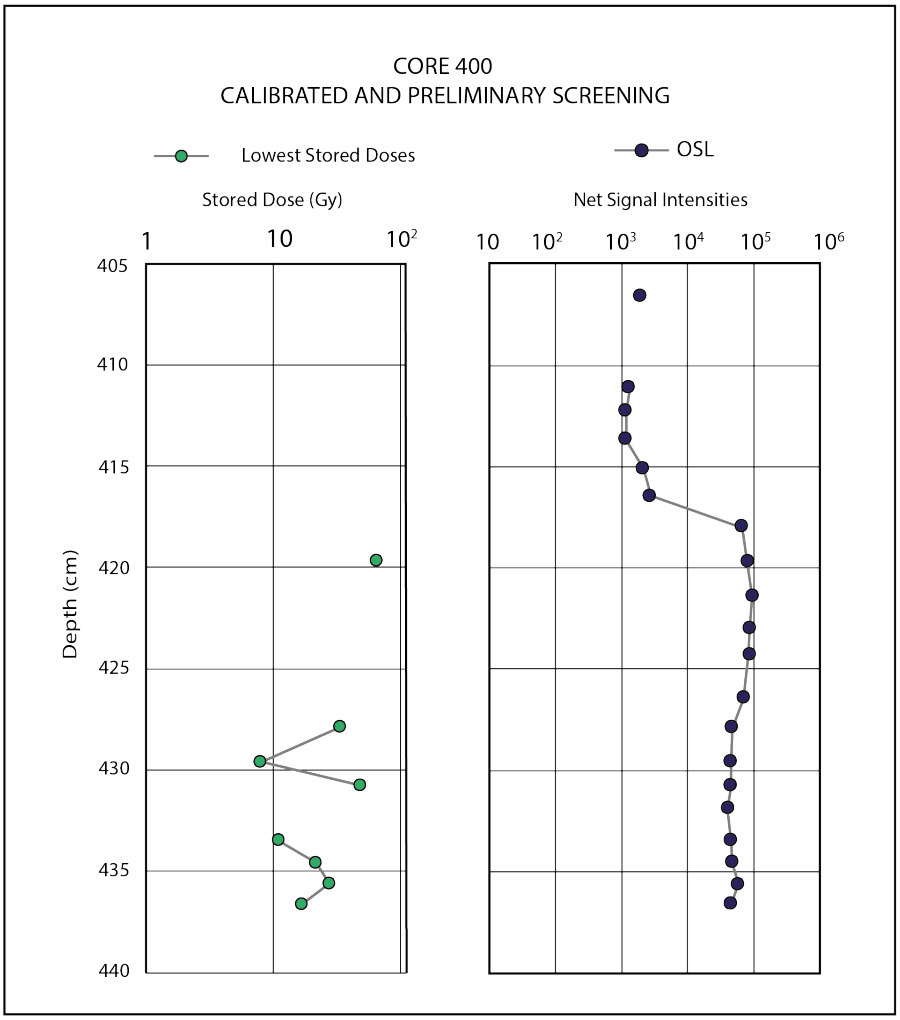

Figure 22. Comparison between Calibrated (left) and Preliminary (right) Screenings for Core 400

III.2.1.2. Core **401**

The results of the preliminary screening of core **401** determined that: (a) the OSL signal in the sediment increases with depth, (b) the first silt sample has a smaller signal than core **400**, and (c) that the last eight sub-samples have approximately the same signal. The calibrated screening provided slightly different results (Fig. 23). Core **401** still has a much more comprehensible stratigraphy than core **401**, and the last silt samples, except for the bottommost three, produced a similar stored dose. These

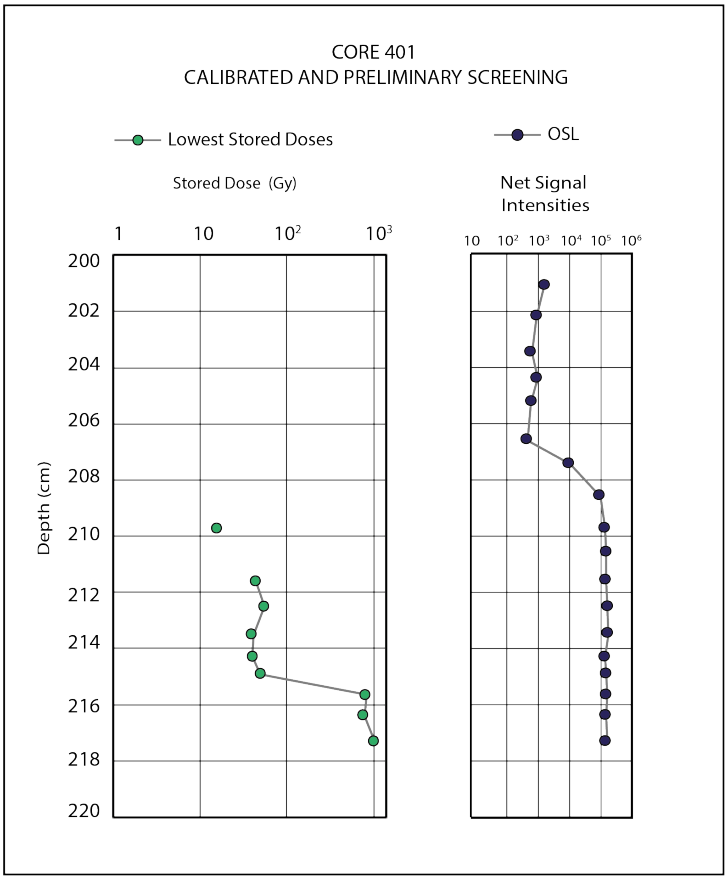

Figure 23. Comparison between Calibrated (left) and Preliminary (right) Screenings for Core 401

bottommost three samples (**401P**, **401Q**, **401R**) produced an oversaturated signal in the calibrated screening. This result was not produced by the preliminary screening because the calibrated screening reads the signal just from a thin layer of quartz, while the preliminary screening reads the unprocessed sample that has these few quartz grains within the sediment. Samples **401G** at the bottom of the sand produced a higher signal than the sand above it during the preliminary screening. This result was not mirrored in the calibrated screening as the sand samples are too insensitive to register a stored dose. These signals cannot be dismissed as they do still register valid intensity that may indicate a pocket of sand not moving with the same frequency as the rest.

III.2.1.3. Isolated Marine Samples

The isolated samples taken from underneath artifacts were expected to show variation in detail between the preliminary and calibrated screenings. Results differ between which samples produced signals higher than in the comparison sub-sample within the core, however, both screenings were able to make similar distinctions between samples with high and low OSL signals (Table 10). The calibrated results are best for date determinations, but when it comes to comparing sediment, preliminary screening is able to differentiate between moderate and small signals because it reads a bulk sample, instead of a few grains. This of course means samples analyzed in the preliminary screening will be mixed and present an average between grains with residual luminescence and grains that are bleached. However, if the samples being compared are

of the same sediment type and environment, they should hold similar ranges. Both screenings indicated high OSL signals from the three silt samples, and because of the low sensitivity of the quartz, signals for the sand samples were close to zero with high errors. The preliminary screening was able to pick up higher signals within the sand

Comparison between Calibrated and Preliminary Screenings					
Sample	Type	Location	Stored Dose (Gy)	Signal Intensity (Photon Counts)	Characterization of signal
399A	Silt beneath anchor	SE	31.3 ± 6.2	82,899 ± 290	High
399B	Sand beneath anchor	SE	--	3,032 ± 65	Moderate
399C	Silt beneath same anchor as **399B**	SE	118.8 ± 72.8	159,531 ± 402	High
399D	Sand beneath architectural block	SE	--	4,078 ± 73	Moderate
399E	Sand beneath anchor	SE	0.9 ± 0.7	1.395 ± 53	Moderate
399F	Surface sand	SE	--	566 ± 43	Low
399G	Sand beneath ceramic	NW	--	--	
399H	Sand beneath ceramic	NW	--	946 ± 46	Low-moderate
399I	Sand beneath ceramic	NW	--	1,489 ± 55	Moderate
399J	Surface sand	NW	0.2 ± 0.2	319 ± 42	Low
399K	Silt beneath ceramic base	NW	36.0 ± 15.0	457,408 ± 679	High

Table 10. Comparison between Calibrated (Stored Doses) and Preliminary (Signal Intensities) Screening Results for Isolated Marine Samples Preliminary Screening results are measured in signal intensities (photon counts) and calibrated screening results are measured in stored doses (Gy). Stored Doses with high errors are highlighted pink.

samples underneath artifacts than the surface sand samples. From the southeast sector of site, sample **399D** from beneath an architectural block is 7.2 times higher than surface-sand sample (**399F**) from the same area. Sample **399B** from beneath an anchor in the same sector of the site is 5.45 times higher than the surface sand. Additionally, in the

northwest, samples **399I** and **399H** produced signals from approximately 3-4.5 times higher than the surface-sand sample (**399J**).

III.2.1.4. Terrestrial Sections

The results of the terrestrial samples collected from the scarp on shore produced trends similar to the preliminary and calibrated screenings (Figs. 24, 25): (a) there is a

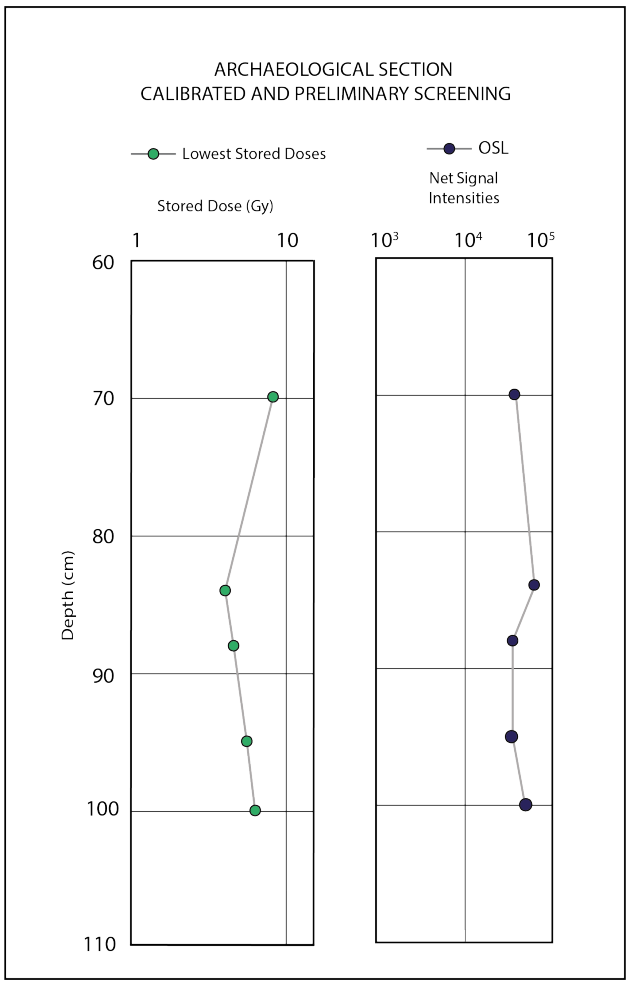

Figure 24. Comparison between Calibrated (left) and Preliminary (right) Screenings for Terrestrial Archaeological Section (398A-E**)**

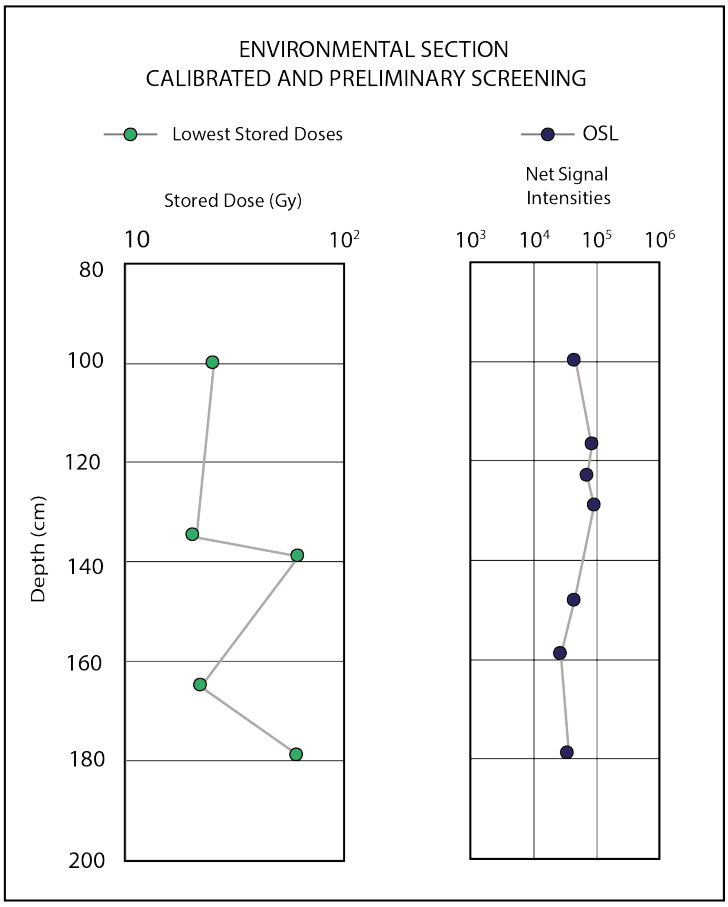

Figure 25. Comparison between Calibrated (left) and Preliminary (right) Screenings for Terrestrial Environmental Section (398G-L**)** Samples **398H** and **398I** were unsuccessful in the calibrated screening and are not shown in the graph.

higher OSL signal in the environmental section than in the archaeological section, and (b) the archaeological section is characterized by similar signals. The environmental section looks fairly different due to **398G** and **398H** being too insensitive to produce a signal in the calibrated screening. Between the two screenings, however, the bottom 29.0 cm (**398J**-**L**) provide the same pattern, with **398J** and **398L** having very similar signals, while **398K** has a signal with almost half the intensity.

III.2.1.5. Preliminary and Calibrated Screenings, Compared

The results of preliminary and calibrated screening of core **400**, core **401**, isolated samples, environmental section, and archaeological section have been presented in a graph for comparison (Fig. 26). The x-axis is the calibrated screening stored doses, and the y-axis is the photon counts of the preliminary screening. If the results present the

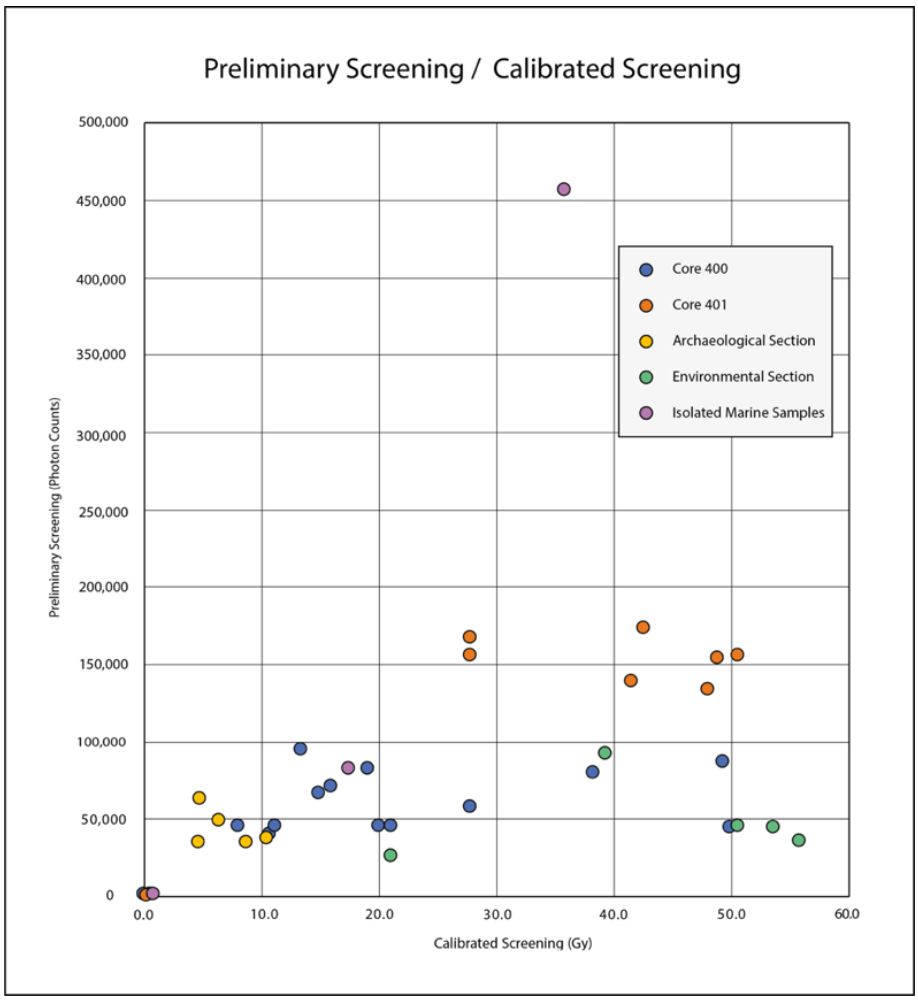

Figure 26. Plot comparing Preliminary and Calibrated Screening Results

same patterns, such as if one sample reads the highest signal from both methods, the point will be plotted towards the top right. This means that if the two methods are in agreement with each other, the points should be plotted in a diagonal line with the right side rising upwards. Each color in the graph corresponds to a different dataset. None of the datasets forms a clear line, but Core **400** is the closest to diagonal. Despite this, broad determinations about whether each sample has high or low signal intensity can be made. This is what was expected for the preliminary screening, and it allows archaeologists to sample sediment with intensities that are not bleached, oversaturated or insensitive.

The results of the preliminary screening were influenced by factors of grain size and minerology that were removed during calibrated screening. It must also be taken into consideration that less silt than sand appears in the isolated marine samples collected at Maroni *Tsaroukkas,* due to the fact that I only sampled a thin layer (approx. 1.0 cm) surface of silt from beneath the anchors.

The portable unit was successful in categorizing sediment with minimal effort: the marine cores, marine isolated samples, and terrestrial sections could be categorized by low (bleached), moderate (archaeological) and high (geological, earlier than human occupation) intensities. Additionally, despite the silt sample having less quartz, a signal-depth progression was still visible.

Eleven isolated sediment samples and two cores were taken within three approximately 40-minute dives by two divers, one of whom had a sprained ankle and

could not use fins. The marine cores additionally took much more time in these dives due to inadequate coring techniques for dense silt. Presumably, in better health conditions and with focus on a small area of site, one buddy team could collect approximately 20 isolated samples within an hour under water. The resulting data could then be read ashore in under an hour. This is a large amount of data that can be collected within a short time frame with little energy. As for application, the data read in the field could instruct further sampling for calibrated determinations, and could be especially useful to determine a broader horizontal view of the disturbances in the sediment underwater (such as on the top layer of silt and the collection of sand).

III.2.3. Artifact Movement

A major goal of the sampling project at the Maroni *Tsaroukkas* anchorage was to understand whether OSL measurements are able to determine if an artifact has moved on the sea floor. The interpretation of the calibrated screening of the isolated samples differs from those collected from the cores. In order to interpret the cores, the lowest signal of the paired aliquots from a given sample was used. The higher signals are not used to avoid residual luminescence from previous periods of burial. This cannot be done with the isolated samples from beneath artifacts. Those samples are from the surface of the stratigraphy, and it is likely that the lowest signal represents the grains that contaminate the sample. To interpret these samples reliably, upwards of 20 aliquots must be read and the trend of the majority and average patterns must be taken into consideration. In order to understand artifact movement, the sediment below a large

artifact was compared to sediment collected in the core within the same layer: artifacts were often sitting on the surface of the silt, therefore they were compared to surface of the silt in the nearby core. When sand was collected beneath an artifact it was compared to all the sand signals in the cores due to the frequent movement of sand. If the sediment has a higher OSL signal beneath the artifact than the comparative sample within the core, then the artifact may have been in place for a long time, blocking the sediment from the sun. If the sediment has a smaller signal, then the sediment has been exposed to the sun or intrusive sediment has washed beneath the artifact. It is assumed that an artifact sitting upon sediment with a higher signal is close to original deposition. However, variation on the surface of the silt is acknowledged and will be discussed later in this chapter (page 101).

399A was the only sample to consistently produce a signal higher than the equivalent sample in the core. **399A** was taken from the silt underneath an anchor in the southeastern sector of the site. Although not understanding the variability of signals on the surface of the silt, **399A**, approximately 2 times higher than the top of the silt in the core, tells us that the artifact may have obscured the silt from the sun for a longer time than it takes for the silt to be exposed by the sand. Depletion indices determined during preliminary screening indicate that sediment was well-bleached during deposition. **399A** and **399C** were the only samples from beneath artifacts with depletion indices above 2.0, indicating the signal does not hold residual luminescence.

While **399A** consistently indicates the artifact overlying it has not moved, **399C**, taken from silt beneath an anchor in the southeastern part of the anchorage, may suggest

movement. Natural signals derived for the aliquots of sample **399C** during the SAR protocol were frequently lower than the top of the silt in core **400**. Therefore, the sediment underlying this anchor has been exposed to the sun more recently than the silt underlying the sand, and may indicate this anchor was moved recently into this position.

Preliminary determinations from larger sediment samples distinguished signal intensities within the sands as well. The sand samples from beneath all the artifacts have signal intensities higher than the surface sand from the corresponding area (**399F** in the southeast and **399J** in the northwest): from 2.46 to 7.2 times higher. Although the sensitivity of the quartz in the sand dispensed for the calibrated screening was too low for a stored dose to be determined, preliminary screening can provide relevant data to fill in the blanks.

These data are presented as an experiment in how OSL can suggest whether an artifact on the sea floor has moved or not. Specifically, the OSL data helps identify sediments exposed to the sun at different times, and how they might lead to conclusions about the positioning of associated artifacts.

II.2.4. Formation of the Site

With additional cores, conclusions about site formation may change, but the two cores discussed here provide information for the sedimentation processes on site. On the seabed off Maroni *Tsaroukkas*, silt was deposited gradually for thousands of years. This

could be due to run-off from the now silted-up river just east of the site.[111] From core **401**, 2.0 m below sea-level and approximately 50.0 m from shore to the west, the accumulated silt seems to have been eroded by wave action, revealing an older sediment deposit. Silt then began to be deposited again. Core **400**, taken from 4.0 m below sea level to the southeast of site, has a deeper deposit of silt with a slight rise in OSL signal. This may be because of the core's proximity to the mouth of the river. More cores from this area are needed in order to understand the river's involvement in sedimentation. After these silt deposits were formed, the sand was introduced. The majority of the site is covered in uniform grey-beige sand. In the northwest corner of the site the sand is frequently a darker grey-brown, with coarser grains and many pebble inclusions.[112] On top of and below the sand there are swaths of cobbles and boulders across the site. The presence of these cobbles and boulders increases to the southeast where they are found mixed with ceramic sherds.

The beach next to the site consists of pebbles, cobbles and boulders, suggesting this is not the source of the sand, but that the sand has moved back and forth between the shallow coast and deeper water. The dark grey sand with inclusions of cobbles in the northwestern corner of the site is similar to the old beach strata from the scarp on shore, suggesting a possible origin. Manning et al. believe the anchorage was cupped between two arms of land protruding from the mainland to form a sheltered bay.[113] The old beach

---

[111] Nichols 2009, 216.
[112] Munsell colors were not assigned in the field, but will be a necessity for future sample collection.
[113] Manning et al. 2002, 113-14.

strata on shore also suggest a significant amount of erosion. However, John Leonard believes the erosion of these arms would have caused a large accumulation of sediment, enough to render the anchorage invisible, yet this sediment is not present.[114] In order to reconstruct what this area would have looked like for ancient sailors, further examinations are needed from a terrestrial standpoint.

III.2. Future Data Collection

There are three types of samples that need to be taken at the anchorage to clarify results from the 2019 OSL sampling program: (a) samples to characterize the variety of signals from the top silt layer, (b) samples from sediment beneath artifacts that has been previously sampled to understand repeatability of the results, and (c) samples to test bleachability of the sediment with slightly less light exposure. Additional samples that could be collected for a secondary stage of analysis are: (a) new terrestrial samples from the environmental and archaeological section, and (b) deeper marine cores for additional analysis to complement OSL determinations.

The challenge of the sampling program is comparing isolated samples of sediment beneath artifacts to sediment in the cores. Without more cores and more samples, it is not possible to know how much variation in OSL signal exists across the surface of the silt. This makes it difficult to compare the sample from underneath an artifact to the silt sub-sample from one core. There are many ways future sampling

[114] Karyda 2016, 86; Leonard 1995, 238.

strategies can account for this deficit. More cores surely need to be taken across the site. Some may capture a longer stratigraphy, but not all need to be deep. To determine the OSL signal of the top layer of silt, where many of the artifacts sit, cores approximately 5.0 cm long could be taken in close proximity to the artifact. This would provide a more reliable comparison between the silt obscured by the artifact and the silt exposed during movement of the sand. It may also be useful on this site to obtain small cores beneath the artifacts, rather than isolated samples, in order to see how much variation there is in the stratigraphic record between the two (or more) samples being compared.

Repeatability of the results from the area of sediment below the artifact is another concern. Additional samples should be taken from beneath the anchors that have been already been sampled in order to see if the results are consistent, or if the collected sample was from a pocket of sediment that holds a different OSL signal. The area of sediment and depth of disturbance from previous sampling activities under the artifacts was recorded. New samples will be collected from the opposite side to determine the consistency of the luminescence signal within the sediment beneath the artifacts. Repeatability determinations will be the most useful from the anchors that were sitting on top of silt (**399A** and **399C**). In the future, it may be worth taking two samples from different areas under the anchors to understand whether the luminescence signal is consistent in this small area.

Additionally, from the southeast sector of site, sample **399D** was the only one taken from a depth (6.0 m) deeper than the others (4.0 m). This sample registered a higher signal than in the sand from core **400** (4.0 m). In order to understand whether this

higher signal is a result of sand accumulation, or of less exposure to sunlight, this area must be sampled more thoroughly.

Of lesser importance is revisitation of the environmental section. The results from these sections provided an initial interpretation, but because the surface was not adequately removed, it is difficult to understand how much this mixing has affected the signals. Ideally, 10.0 cm or more should be taken off the face of the scarp in order to prevent contamination from sun exposure and erosion. Samples collected from cleaner contexts could determine the date of the old beach at the bottom of the scarp, and provide more reliable data for comparison with the marine samples.

There are many different methods of analyzing sedimentation that can complement OSL signals. Additional cores can be collected to utilize x-radiographs, determine radiocarbon dates, and identify micropaleontological or bioarchaeological material within a stratigraphic sequence. X-radiographs can be taken to view sediment changes that are not apparent to the human eye. This is useful for accurately dividing strata of sediment when extracting samples from the cores. Radiocarbon C^{14} dating is a vastly popular method of absolute dating.[115] Within the cores, plant remains or small microfaunal remains may provide the opportunity to obtain radiocarbon dates. The comparison between radiocarbon and OSL dates could enhance OSL data, and refine the dates of individual strata. Additionally, the species of any micro faunal remains can be identified which may provide information about the evolution of the coastal

[115] Renfrew 2014, 12.

environment. For example, the presence of certain species that only reside in lagoonal or still water could indicate whether the coastal area was once a sheltered environment.[116] A similar geoarchaeological study has been performed at the ancient harbor of Caesarea Maritima, Israel (21 BCE to 490 CE). [117] Using a combination of foraminiferal analysis and ^{14}C dating of marine cores, the following contexts were identified: (a) before the construction of the harbor, (b) construction of the harbor, (c) active harbor, and (d) inactive harbor.[118] This was due to the presence of different foraminiferal biofacies that reside only in low energy muddy substrates, and others that reside in higher energy environments.[119] Closer to Maroni *Tsaroukkas*, the Bronze Age site of Kition *Bamboula*, in the southeastern Cyprus, was once a harbor that is now 2.0 m above sea level and 400.0 m inland.[120] In order to understand the drastic environmental change at this site, 17 cores were drilled and two were chosen for sedimentological and paleontological analysis, accompanied by ^{14}C dating.[121] The two cores were selected from the middle of the harbor basin. Five sedimentary units could be separated that indicate the evolution of the harbor area. From the presence or absence of foraminifera, posidonia and shells within the substrate, the study concluded that the harbor was once an open bay that

[116] See Morhange et al. (2000, 212) who analyze changes to the coastal environment around Phoenician military harbour of Kition Bamboula, Cyprus using macrofaunal remain in cores.
[117] Reinhardt et al. 1994, 37.
[118] Reinhardt et al. 1994, 37.
[119] Reinhardt et al. 1994, 37.
[120] Morhange et al. 2000, 205.
[121] Morhange et al. 2000, 205.

quickly became closed off to the Mediterranean, likely due to man-made modifications (post 400 CE).[122]

Although these additional techniques provide new information, alone they would not aid the anchorage at Maroni *Tsaroukkas*, as the archaeological material has little to no vertical stratigraphy. Any information derived from cores is likely to be older than the Late Bronze Age. OSL is therefore ideal for this type of analysis as it can identify movement of sediment from region to region and patterns that are not only vertical, but horizontal.

In summary, on the basis of this experimental analysis, the results point to three sediment samples that will further enhance the current interpretations of artifact movement under water: (a) layered, isolated samples beneath artifacts and next to artifacts for better comparison (b) repetitive samples from beneath previously sampled anchors to understand consistency of the results, and (c) samples to test how sediment in slightly deeper water are being bleached.

III.3. Conclusion

Analysis of sediments by means of OSL has never been attempted at an ancient submerged site in the Mediterranean. OSL functions as a tool for dating stratigraphic records and identifying disturbances within them. Accordingly, OSL has been utilized on

[122] Morhange et al. 2000, 222.

terrestrial sites for decades. The challenges of the underwater environment create complications for capturing measurable OSL signals.

The 2019 sampling program at the anchorage of Maroni *Tsaroukkas,* Cyprus set out to describe sediment deposition, disturbances, and their relationship to the archaeological material. Despite issues of sediment mixing and lack of bleaching, this experimental application proved that accurate data can be collected and assessed from shallow underwater sites. The 2019 sampling program sought to determine if these disturbances as well as stratigraphic identifications could be made using preliminary and calibrated screenings, and connected with artifacts under water.

Two of 11 isolated samples taken beneath the artifacts on site produced signals. **399C** seems to represent a disturbance to the silt beneath an anchor, suggesting it has recently been moved to this position. Sample **399A**, from silt beneath an anchor, is older than the silt at the top of the corresponding core, suggesting this artifact has blocked the silt below it from the sun for a longer time than the sand has been blocking the silt. Thorough sampling in the future will serve to secure these results.

Eight sand samples did not produce a signal, but this is not an indication of failure. The three silt samples were expected to produce an OSL signal, the two surface-sand samples were expected to be bleached, while the six sand samples from beneath artifacts were expected to produce a slightly higher signal than the surface sands. Merging both the calibrated and preliminary screening results allows for the categorization of sand and silt signal intensities that can inform the accumulation and movement of sediments on site at Maroni *Tsaroukkas.*

Initial conclusions about sedimentation processes were also possible through OSL sampling on site. Differences in silt accumulation can be seen between the northwest and southwest, possibly due to the outflow of the now inactive river. This is a working theory that I intend to explore in the future.

In conclusion, terrestrial and underwater excavations tackle very different environments. Terrestrial excavations must decipher stratigraphic changes and OSL is just one of the tools that are used. Sediment itself holds an immense amount of information on terrestrial sites, and archaeologists spend a large amount of time excavating, sampling and analyzing sediment. Many methodologies have been employed to derive information from the sediment itself: micromorphology, phytolith sampling, X-ray fluorescence, and sieving for zooarchaeological and ethnoarchaeological material are just some of these tools. Many of these methods are not applicable to sediment underwater that is constantly in flux. The benefit of OSL to derive information about sediment movement makes this method particularly well-suited to the horizontal stratigraphic record of an anchorage like Maroni *Tsaroukkas*. Microfaunal analysis and radiocarbon dating are useful to characterize older sequences of a site, but OSL has the unique ability to see changes of sedimentation processes within a short stratigraphic record, and from one localized area to the next, allowing estimation about the movement of larger, heavier artifacts.

REFERENCES

Aitken, M. J., D. W. Zimmerman, and S. J. Fleming. 1968. "Thermoluminescent Dating of Ancient Pottery." *Nature* 219: 442-45.

Aitken, M. J. 1998. *An Introduction to Optical Dating: The Dating of Quaternary Sediments by the Use of Photon-Stimulated Luminescence.* Oxford: Oxford University Press.

Andreou, G. M. 2018. "Monitoring the impact of coastal erosion on archaeological sites: the Cyprus Ancient Shoreline Project." *Antiquity* 92: 1-6.

Araujo, A. G. M. 2013. "Bioturbation and the Upward Movement of Sediment Particles and Archaeological Materials: Comments on Bueno et al." *Journal of Archaeological Science* 40: 2124-127.

Atkins, C. 2020. "Of Unfinished Anchors and Maritime Trade Networks: A View from Maroni Tsaroukkas, Cyprus." Archaeological Institute of America 121st Annual Meeting Abstracts 43: 14

Bowens, A. 2009. *Underwater Archaeology: The NAS Guide to Principles and Practice.* 2nd ed. West Sussex: John Wiley and Sons Ltd.

Brennan, M. L. 2016. "Quantifying Impacts of Trawling to Shipwrecks." In *Site Formation Processes of Submerged Shipwrecks* edited by M. E. Keith, 157-78. Florida: University Press Florida.

Cadogan, G. 1992. "The British Museum's Work at Maroni." In *Studies in Honour of Vassos Karageorghis* edited by G. C. Ionnides, 123-26. Nicosia: Society of Cypriot Studies.

Carter, J., A. J. Creswell, T. C. Kinnaird, L. A. Carmichael, S. Murphy, and D. C. W. Sanderson. 2018. "Non-Poisson Variations in Photomultipliers and Implications for Luminescence Dating." *Radiation Measurements* 120: 267-73.

Chen, R. and V. Pagonis. 2011. *Thermally and Optically Stimulated Luminescence: A Simulation Approach.* West Sussex: John Wiley & Sons Ltd.

Clark, P. R. 1992. "Contrasts in the Recording and Interpretation of 'Rural' and 'Urban' Stratification." In *Interpretation of Stratigraphy: A Review of the Art, Proceedings of a Conference Held on 18th June, 1992 at the City of Lincoln*

Archaeology Unit edited by K. Steane, J. Mann, and H. Palmer-Brown, 17-19. Lincoln: City of Lincoln Archaeology Unit.

Duller, G. A. T. 2016. *Analyst v4.31.9: User Manual.* Wales: Aberystwyth University.

DTU Nutech. 2015. "Guide to 'The Risø TL/OSL Reader'" Denmark: DTU Nutech. https://www.nutech.dtu.dk/english/products-and-services/radiation instruments/tl_osl_reader/software.

Farrand, W. R. and T. W. Jacobsen. 2000. *Depositional History of Franchthi Cave: Sediments, Stratigraphy and Chronology.* Bloomington: Indiana University Press.

Fitzsimmons, K. E. 2011. "An Assessment of the Luminescence Sensitivity of Australian Quartz with Respect to Sediment History." *Geochronometria* 38: 199-208.

Folk, R. L. 1980. *Petrology of Sedimentary Rocks.* 2nd ed. Austin: Hemphill Publishing Company.

Ford, B., C. Sowden, K. Farnsworth, and M. Scott Harris. 2016. "Coastal and Inland Geologic and Geomorphic Processes." In *Site Formation Processes of Submerged Shipwrecks,* edited by M. E. Keith, 17-43. Gainesville, Florida: University Press Florida.

Franklin, A. D., J. R. Prescott, and R. B. Scholefield. 1995. "The Mechanism of Thermoluminescence in an Australian Sedimentary Quartz." *Journal of Luminescence* 63: 317-26.

Fulton, C., A. Viduka, A. Hutchison, J. Hollick, A. Woods, D. Sewell, and S. Manning. 2016. "Use of Photogrammetry for Non-Disturbance Underwater Survey." *Advances in Archaeological Practice* 4: 17-30.

Harris, E. C. 1989. *Principles of Archaeological Stratigraphy.* 2nd ed. San Diego: Academic Press.

Heydari, M. and G. Guérin. 2018. "OSL Signal Saturation and Dose Rate Variability: Investigating the Behaviour of Different Statistical Models." *Radiation Measurements* 120: 96-103.

Huntley, D. J., D. I. Godfrey-Smith, and M. L. W. Thewalt. 1985. "Optical Dating of Sediments." *Nature* 313: 105-7.

Jacobs, Z. 2008. “Luminescence Chronologies for Coastal and Marine Sediments.” *Boreas* 37: 508-35.

Kapitän, G. 1969. “The Church Wreck off Marzamemi.” *Archaeology* 22: 122-33.

Karyda, E. 2016. “Sailing from Coast to Coast: Cabotage on the Cypriot South Coast.” In *Approaching Cyprus: Proceedings of the Post-Graduate Conference of Cypriot Archaeology (PoCA) held at the University of East Anglia, Norwich, 1st 3rd November, 2013,* edited by R. Maguire and J. Chick, 78-95. Cambridge: Cambridge Scholars Publishing.

Keith, M. E. and Evans, A. M. 2016. “Sediment and Site Formation in the Marine Environment.” In *Site Formation Processes of Submerged Shipwrecks,* edited by M. E. Keith, 44-69. Gainesville, Florida: University Press Florida.

Kennedy, G. C. and L. Knopf. 1960. “Dating by Thermoluminescence.” *Archaeology* 13: 147-48.

Kinnaird, T., D. C. Sanderson, C. Burbidge, and E. Peltenburg. 2007. “OSL Dating of Neolithic Kissonerga-Mylouthkia, Cyprus.” *Neolithics* 7: 51-57.

Kinnaird, T., J. E. Dixon, A. H. F. Roberston, E. Peltenburg, and D. C. W. Sanderson. 2013. “Insights on Topography Development in the Vasilikós and Dhiarizos Valleys, Cyprus, from Integrated OSL and Landscape Studies.” *Mediterranean Archaeology and Archaeometry* 13: 49-62.

Kinnaird, T., J. Bolòs, A. Turner, and S. Turner. 2017. “Optically-Stimulated Luminescence Profiling and Dating of Historic Agricultural Terraces in Catalonia (Spain).” *Journal of Archaeological Science* 78: 66-77.

Leidwanger, J. 2018. “New Investigations of the 6th-c. A. D. ‘Church Wreck’ at Marzamemi, Sicily.” *Journal of Roman Archaeology* 31: 339-56.

Leonard, J. R. 1995. “Evidence for Roman Ports, Harbours and Anchorages in Cyprus.” In *Cyprus and the Sea,* edited by V. Karageorghis and D. Michaelides, 228-46. Nicosia: University of Cyprus.

Madsen, A. T., A. S. Murray, T. J. Andersen, M. Pejrup, and H. Breuning-Madsen. 2005. “Optically Stimulated Luminescence Dating of Young Estuarine Sediments: A Comparison with ^{210}PB and ^{137}Cs Dating.” *Marine Geology* 214: 251-68.

Manning, S. W., S. J. Monks, L. Steel, E. Ribeiro, and J. M. Weinstein. 1998. "Late Cypriot Tombs at Maroni Tsaroukkas, Cyprus." *Annual of the British School at Athens* 93: 297-351.

Manning, S. W., D. A. Sewell, and E. Herscher. 2002. "Late Cypriot I A Maritime Trade in Action: Underwater Survey at Maroni Tsaroukkas and the Contemporary East Mediterranean Trading System." *Annual of the British School at Athens* 97: 97-162.

Manning, S. W., G. Andreou, K. D. Fisher, P. Gerard-Little, C. Kearns, J. F. Leon, D. A. Sewell, and T. M. Urban. 2014. "Becoming Urban: Investigating the Anatomy of the Late Bronze Age Complex, Maroni, Cyprus." *Journal of Mediterranean Archaeology* 27: 3-32.

Mellett, C. L. 2013. "Luminescence Dating." In *Geomorphological Techniques,* edited by Cook, S. J., Clarke, L. E., Nield, J. M., 1-11. London: British Society for Geomorphology.

Morhange, C., J. P. Goiran, M. Bourcier, P. Carbonel, J. Le Campion, J. M. Rouchy, and M. Yon. 2000. "Recent Holocene Paleo-Environmental Evolution and Coastline Changes of Kition, Larnaca, Cyprus, Mediterranean Sea." *Marine Geology* 170: 205-30.

Murray, A. S. and A. G. Wintle. 2000. "Luminescence Dating of Quartz using an Improved Single Aliquot Regenerative-Dose Protocol." *Radiation Measurements* 32: 57-73.

Murray, A. S. and S. Funder. 2003. "Optically Stimulated Luminescence Dating of a Danish Eamian Coastal Marine Deposit: A Test of Accuracy." *Quaternary Science Review* 2: 1177-83.

Nichols, G. 2009. *Sedimentology and Stratigraphy*. 2nd ed. West Sussex: John Wiley & Sons.

Olley, J. M., P. De Deckker, R. G. Roberts, L. K. Fifield, H. Yoshida, and G. Hancock. 2004. "Optical Dating of Deep-Sea Sediments Using Single Grains of Quartz: a Comparison with Radiocarbon." *Sedimentary Geology* 169: 175-89.

Parker, A. J. 1981. "Stratification and Contamination in Ancient Mediterranean Shipwrecks." *The International Journal of Nautical Archaeology* 10: 309-35.

Reinhardt, E., C. Schroder-Adams, and R. T. Patterson. 1994. "Geoarchaeology of the Ancient Harbor Site of Caesarea Maritima, Israel; Evidence from Sedimentology

and Paleoecology of Benthic Foraminifera." *Journal of Foraminiferal Research* 24: 37-48.

Renfrew, C. 2014. Forward to *Radiocarbon Dating: An Archaeological Perspective,* 2nd ed, by R. E. Taylor, O. Bar-Yosef. Walnut Creek, California: Left Coast Press.

Roberts, G. R., Z. Jacobs, B. Li, N. R. Jankowski, A. C. Cunningham, and A. B. Rosenfeld. 2015. "Optical Dating in Archaeology: Thirty Years in retrospect and Grand Challenges for the future." *Journal of Archaeological Science* 56: 41-60.

Roberts, H. M., G. A. T. Duller, M. Gunn, C. R. Cousins, R. E. Cross, and D. Langstaff. 2018. "Strategies for Equivalent Dose Determination without Heating, Suitable for Portable Luminescence Readers." *Radiation Measurements* 120: 170-5.

Sanderson, D. C. W., P. Bishop, I. Houston, M. Boonsener. 2001. "Luminescence Characterisation of Quartz-Rich Cover Sand from NE Thailand." *Quaternary Science Reviews* 20: 893-900.

Sanderson, D. C. W., P. Bishop, M. Stark, S. Alexander, and D. Penny. 2007. "Luminescence Dating of Canal Sediments from Angkor Borei, Mekong Delta, Southern Cambodia." *Quaternary Geochronology* 2: 322-29.

Sanderson, D. C. W. and S. Murphy. 2010. "Using Simple Portable OSL Measurements and Laboratory Characterisation to Help Understand Complex and Heterogenous Sediment Sequences for Luminescence Dating." *Quaternary Geochronology* 5: 299-305.

Sanderson, D. C. W. and T. C. Kinnaird. 2019. "Optically Stimulated Luminescence Dating as a Geochronological Tool for Late Quaternary Sediments in the Red Sea Region." In *Geological Setting, Palaeoenvironment and Archaeology of the Red Sea* edited by N. M. A. Rasul and L. C. F. Stewart, 685-707. Cham, Switzerland: Springer International Publishing.

Schirmir, W. 1998. "Havara on Cyprus: A Surficial Calcareous Deposit." *Eiszeitalter und Gegenwart* 48: 110-17.

Sharma, S. K., S. Chawla, M. D. Sastry, M. Gaonkar, S. Mane, V. Balaram, and A. K. Singhvi. 2017. "Understanding the Reasons for Variations in Luminescence Sensitivity of Natural Quartz Using Spectroscopic and Chemical Studies." *Proceedings of the Indian National Science Academy* 83: 645-53.

Stang, D. M., E. J. Rhodes, and A. M. Heimsath. 2012. "Assessing Soil Mixing Processes and Rates using a Portable OSL-IRSL Reader: Preliminary Determinations." *Quaternary Geochronology* 10: 314-19.

Stuut, J., I. Smalley, and K. O'Hara-Dhand. 2009. "Aeolian Dust in Europe: African Sources and European Deposits." *Quaternary International* 198: 234-45.

Thiel, C., S. Tsukamoto, K. Tokuyasu, J. Buylaert, A. S. Murray, L. Tanaka, and M. Shirai. 2015. "Testing the Application of Quartz and Feldspar Luminescence Dating to MIS 5 Japanese Marine Deposits." *Quaternary Geochronology* 29: 16-29.

Yoshida, H., R. G. Roberts, J. M. Olley, G. M. Laslett, and R. F. Galbraith. 2000. "Extending the Age Range of Optical Dating using Single 'Supergrains' of Quartz." *Radiation Measurements* 32: 439-46.

Yukihara, E. G. and S. W. S. McKeever. 2011. *Optically Stimulated Luminescence: Fundamentals and Applications.* West Sussex: John Wiley & Sons Ltd.

Zheng, C. X., L. P. Zhou, and J. T. Qin. 2009. "Difference in Luminescence Sensitivity of Coarse-Grained Quartz from Deserts of Northern China." *Radiation Measurements* 44: 534-37.

APPENDIX A

Preliminary Screening Core **400**					
Sample Number	OSL Photon Counts	OSL Depletion	IRSL Photon Counts	IRSL Depletion	IRSL/OSL
400A	1,933 ± 57	1.5	--	--	-0.02
400B	1,206 ± 49	1	--	--	0.04
400C	1,314 ± 50	1	--	--	-0.01
400D	1,188 ± 49	1	--	--	0.01
400E	1,152 ± 48	1.2	--	--	0.02
400F	2,111 ± 57	2.4	--	--	0.00
400G	2,702 ± 61	1.4	111 ± 34	2.5	0.04
400H	66,679 ± 261	1.8	5,922 ± 85	1.2	0.09
400I	80,073 ± 286	1.8	8,383 ± 97	1.2	0.10
400J	95,429 ± 311	1.8	8,750 ± 99	1.2	0.09
400K	87,744 ± 299	1.8	9,927 ± 106	1.3	0.11
400L	83,272 ± 292	1.9	12,029 ± 116	1.3	0.14
400M	71,012 ± 270	1.8	10,285 ± 110	1.3	0.14
400N	46,273 ± 218	1.7	7,614 ± 94	1.4	0.16
400O	45,546 ± 217	1.9	7,120 ± 92	1.3	0.16
400P	45,230 ± 217	1.7	8,426 ± 99	1.3	0.19
400Q	40,336 ± 205	1.8	6,602 ± 89	1.3	0.16
400R	46,095 ± 218	1.8	7,562 ± 96	1.4	0.16
400S	46,628 ± 219	1.9	7,257 ± 92	1.3	0.16
400T	58,596 ± 245	1.9	8,814 ± 99	1.2	0.15
400U	45,786 ± 218	1.9	7,205 ± 92	1.4	0.16

Table A.1. Preliminary Screening Results for Core 400

Preliminary Screening Core **401**					
Sample Number	OSL Photon Counts	OSL Depletion	IRSL Photon Counts	IRSL Depletion	IRSL/OSL
401A	1,578 ± 53	1.3	272 ± 38	0.9	0.17
401B	913 ± 47	1	--	--	--
401C	631 ± 43	1	--	--	--
401D	968 ± 46	1.3	--	--	--
401E	597 ± 43	1	--	--	--
401F	462 ± 49	1	--	--	--
401G	10,462 ± 108	1.5	300 ± 41	1.7	0.03
401H	100,438 ± 320	1.5	6,008 ± 86	1.2	0.06
401I	139,431 ± 376	1.5	10,482 ± 108	1.3	0.08
401J	156,564 ± 398	1.6	9,942 ± 107	1.3	0.06
401K	153,987 ± 395	1.6	11,318 ± 113	1.3	0.07
401L	167,987 ± 412	1.6	16,326 ± 133	1.3	0.10
401M	173,854 ± 419	1.6	14,003 ± 124	1.3	0.08
401N	133,812 ± 369	1.6	10,492 ± 110	1.3	0.08
401O	156,415 ± 398	1.5	10,768 ± 110	1.2	0.07
401P	160,530 ± 403	1.5	12,562 ± 118	1.3	0.08
401Q	155,183 ± 397	1.5	13,636 ± 122	1.3	0.09
401R	161,574 ± 405	1.7	14,796 ± 127	1.3	0.09

Table A.2. Preliminary Screening Results for Core 401

Preliminary Screening Isolated Marine Samples							
Sample Number	Type	Location	OSL Photon Counts	OSL Depletion	IRSL Photon Counts	IRSL Depletion	IRSL/OSL
399A	Silt beneath anchor	SE	82,899 ± 290	2.1	12,430 ± 177	1.5	0.15
399B	Sand beneath anchor	SE	3,032 ± 65	1.9	194 ± 37	1.5	0.06
399C	Silt beneath same anchor as **399B**	SE	159,531 ± 402	2.3	19,628 ± 145	1.5	0.12
399D	Sand beneath architectural block	SE	4,078 ± 73	1.7	98 ± 37	2.6	0.02
399E	Sand beneath anchor	SE	1,395 ± 53	1.4	--	--	--
399F	Surface sand	SE	566 ± 43	1	--	--	--
399G	Sand beneath ceramic	NW	--	--	--	--	-
399H	Sand beneath ceramic	NW	946 ± 46	1.1	29 ± 34	3.1	
399I	Sand beneath ceramic	NW	1,489 ± 55	1.1	--	1.9	
399J	Surface sane	NW	319 ± 42	1.1	--	--	0.03
399K	Silt beneath ceramic base	NW	457,408 ± 679	1.8	29,201 ± 175	1.3	--

Table A.3. Preliminary Screening Results for Isolated Marine Samples (399 A-K)

Preliminary Screening Archaeological Section						
Sample Number	Lithostratigraphy	OSL Photon Counts	OSL Depletion	IRSL Photon Counts	IRSL Depletion	IRSL/OSL
398A	Orange clayey sand (collapse)	38,050 ± 198	2.3	3,894 ± 71	1.5	0.10
398B	Orange clayey sand within layer of collapse	63.190 ± 253	2.7	5,385 ± 80	1.5	0.09
398C	Orange clayey sand above plaster surface	35.444 ± 192	2.0	3,246 ± 66	1.3	0.09
398D	Orange clayey sand below plaster surface	34.905 ± 189	2.1	3,562 ± 68	1.5	0.10
398E	Orange-gray clayey-sand	49.211 ± 224	2.3	5,697 ± 82	1.5	0.12

Table A.4. Preliminary Screening Results for Terrestrial Samples: Archaeological Section (398 A-E)

Preliminary Screening Environmental Section						
Sample Number	Lithostratigraphy	OSL Photon Counts	OSL Depletion	IRSL Photon Counts	IRSL Depletion	IRSL/OSL
398F	Light orange-beige clayey sand	46 ± 218	1.7	5,206 ± 80	1.6	0.11
398G	Chalk	86 ± 296	2.1	18.267 ± 140	1.5	0.21
398H	Light orange -beige clayey sand	72 ± 271	2.0	9,889 ± 106	1.4	0.14
398I	Light orange-beige clayey sand	93 ± 307	2.0	12,855 ± 118	1.5	0.14
398J	Orange sandy clay	45 ± 215	1.9	6,973 ± 91	1.6	0.15
398K	Light gray-orange sand with small pebbles	27 ± 168	1.5	1.848 ± 53	1.3	0.07
398L	Dark gray-orange sand with small pebbles	36 ± 194	1.6	2,435 ± 59	1.4	0.07

Table A.5. Preliminary Screening Results for Terrestrial Samples: Environmental Section (398 F-L)

Calibrated Screening Core **400**

		Stored Dose (Gy)			Sensitivity (Gy^{-1})		
Sample	Depth	Aliquot 1	Aliquot 2	Average	Aliquot 1	Aliquot 2	Average
400A	406.6	0.02 ± 0.26	--	--	349 ± 19	--	--
400B		--	--	--	--	--	--
400C	411.1	0.5 ± 2.25	--	--	282 ± 17	--	--
400D	412.3	--	--	--	203 ± 14	--	--
400E	413.7	--		--	2,597 ± 51	--	--
400F	415.1	--	0.6 ± 0.1	--	235 ± 15	1,432 ± 38	834
400G	416.45	--	--	--	116 ± 11	568 ± 24	342
400H	418	12.4 ± 2.6	17.3 ± 12.4	14.8	910 ± 30	127 ± 11	518
400I	419.7	9.3 ± 2.4	67.4 ± 3.5	38.3	519 ± 23	2,613 ± 51	1,566
400J	421.4	13.6 ±4.0	13.2 ± 3.2	13.4	574 ± 24	648 ± 25	611
400K	423	42.7 ± 9.4	56 ± 30.5	49.4	401 ± 20	1874 ± 43	1137
400L	424.3	24.5 ± 8.4	13.7 ± 78.5	19.1	309 ± 18	239 ± 15	274
400M	426.45	18.0 ± 6.6	13.9 ± 3.8	15.9	340 ± 18	554 ± 24	446
400N	427.9	6.1 ± 2.1	33.8 ± 3.5	20.0	470 ± 22	1,971 ± 44	1,220
400O	429.6	8.1 ± 0.9	--	--	1,508 ± 39	--	--
400P	430.75	49.9 ± 4.0	--	--	7,309 ± 85	--	--
400Q	431.9	10.7 ± 4.4	--	--	355 ± 19	--	--
400R	433.5	11.2 ± 0.9	--	--	2,234 ± 47	--	--
400S	434.6	103.5 ± 12.6	22 ± 2	62.7	13,291 ± 115	2,365 ± 49	5,462
400T	435.6	27.8 ± 2.4	--	--	5,651 ± 75	--	--
400U	436.6	16.8 ± 2.6	25.4 ± 2.1	21.1	2,035 ± 45	5,099 ± 71	3,567

Table A.6. Calibrated Screening Results for Core 400 Results highlighted pink have stored doses with error values above 20% and are not considered viable for drawing conclusions.

Calibrated Screening Core **401**							
		Stored Dose (Gy)			Sensitivity (Gy^{-1})		
Sample	Depth	Aliquot 1	Aliquot 2	Average	Aliquot 1	Aliquot 2	Average
401A	201.1	--	1.1 ± 3.4	--	135 ± 12	50 ± 7	92
401B	202.2	1.4 ± 2.6	--	--	91 ± 10	345 ± 19	218
401C	203.5	--	--	--	1528 ± 39	176 ± 13	852
401D	204.4	0.4 ± 1.5	--	--	128 ± 11	36 ± 6	82
401E	205.25	--	0.5 ± 0.4	--	193 ± 14	349 ± 19	271
401F	206.6	--	--	--	269 ± 16	247 ± 16	26
401G	207.45	--	--	--	--	177 ± 13	88
401H	208.6	124.8 ± 361.6	159.9 ± 42.7	142.4	20 ± 4	102 ± 10	61
401I	209.7	15.4 ± 2.5	67.6 ± 5.6	41.5	1,444 ± 38	3,266 ± 57	2,355
401J	210.6	--	55.4 ± 9.1	--	3,050 ± 55	332 ± 18	1,691
401K	211.6	53.8 ± 7.9	43.8 ± 7	48.8	4,357 ± 66	2,058 ± 45	3,207
401L	212.5	--	55.6 ± 2.9	--	3,270 ± 57	2,877 ± 54	3,073
401M	213.5	43.5 ± 2	41.5 ± 6	42.6	3,408 ± 58	9,921 ± 100	6,664
401N	214.3	41.3 ± 1.9	54.6 ± 2.9	48.0	3,875 ± 62	2,734 ± 52	3,304
401O	214.9	53.7 ± 9.7	47.6 ± 2.1	50.6	3,058 ± 55	4,664 ± 68	3,861
401P	215.65	761.4 ± 116.8	828.4 ± 31.7	794.9	3,129 ± 56	7,965 ± 89	5,547
401Q	216.4	853.7 ± 32.8	782.7 ± 42.2	818.2	7,049 ± 84	2,767 ± 53	4,908
401R	217.3	1,356.5 ± 49.1	1,031.9 ± 48.9	1194.2	15,306 ± 124	3,432 ± 59	9,369

Table A.7. Calibrated Screening Results for Core 401 Results highlighted pink have stored doses with error values above 20% and are not considered viable for drawing conclusions.

Calibrated Screening of Isolated Marine Samples									
				Stored Dose (Gy)			Sensitivity (Gy^{-1})		
Sample	Type	Location	Depth (cm)	Aliquot 1	Aliquot 2	Average	Aliquot 1	Aliquot 2	Average
399A	Silt beneath anchor	SE	300.0	3.5 ± 0.8	31.3 ± 6.1	17.4	522 ± 23	659 ± 26	591
399B	Sand beneath anchor	SE	450.0	--	--	--	--	--	--
399C	Silt beneath same anchor as **399B**	SE	450.0	118.8 ± 72.8	--	--	92 ± 10	--	--
399D	Sand beneath architectural block	SE	600.0	--	--	--	953 ± 31	570 ± 24	762
399E	Sand beneath anchor	SE	300.0	--	0.9 ± 0.7	--	76 ± 9	224 ± 15	150
399F	Surface sand	SE	300.0	--	--	--	--	--	--
399G	Sand beneath ceramic	NW	200.0	--	--	--	97 ± 10	319 ± 18	208
399H	Sand beneath ceramic	NW	200.0	--	--	--	118 ± 11	--	--
399I	Sand beneath ceramic	NW	200.0	--	--	--	166 ± 13	155 ± 12	161
399J	Surface sand	NW	200.0	--	0.2 ± 0.2	--	--	519 ± 23	--
399K	Silt beneath ceramic base	NW	200.0	54 ± 14	18 ± 6.5	36	1211 ± 35	328 ± 18	769

Table A.8. Calibrated Screening Results for Isolated Marine Samples (399 A-K) Results highlighted pink have stored doses with error values above 20% and are not considered viable for drawing conclusions.

Calibrated Screening Archaeological Section							
		Stored Dose (Gy)			Sensitivity (Gy^{-1})		
Sample	Depth	Aliquot 1	Aliquot 2	Average	Aliquot 1	Aliquot 2	Average
398A	60	12.2 ± 1.1	8.65 ± 0.8	10.4	3,380 ± 58	2,317 ± 48	2,849
398B	70	4.05 ± 0.4	5.53 ± 0.3	4.8	1,248 ± 35	2,982 ± 55	2,115
398C	85	4.62 ± 0.4	4.74 ± 0.4	4.7	1,556 ± 39	2,289 ± 48	1,922
398D	95	5.57 ± 0.2	11.84 ± 1.1	8.7	6,229 ± 79	10,409 ± 102	8,319
398E	100	6.36 ± 0.4	6.50 ± 0.5	6.4	2,856 ± 53	2,905 ± 54	2,881

Table A.9. Calibrated Screening Results for Terrestrial Samples: Archaeological Section (398 A-E)

Calibrated Screening Environmental Section							
		Stored Dose (Gy)			Sensitivity (Gy^{-1})		
Sample	Depth (cm)	Aliquot 1	Aliquot 2	Average	Aliquot 1	Aliquot 2	Average
398F	100.0	76.6 ± 5.2	24.6 ± 3.3	50.6	5,355 ± 73	3,891 ± 62	4,623
398G	117.0	--	--	--	--	--	--
398H	129.0	--	--	--	--	--	--
398I	135.0	59.2 ± 21.6	19.5 ± 3.9	39.3	252 ± 16	1,108 ± 33	680
398J	150.0	47.7 ± 9.9	59.5 ± 10.3	53.6	486 ± 22	1,125 ± 34	806
398K	165.0	20.8 ± 4.2	21.2 ± 6	21	1,192 ± 35	476 ± 22	834
398L	179.0	47.6 ± 4.4	64 ± 19.6	55.8	1,175 ± 34	591 ± 24	883

Table A.10. Calibrated Screening Results for Terrestrial Samples: Environmental Section (398 F-L) Results highlighted pink have stored doses with error values above 20% and are not considered viable for drawing conclusions.

SAR **399A**							
Aliquot	Grain Size	Preheat Temperature	Stored Dose	Sensitivity	Recuperation % (from zero dose)	Recycling Ratio (from repeat dose)	IR Response (from IRSL dose)
1	200	220	--	--	--	--	--
2	200	220	--	--	--	--	--
3	120	220	50.7 ± 3.5	3,130	1.8	1.0	1.5
4	120	220	26.6 ± 4.7	3,485	8.0	1.2	2.3
5	120	220	--	--	--	--	--
6	200	230	0.7 ± 0.4	2,856	58.9	0.8	0.2
7	200	230	0.3 ± 0.6	3,078	74.3	1.4	-3.8
8	200	230	6.3 ± 2.7	3,406	12.9	1.0	1.6
9	120	230	2.4 ± 0.4	3,193	22.2	1.1	-0.5
10	120	230	7 ± 3.5	2,843	50.9	1.1	16.7
11	200	240	21.7 ± 14.3	3,290	11.0	0.9	-5.1
12	200	240	46.2 ± 7.9	3,358	8.1	0.8	-1.1
13	120	240	--	--	--	--	--
14	120	240	61.2 ± 15.1	2,862	25.0	1.2	-8.3
15	120	240	37.7 ± 10.2	3,615	7.6	1.2	2.8
16	200	250	--	--	--	--	--
17	200	250	26.3 ± 9.1	3,694	12.6	1.0	4.0
18	200	250	4.9 ± 1	2,524	20.5	0.7	1.2
19	120	250	12.8 ± 2.2	2,798	21.0	1.1	-0.6
20	120	250	0.9 ± 0.4	2,774	-39.5	1.1	7.4
21	200	260	98.9 ± 53.4	2,482	13.5	1.1	1.5
22	200	260	26.4 ± 6.5	3,246	14.6	1.2	-0.2
23	120	260	7.97 ± 5.5	2,706	34.6	0.9	3.7
24	120	260	29.46 ± 31.1	2,463	0.6	3.0	-12.5

Table A.11. Single Aliquot Regenerative Protocol Results for Marine Sample 399A Results highlighted pink have stored doses with error values above 20% and are not considered viable for drawing conclusions.

SAR **399C**							
Aliquot	Grain Size	Preheat Temperature	Stored Dose	Sensitivity	Recuperation % (from zero dose)	Recycling Ratio (from repeat dose)	IR Response (from IRSL dose)
1	200	220	--	3,105	123.6	0.9	-3.3
2	200	220	8.7 ± 2.7	4,862	46.3	0.9	1.3
3	120	220	--	3,432	5.1	0.8	0.4
4	120	220	11.7 ± 0.9	3,431	5.1	1.0	-1.0
5	120	220	0.8 ± 0.6	3,737	13.1	1.0	-1.7
6	200	230	0.5 ± 0.5	3,020	2.5	1.2	4.0
7	200	230	4.6 ± 2.1	3,078	11.0	2.0	-0.2
8	200	230	1.7 ± 9	3,086	83.5	2.1	-23.9
9	120	230	8.5 ± 6.9	3,012	27.0	0.7	8.8
10	120	230	--	--	--	--	--
11	200	240	--	3,127	190.2	1.3	4.0
12	200	240	--	--	--	--	--
13	120	240	46 ± 5.5	2,858	2.0	0.9	0.2
14	120	240	14.9 ± 4.9	2,735	12.3	2.0	12.3
15	120	240	3.6 ± 0.4	3,415	36.6	1.0	-0.9
16	200	250	7.4 ± 2.3	3,174	17.8	1.2	3.0
17	200	250	18.1 ± 9.9	2,715	17.8	1.1	-2.1
18	200	250	--	--	--	--	--
19	120	250	--	3,294	1.3	4.5	-7.8
20	120	250	18.4 ± 8.4	2,867	12.0	0.8	-2.6
21	200	260	--	--	--	--	--
22	200	260	--	--	--	--	--
23	120	260	18.4 ± 5.8	2,962	15.4	1.8	-15.6
24	120	260	5.6 ± 0.8	2,708	35.3	0.9	-0.2

Table A.12. Single Aliquot Regenerative Protocol Results for Marine Sample 399C Results highlighted pink have stored doses with error values above 20% and are not considered viable for drawing conclusions.

SAR **399D**							
Aliquot	Grain Size	Preheat Temperature	Stored Dose	Sensitivity	Recuperation % (from zero dose)	Recycling Ratio (from repeat dose)	IR Response (from IRSL dose)
1	200	220	--	--	--	--	--
2	200	220	-1.8 ± 0.9	4,323	7,107.6	0.7	-1.5
3	120	220	--	--	--	--	--
4	120	220	-0.1 ± 1.4	2,961	-484.2	2.1	1.6
5	120	220	--	--	--	--	--
6	200	230	-4.4 ± 6.8	3,083	-148.3	-0.7	-2.8
7	200	230	-1 ± 1.4	2,770	-95.0	1.0	2.5
8	200	230	13.6 ± 4.9	3,341	2.1	1.2	3.5
9	120	230	--	--	--	--	--
10	120	230	-0.3 ± 0.2	3,224	-86.0	0.8	--
11	200	240	--	--	--	--	--
12	200	240	--	--	--	--	--
13	120	240	-1.2 ± 1.4	3,066	230.3	0.4	-1.1
14	120	240	-2.3 ± 2.7	2,717	-1,037.7	0.9	-6.2
15	120	240	-0.5 ± 0.7	3,041	8.4	0.7	-4.9
16	200	250	-1 ± 1	2,992	504.0	1.3	6.5
17	200	250	1.1 ± 31.7	3,080	28.5	37.9	1.7
18	200	250	--	--	--	--	--
19	120	250	--	--	--	--	--
20	120	250	-0.2 ± 1.1	2,661	256.5	0.4	5.5
21	200	260	--	--	--	--	--
22	200	260	-11 ± 70.4	2,978	-2.8	-0.5	9.4
23	120	260	-0.1 ± 0.4	3,191	94.9	0.9	-0.7
24	120	260	-0.6 ± 0.9	3,128	241.0	0.9	-0.7

Table A.13. Single Aliquot Regenerative Protocol Results for Marine Sample 399D Results highlighted pink have stored doses with error values above 20% and are not considered viable for drawing conclusions.

SAR **399F**							
Aliquot	Grain Size	Preheat Temperature	Stored Dose	Sensitivity	Recuperation % (from zero dose)	Recycling Ratio (from repeat dose)	IR Response (from IRSL dose)
1	200	220	-1.2 ± 0.6	3,419	-46.7	0.8	3.2
2	200	220	--	--	--	--	--
3	120	220	-1.1 ± 1.2	3,637	-62.7	1.7	-2.0
4	120	220	-3.0 ± 2.8	3,436	-663.1	0.6	-2.8
5	120	220	--	3,427	80.9	1.4	-4.8
6	200	230	4.9 ± 3.5	2,971	99.5	-1.2	-19.0
7	200	230	-0.5 ± 0.2	3,309	295.8	0.8	0.4
8	200	230	--	--	--	--	--
9	120	230	--	--	--	--	--
10	120	230	-1.1 ± 7.1	3,711	-99.7	0.2	-7.8
11	200	240	-3.2 ± 2.8	2,804	-142.2	0.7	-0.9
12	200	240	-0.5 ± 0.2	2,829	233.3	0.5	2.5
13	120	240	--	--	--	--	--
14	120	240	--	--	--	--	--
15	120	240	3.8 ± 7.1	2,941	17.1	1.3	0.5
16	200	250	-0.3 ± 0.7	2,752	183.3	1.0	-0.1
17	200	250	-0.1 ± 3.6	3,369	110.1	0.6	0.6
18	200	250	--	--	--	--	--
19	120	250	-1.0 ± 0.4	2,860	-234.7	1.1	-0.3
20	120	250	-0.5 ± 0.3	3,956	144.0	1.0	0.7
21	200	260	-2.2 ± 2.4	2,485	-271.1	1.6	6.4
22	200	260	8.9 ± 10.9	3,419	-46.7	0.8	3.2
23	120	260	-2.0 ± 8.4	3,637	-62.7	1.7	-2.0
24	120	260	-0.7 ± 1.9	3,436	-663.1	0.6	-2.8

Table A.14. Single Aliquot Regenerative Protocol Results for Marine Sample 399D Results highlighted pink have stored doses with error values above 20% and are not considered viable for drawing conclusions.

Mean SAR Values					
Sample	Stored Dose	Sensitivity	Recuperation %	Recycling Ratio	IR Response
399A	27.7	3,192	12.2	1.0	0.3
399C	16.7	3,103	19.7	0.9	-0.5
399D	--	--	--	--	--
399F	--	--	--	--	--

Table A.15. Mean Single Aliquot Regenerative Protocol Results Results highlighted pink have stored doses with error values above 20% and are not considered viable for drawing conclusions.